DYNAMIC HEAT TRANSFER IN COMPOSITE MINIATURE STRUCTURES

By

MARIO ARIET ANTIGA

A DISSERTATION PRESENTED TO THE GRADUATE COUNCIL OF
THE UNIVERSITY OF FLORIDA
IN PARTIAL FULFILLMENT OF THE REQUIREMENTS FOR THE
DEGREE OF DOCTOR OF PHILOSOPHY

UNIVERSITY OF FLORIDA

April, 1965

ACKNOWLEDGMENTS

The author wishes to express his sincere appreciation to Professor Robert D. Walker, Jr., whose interest, advice and criticism stimulated and guided this research program, to Dr. Herbert E. Schweyer for his guidance and advice throughout his career.

He wishes to thank Mr. Henry R. Wengrow without whose assistance this work would not have been possible, Dr. Mack Tyner and Mr. Marin Fadran for their helpful discussions and suggestions, and the members of his Supervisory Committee Dr. T. M. Reed, Dr. R. G. Blake and Dr. E. W. Kluge. A special appreciation is due Mr. Bruce T. Fairchild, Mr. E. K. Wangrow and Dr. F. F. May for the use of their AMOS program, and Mr. Roberts Vick for his assistance on the drawings.

The author also wishes to acknowledge the financial assistance of the Harry Diamond Laboratories, Army Material Command, and its technical representatives Messrs. R. N. Comyn and Nathan Kaplan, who by their encouragement and support made it possible to conduct this investigation.

TABLE OF CONTENTS

		Page
ACKNOWLEDGMENTS		ii
LIST OF TABLES		vi
LIST OF FIGURES		vii
ABSTRACT		x
CHAPTER		
I.	INTRODUCTION	1
II.	THEORY OF HEAT TRANSMISSION	8
	Geometrical Considerations in Battery Life Optimization	16
III.	ANALOG COMPUTER MODEL	22
	A. Description of the Model	22
	B. Heat Transfer Coefficients	24
	C. Development of the Mathematical Model	27
	D. Analog Computer Solution	31
	E. Discussion of Results	38
	1. Temperature Histories in a Standard Simulated Battery	42
	2. Effect of Heat Sink on Cell Temperatures	42
	3. Effect of Insulation Parameters on Cell Temperatures	44
	4. Variation of Heat Generator Parameters	46
	5. Variation of Cell Parameters	49
	6. Effect of Rate and Level of Heat Generation by Chemical Reactions in Cells	56

TABLE OF CONTENTS (Continued)

CHAPTER		Page
IV	ANALOG COMPUTER MODEL II	62
	A Description of the Model	62
	B. Development of the Mathematical Model	65
	C Analog Computer Solution	67
	D Discussion of Results	67
	1 Geometrical Shape of Insulation Elements	76
	2 Simulation of Standard Thermal Battery	78
	3 Effect of a Metal Layer Next to the Core on Core Temperature	80
	4 Effect of Varying Insulation Arrangements on Core Temperature	80
V	DIGITAL COMPUTER MODEL III	88
	A. Description of the Model	89
	B. Development of the Mathematical Model	90
	C Finite Differences Approximation	94
	D Development of the Computer Program	94
	E The AMPS Program	97
	F Discussion of Results	99
	1. Simulation of Standard Thermal Battery	101
	2. Effect of Varying Insulation Arrangements on Core Temperature	104
	3 Effect of Idealized Insulating Materials on Core Temperature	108
	4. Effect of Core Radius on Core Temperature	109
	5. Effect of Intra-Cell Heat Generation	114

TABLE OF CONTENTS (Continued)

CHAPTER		Page
	6. Effect of Heat Sink Temperature on Core Temperature	114
	7. Effect of Changes in the Heat Capacity of the Heat Generators on the Core Temperature	114
	8. Core Temperature of Improved Thermal Battery	118
	9. Effect on Core Temperature of Delayed Heat Generation Within the Insulation	118
	10. Effect of Change in the Volume of the Battery on Core Temperature	121
VI.	CONCLUSIONS AND RECOMMENDATIONS	123
LIST OF SYMBOLS		125
LITERATURE CITED		127
APPENDICES		130
A.	Details of Analog Model I	131
B.	Details of Analog Model II	138
C.	Details of Digital Model III	148
E.	Details of the Computer Program	156
BIOGRAPHICAL SKETCH		209

LIST OF TABLES

Table		Page
1	Differential-Difference Equations for Mathematical Model I	28
2	Coefficients for Programmed Differential-Difference Equations Model I	32
3	Average Physical Properties and Dimensions of Thermal Battery Components Model I	36
4	Effect of Parameters and Changes on the Life to 400°C of a Simulated Thermal Battery	40
5	Differential-Difference Equations for Mathematical Model II	69
6	Coefficients for Programmed Differential-Difference Equations Model II	71
7	Average Physical Properties and Dimensions of Thermal Battery Components Model II	75
8	Effect of Changes in the Insulation Structure on Life to 400°C of Simulated Thermal Batteries	77
9	Effect of Parameters and Changes on Life to 400°C of a Simulated Thermal Battery	105
A-1	Summary of Runs	132
A-2	Summary of Potentiometer Settings	134
B-1	Summary of Runs	143
B-2	Summary of Potentiometer Settings	144
C-1	Data Used in Simulation of Standard Thermal Battery	150
C-2	Summary of Runs	151

LIST OF FIGURES

Figure		Page
1	Schematic Diagram of Thermal Battery	4
2	Temperature Histories in Homogeneous Right Circular Cylinders	21
3	Schematic Diagram of Battery Described by Model 1	23
4	Analog Computer Diagram of Model 1	30
5	Experimental Versus Computed Results	39
6	Temperature Histories of Elements in Standard Simulated Thermal Battery	43
7	Effect on Cell Temperature of Changing the Temperature of the Heat Sink	45
8	Effect on Cell Temperature of Reducing the Thermal Conductivity of the Insulation	46
9	Effect on Cell Temperature of Increasing the Thermal Conductivity of the Insulation	47
10	Effect on Cell Temperature of Changing the Thickness of the Insulation	48
11	Effect on Cell Temperature of Changing Thickness of Heat Generators	50
12	Effect on Cell Temperature of Compressing Heat Generators	51
13	Effect on Cell Temperature of Changing the Thickness of the Cell	53
14	Effect on Cell Temperature of Changing the Enthalpy of the Cell	55
15	Effect on Cell Temperature of Changing the Magnitude of the Intra-Cell Chemical Heat Generation	57
16	Change of Initial Rate of Intra-Cell Chemical Heat Generation Term	59
17	Change of Decay Rate of Intra-Cell Chemical Heat Generation Term	61

[illegible] FIGURES ([illegible])

[illegible]	[illegible] Diagram of Battery Described by Model II	[illegible]
[illegible]	[illegible] Computer Diagram of Model II	[illegible]
[illegible]	[illegible] Histories in Standard Simulated Thermal [illegible]	[illegible]
[illegible]	[illegible] Histories in Simulated Thermal Battery [illegible] Sent to Core	8[illegible]
[illegible]	[illegible] Histories in Simulated Thermal Battery [illegible] Insulation Arrangement	[illegible]
[illegible]	[illegible] Histories in Simulated Thermal Battery [illegible] Insulation Arrangement	[illegible]
[illegible]	[illegible] Histories in Simulated Thermal Battery [illegible] Varying Insulation Arrangement	8[illegible]
[illegible]	[illegible] Histories on Simulated Thermal Battery [illegible] Varying Insulation Arrangement	8[illegible]
[illegible]	[illegible] Diagram of Battery Described by Model III	93
[illegible]	[illegible] Profiles in Standard Simulated Thermal [illegible]	103
[illegible]	[illegible] on Cell Temperature of Various Insulation Arrangements	107
[illegible]	Effect on Cell Temperature of Idealized Changes in the Thermal Properties of the Insulation	110
[illegible]	Effect on Insulation Temperature of Idealized Changes in Thermal Properties of the Insulation	111
[illegible]	[illegible]rect on Cell Temperature of Different Idealized Insulations	112
[illegible]	[illegible] Cell Temperature of Changes in Core Radius	113
[illegible]	[illegible] Temperature of Changes in the Intra-[illegible] Generation	[illegible]5
[illegible]	[illegible] on Cell [illegible]ture of the Heat Sink Tempera-[illegible]	1[illegible]

LIST OF FIGURES (Continued)

Figure		Page
35	Effect on Cell Temperature of Changes in the Heat Capacity of the Heat Generators	117
36	Effect on Cell Temperature of Suggested Design Improvements	119
37	Effect on Cell Temperature of Delayed Heat Generation Within the Insulation	120
38	Effect on Cell Temperature of a Change in the Volume of the Battery	122
A-1	Analog Circuit of Heat of Reaction Term	137
B-1	Details of the Shape of Insulation Elements	139
C-1	Analytical Versus Computed Results for the Cooling of a Homogeneous Sphere	149

Abstract of Dissertation Presented to the Graduate Council in
Partial Fulfillment of the Requirements for the
Degree of Doctor of Philosophy

DYNAMIC HEAT TRANSFER IN COMPOSITE
MINIATURE STRUCTURES

By

Marie Ariet Antiga

April, 1965

Chairman: Prof. Robert D. Walker, Jr.
Major Department: Chemical Engineering

The inability to measure temperatures in small objects accurately and at all desirable locations during rapid temperature transients points up the need for valid alternate methods of solving such problems. In this investigation, temperature histories were computed for specific locations in a simulated thermal battery, and the effect of changing the construction configuration and the physical properties of the materials were studied in order to optimize battery life.

Two analog computer models were developed to simulate the thermal battery. These models were based on the assumption of "well-mixed" elements having the thermal resistance "lumped" at the interfaces between adjacent elements. They provided simulations of the temperature histories in thermal batteries which were in satisfactory

agreement with experience. The analog studies provided considerable insight into heat transfer processes in these units, and the effects of changes in configuration and properties of materials. The results of these models were also very helpful in the development of the more accurate digital computer model.

The digital computer model consisted of a sphere having a core made up of an inner well-mixed section and an outer section where temperature gradients existed. The core was surrounded by six concentric spherical layers of insulating materials which could be assigned any value of physical properties. The partial differential equations describing this model were approximated using finite-difference techniques by a system of differential-difference equations which in turn were solved by the Adams-Moulton-Shell numerical integration method. Among the more important findings of this work are:

1. Of the insulation materials and configurations studied maximum battery life is achieved with all-Thermoflex insulation.

2. If it is necessary to use layers of more than one insulation material, maximum battery life is achieved with as much Thermoflex as possible adjacent to the core.

3. Insulation layers prepared by mixing a poor insulator with a good one are less efficient than proper arrangements of layers consisting of pure materials.

4. An increase in the volumetric heat capacity of the heat generators leads to an increase in the battery life.

5. An increase in the intra-cell heat of reaction leads to

an increase in battery life providing it is spread over a sufficiently long period of time.

6. Placement of suitable heat generators in the insulation leads to substantially increased battery life.

7. An increase in battery size generally results in an increase in battery life because the capacity of the heat reservoir increases more rapidly than the rate of heat losses. Conversely, the smaller the battery the more serious the heat transfer problem.

8. The sphere is the most efficient shape because it has the smallest area for a given volume. The greater the deviation of an actual shape from a sphere the greater the heat transfer problem.

9. The high cut-off temperature imposed by a high-melting electrolyte leads to an optimum core to insulation volume ratio. For the system studied this optimum ratio turned out to be close to that chosen for the standard.

10. The optimum insulator for a high cut-off temperature is not the insulator with the lowest thermal diffusivity, it is, rather, the one with the lowest thermal conductivity and a value of the volumetric heat capacity which is a function of the cut-off temperature.

CHAPTER 1

INTRODUCTION

The construction and operation of thermal batteries was first discussed by Goodrich (1), who defined them as electrochemical power supplies based upon electrolytes of various inorganic salts which remain solid and nonconducting at all storage temperatures. He indicated that for isolated performance, an integral heat generating source (based on chemical reaction using gaseous, liquid or solid fuels) is required to raise the temperature of the cell above its melting point. Vissel (2), and Selis et al. (3) have presented descriptions of different electrochemical systems, such as $Mg/LiCl-KCl-K_2Cr_2O_4/Ni$ and $Mg/LiCl-KCl/PsO_x,Ni$ which perform satisfactorily in thermal batteries.

McKee (4) enumerated the following advantages of thermal batteries:

1. Permit high voltages
2. Large currents may be drawn from them
3. Indefinite storage
4. Operation over a wide range of temperature extremes
5. No maintenance
6. Use in any position
7. Ruggedness

He stated that the chief limitation is that they are relatively short lived, the implication being that this results from loss of heat, for otherwise life could be increased essentially indefinitely by adding

more call reactants. Johnson (5), and Hill (6) presented data on heat generating systems which can achieve temperatures of about 700°C in about 1 second. Some of these systems contain zinc metal while others are based on $KMnO_4$, CaF_2, MgF_2, Fe, etc. Numerous other systems have been devised from study of the thermodynamic properties of the reactants and products of reactions.

Possibly the classic case of utilizing a chemical reaction to produce heat is the thermite process. Generally the reactants in these reactions are in the form of very fine powder and are chosen so as to be gaseous, or nearly so. These reactions are essentially instantaneous, and they give off a great deal of heat. Temperatures of the order of 2000°C are commonly attained.

The design of thermal batteries constitutes a challenging complex engineering problem because of the stringent heat transfer limitations required to construct a useful unit. The chemical composition of the materials which compose the thermal battery and the details of its construction are subject to security classification. Not enough unclassified information is available to permit the heat transfer problem to be defined meaningfully.

A thermal battery can be thought of as an assembly of three main types of elements:

1. <u>Heat generators</u>, which constitute an essentially instantaneous heat source;

2. <u>Electrolytic cells</u>, which become activated when the

electrolyte, which is solid at ambient temperature, melts as it receives heat given off by the heat generators.

3. Insulation, which serves to decrease the rate of heat loss from the assembly to the surroundings.

In a thermal battery the heat generators and electrolytic cells, which may be shaped in the form of flat circular cylinders, can be arranged in a stack in which each cell is in contact with two generators and vice versa. This cell-generator core is then surrounded by the insulation. A schematic diagram of such a unit is shown in Figure 1.

The operation of the battery is initiated when the heat generators are set off. The large quantity of heat given off almost instantaneously by these generators is transferred rapidly to the electrochemical cells with the result that the solid electrolyte melts and the cell begins to generate electrical power. The assembly loses heat to the surroundings owing to its high relative temperature, and the electrochemical reaction within the cell proceeds until the electrolyte approaches its freezing point. In this work the elapsed time between the reaching 400°C and cooling back to 400°C is referred to as the life of the battery.

In a heat transfer study one of the obvious objectives would be to maximize the life of the battery for a given battery volume subject to other constructional and operational constraints. Maximization of battery life above 400°C can, therefore, make the primary objective of this investigation. The life of a thermal battery can be estimated reasonably well if temperature histories can be obtained at the required

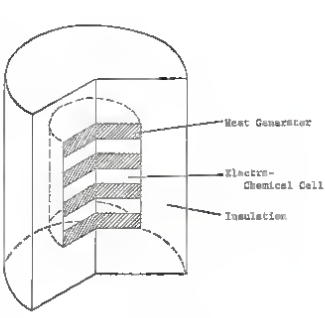

Figure 1 Schematic Diagram of Thermal Battery

locations within the battery. Although it might appear that the desired time-temperature relations could be obtained either by direct measurement or by classical mathematical methods, further consideration of the problem will reveal inherent limitations in both the experimental and the formal computational approaches.

Although thermometers, thermocouples, and similar devices are generally quite adequate temperature measurement instruments for many physical phenomena, there exist other situations, such as that encountered here, where the instrumental response will not be adequate. For example, large differences may arise between the indicated and actual temperatures of an object as a result of response lags of the sensing device during rapid temperature changes, or as a result of heat losses through the measuring device if the object under study is small in size relative to the sensing device. Such errors are in general difficult to evaluate.

Alternatively the temperature histories at points of interest may be obtained by solving the mathematical model which describes the given physical situation. For the case of unsteady-state heat transfer, the mathematical model will consist of one or more partial differential equations. Even if the errors associated with a temperature measuring device should not be serious, a valid calculation procedure would have a tremendous advantage of producing temperature histories of numerous points simultaneously. Moreover, the experimental approach would subject the system to the disruptive influence of the numerous measuring devices required for direct measurements. Where the object under study is

relatively small the errors resulting from heat losses through the various measuring instruments might be the most significant mode of heat loss thereby making the observations meaningless.

Another significant advantage of the mathematical model approach to this problem as compared to the experimental approach is that the experimental testing of the battery requires a statistical analysis involving numerous replications because of the random variations of the materials making up the battery. In the mathematical model, materials having exact properties are assumed and hence valid conclusions can be drawn from a much smaller number of trials.

There is another consideration which is very significant from the design viewpoint, namely, the mathematical model allows for the possibility of evaluating the performance of a battery constructed of idealized materials. If the results indicate that a significant improvement could be obtained with such materials, efforts could be directed towards the development of these materials.

In many cases of practical interest, such as the one under consideration, formal mathematical solutions of partial differential equations are very difficult or impossible to evaluate because materials may not be homogeneous, thermal properties may vary, or the boundary or initial conditions may be complex. However, the availability of electronic computers makes possible the solution of complex mathematical models by various approximation techniques.

In this study, mathematical models of the dynamic heat transfer in thermal batteries were developed with simplifying assumptions which

made their solution on the computers possible. In the initial stage of the investigation the analog computer was utilized. With the insight gained from the analog studies, a more complete mathematical model was developed and programmed for the IBM 709 digital computer.

The investigation had two chief objectives:

1. To provide temperature histories for specific locations within a battery.

2. To study the effect of changing the construction configurations and properties of the materials required for the construction of the battery so that design specifications could be made to optimize its performance.

The optimization criterion was defined as the maximum life of the battery. Thus, the configuration yielding the maximum battery life was considered optimum. As mentioned before, the effect of idealized materials was studied with the idea that if the inclusion of certain idealized material increased the life of the assembly significantly, the desirability of developing such a material would be indicated.

CHAPTER II

THEORY OF HEAT TRANSMISSION

The second law of thermodynamics states that heat energy always flows in the direction of the negative temperature gradient, i.e., from a hot body to a cooler one.

There are three distinct methods by which this migration of heat takes place:

1. Conduction, in which the heat passes through the substance of the body itself.

2. Convection, in which heat is transferred by relative motion of portions of the heated body.

3. Radiation, in which heat is transferred directly between portions of the body by electromagnetic radiation.

Although the three kinds of heat transmission generally occur together, fortunately one or the other often prevails in practical cases. Therefore, separate laws governing each kind of heat transfer have been developed and may be used in such cases. Superposition of these laws is also often possible and used (7).

The basic law of heat conduction is,

$$\frac{Q}{A} = -k\frac{\Delta T}{\Delta L} \qquad \text{(II-1)}$$

In this and the next two equations, Q, denotes the time rate of heat flow, i.e., the heat energy flowing through a constant area, A, in unit time. The rate of heat flow, Q, may be considered constant for the time

being. Equation (II-1) relates to steady state transfer in a plane plate of thickness ΔL with a perfectly insulated edge: the two free surfaces being held at the temperature difference ΔT. The parameter, k, which may be considered a constant for the time being, is called thermal conductivity.

Equation (II-1) originates from Biot (8), but it is generally called Fourier's equation because Fourier (9) used it as a fundamental equation in his analytic theory of heat.

For heat convection the following equation was first recommended by Newton (10):

$$Q = HA\Delta T \qquad \text{(II-2)}$$

Equation (II-2) relates to the heat transfer between a surface and a fluid in contact with it, the temperature difference being ΔT. The factor H is called surface coefficient of heat transfer, film coefficient of heat transfer, or simply coefficient of heat transfer. This expression is often referred to as Newton's cooling law, but it is really a definition of H. This point will be discussed later in more detail.

For the total radiation, equations of the form

$$Q = \sigma A T^4 \qquad \text{(II-3)}$$

have been used since Stefan (11) found this relation and Boltzmann (12) proved it theoretically for a perfectly black surface. Equation (II-3) relates to the emission of radiation from a surface at the absolute temperature T. The factor σ is a natural constant known as the Stefan-Boltzmann constant, or the constant of total black-body

radiation. For surfaces not absolutely black, σ must be modified if the Stefan-Boltzmann law is to be applicable.

The basic equation of heat accumulation for small linear changes of temperature is

$$Q = \rho C_p V \frac{\Delta T}{\Delta t} \qquad \text{(II-4)}$$

where Q is the heat accumulation in unit time, in the volume, V, of a medium of density, ρ, and specific heat, C_p, when the temperature increases by ΔT in a time interval Δt.

From the above fundamental relations a great deal of knowledge has been developed. The application of mathematics permits the evaluation of heat transfer processes by different modes, in different geometrical shapes, and subject to varied initial and boundary specifications. Carslaw and Jaeger (13) have presented a very complete formal mathematical treatment of heat conduction problems. Jakob (7) considered all forms of heat transfer in his work, and provided theoretical or empirical solutions to a great variety of heat transfer problems. Maddox (14) presents a very complete treatment of the heat transfer problem from the practical design engineering point of view.

Specifically in the field of heat transfer by conduction, many physical situations can be described by relations which are amenable to solution by formal mathematical techniques. Other studies (15,16,17) have treated composite bodies, mostly the laminated wall having no interfacial resistance. However, Sinde (18) considered a composite system having resistance between layers.

In most of the formal mathematical solutions to heat conduction

problems the assumption of constant thermal and physical properties is usually made. Friedman (19), and Yang (28) have studied the effect of these assumptions and have shown that in some situations significant errors may result from their use. The solutions to most realistic problems involving conduction heat transfer usually involve infinite series of terms which may or may not converge rapidly. Therefore, it is sometimes quite difficult to obtain a numerical answer from the general mathematical solution.

In order to make the results of formal mathematical treatment more applicable to practical problems Gurney and Lurie (21), Kreisher (22), Olson and Schulte (23), Newman (24), and others (14,25,26,27) have presented graphs or charts showing temperature versus time or geometrical location for different parameters. Such parameters as thermal diffusivity, $\alpha = \frac{k}{\rho C_p}$, surface convection coefficients, and geometric shapes are usually employed. The geometrical shapes considered are limited to homogeneous infinite planes, infinite cylinders, spheres or objects of such shape that heat flow can be considered unidirectional.

It is generally conceded that formal mathematical methods are capable of solving only the simpler situations of geometry and boundary conditions in heat conduction problems. Many practical situations yield a mathematical model which can only be solved by approximation methods. Numerical, graphical and analog techniques are the most common tools for handling complex heat conduction problems. Although these methods are approximate, they can, in principle, be extended to any degree of

closeness of approach to the exact solution given by formal mathematical techniques. Their only limitation is the amount of effort (time and/or money) involved. In addition, as mentioned before, the formal mathematical solution also requires considerable effort if a precise numerical answer is desired owing to the usual infinite series form of the solution. Later, an example will be given of a problem where an approximate approach actually required less effort to yield an answer of a given accuracy than the effort required to evaluate the formal mathematical solution to the same degree of accuracy.

Graphical methods for solving heat conduction problems were first developed by Binder (28), and Schmidt (29) based on the calculus of finite differences. Many improvements and extensions of the basic method have been made (30,31). The work of Longwell (32) is of particular significance to this investigation because it treats graphically the motion of the freezing boundary in the heat transfer process involving the phase change from liquid to solid. This is probably the mechanism by which the electrochemical cells become inoperative. In general it can be stated that graphical methods are useful only when low accuracy is sufficient in the solution of a problem. If a high degree of accuracy in the solution is attempted, this procedure becomes prohibitively cumbersome.

It has been known for many years that different physical phenomena can be described by the same mathematical relations, in such cases they are said to be analogous processes. Langmuir, Adams and Meikle (33) seem to have been the first to make use of the analogy between

thermal and electrical conduction; they solved a problem based on the similarity between a flow-temperature field and an electrical flow-voltage field of the same geometrical configuration.

Zoukas (34), and Paschkis (35) developed large-scale, permanent analog devices whose principal elements were resistors and condensers, and they were able to solve unsteady-state heat transfer problems. The chief drawback of these analog devices is that they are expensive to construct, and are usually capable of simulating only the type of system for which they were specifically designed. Even relatively minor modifications of the original system can be cumbersome and expensive.

The type of analog devices discussed above depend for their operation upon the existence of a direct physical analogy between the analog and the prototype system under study. Such an analogy is recognized by comparing the characteristic equations describing the dynamic or static behavior of the two systems. An analogy is said to exist if these characteristic equations are identical in form, and the initial and boundary conditions are the same. Such a similarity is possible only if there is a one-to-one correspondence between elements in the analog and in the prototype system. For every element in the original system there must be present in the analog system an element having similar properties, i.e., an element having a similar excitation-response relationship, furthermore, the elements in the analog must be interconnected in the same fashion as the elements in the original system.

The other major class of analog system includes mathematical rather than physical analogs. The behavior of the system under study,

or the problem to be solved is first expressed as a set of algebraic or differential equations. An assemblage of computing units or elements each capable of performing some specific mathematical operation, such as addition, multiplication or integration, is provided, and these units are interconnected so as to generate the solution of the problem (36).

The availability in recent years of high-speed digital computers has augmented the interest in numerical methods based on the calculus of finite differences as an efficient tool for the solution of complex heat flow problems. Emmons (37) utilized the relaxation method developed by Southwell (38) for the solution of two and three-dimensional steady state heat transfer processes. Although the relaxation technique can be used for unsteady-state problems (39), explicit time iteration procedures, such as the one developed by Dusinberre (40), are generally preferred to relaxation methods because they can be adapted more readily to digital computation.

The explicit finite-differences technique has in general the limitation that it is difficult to evaluate the accuracy of the solution. If the criteria of "stability" and "convergence" are satisfied, the accuracy is determined by the number of increments used, and it can be improved at the expense of increased effort (41). The convergence criterion is the requirement that the exact solution be approached by the approximate solution as the number of increments approaches infinity. The stability criterion seems that the error introduced into the computation, owing to the limited number of digits which a given

computer can carry, must not increase in magnitude as the computation proceeds. These criteria have been studied by a number of investigators (41,42,43). Therefore, for a numerical method which is stable and convergent when applied to a system of equations, the finite-difference technique can yield any degree of accuracy desired. The only restriction is the amount of effort required.

Brian (44) and Douglas (45) developed implicit difference methods which are unconditionally stable, usually at the expense of increased computational effort. Yaversky, et al. (46) utilized the explicit type finite-difference formulation, and solved on a digital computer the problem of heating homogeneous cylindrical briquettes. Dickert (47) used the explicit finite-difference approach for the solution on an IBM 650 digital computer of the unsteady-state heat transfer in a composite finite cylinder. Actually the physical model he simulated was a simplified version of the thermal batteries which are the subject of this study.

Horne and Richardson (48) developed a model to simulate the performance of batteries at low ambient temperatures. It was programmed on a digital computer and it was based on well-mixed sections with lumped thermal resistance at the interfaces.

In this investigation, two different mathematical models were developed and solved on an analog computer in order to benefit from the advantageous features of the instrument, such as the essentially instantaneous availability of the answer, the continuous display of the results (usually in an oscilloscope or a plotter), and the immediate

response of the system to a change in one of the parameters. All of these features made the analog computer the initial choice in this study. Later, after sufficient insight had been gained from the analog studies and when increased accuracy was desired, a model was developed to be programmed on the digital computer. The results revealed very interesting aspects of heat transfer phenomena, and provided a good simulation of thermal batteries.

A. Geometrical Considerations in Battery Life Optimization

Some conclusions can be drawn from purely geometrical considerations with respect to the optimum shape of a thermal battery under the criterion of maximum life. Since the rate of heat transfer is directly proportional to the area and the rate of temperature change is inversely proportional to the volume, it is clear that the smaller the area of a body, the lower the rate at which it will loose heat, all other things being equal. Therefore, a hot body of a given volume will remain hot longer, the smaller its area.

If, for the moment, the geometrical shape of the battery is restricted to right circular cylinders, elementary mathematical considerations show that for a cylinder having radius R and height h, the total area is given by

$$A = 2\pi R^2 + 2\pi Rh \qquad \text{(II-5)}$$

while the volume is given by

$$V = \pi R^2 h \qquad \text{(II-6)}$$

If the volume is considered to be fixed, the area can be expressed by

$$A = 2\pi R^2 + 2\pi R \frac{V}{\pi R^2} \qquad \text{(II-7)}$$

which can be differentiated with respect to R and equated to zero to give

$$\frac{dA}{dR} = 4\pi R - \frac{2V}{R^2} = 0 \qquad \text{(II-8)}$$

Equation (II-8) may be solved for the volume to obtain

$$V = 2\pi R^3 \qquad \text{(II-9)}$$

This would be the value of the volume corresponding to a minimum area, but

$$V = \pi R^2 h \qquad \text{(II-10)}$$

hence

$$h = 2R \qquad \text{(II-11)}$$

Equation (II-11) makes clear that the right circular cylinder having the minimum area per unit volume is one having its height equal to its diameter

Similarly it can be shown that for the case of orthogonal parallelepipeds the volume is given by

$$V = xyz \qquad \text{(II-12)}$$

while the area is given by

$$A = 2xy + 2xz + 2yz \qquad \text{(II-13)}$$

If the volume is considered to be fixed the area can be expressed as

$$A = 2xy + \frac{2xV}{xy} + \frac{2yV}{xy} \qquad \text{(II-14)}$$

which can be differentiated partially with respect to x and y to give

$$\frac{\partial A}{\partial x} = 2x - \frac{2V}{x^2} = 0 \qquad \text{(II-15)}$$

$$\frac{\partial A}{\partial y} = 2y - \frac{2V}{y^2} = 0 \qquad \text{(II-16)}$$

These equations may be solved for x and y, respectively, to give

$$x = V^{1/3} \qquad \text{and} \qquad y = V^{1/3} \qquad \text{(II-17)}$$

which results in a value of $x = V^{1/3}$ when substituted into equation (II-12). Hence the orthogonal parallelepiped whose outside area is a minimum for a given total volume is the cube.

Forsyth (48) has shown by the calculus of variations that the sphere is the solid generated by rotation which has the maximum volume for a given area. The sphere is likewise the solid having the maximum volume for a given area out of all possible solids, but this is more difficult to demonstrate rigorously. It can be shown specifically that the sphere has a lower ratio of area to volume for a given volume than the cylinder having equal height and diameter which in turn has a lower ratio than the cube. For a volume of V the radius of the sphere is given by

$$R_s = \left(\frac{3}{4\pi} V\right)^{1/3} \qquad \text{(II-18)}$$

and the area is given by

$$A_s = 4\pi \left(\frac{3V}{4\pi}\right)^{1/3} \qquad \text{(II-19)}$$

For the cylinder, the radius is given by

$$R_c = \left(\frac{1}{\pi} V\right)^{1/3} \qquad \text{(II-20)}$$

and the area

$$A_c = 4\pi \left(\frac{V}{\pi}\right)^{2/3} \qquad \text{(II-21)}$$

Hence, for the same volume V, the ratio of the area of the sphere to the

area of the cylinder is

$$\frac{A_s}{A_c} = \left(\frac{3}{4}\right)^{2/3} = 0.825 \qquad \text{(II-22)}$$

For a cube the side i is given by

$$i = V^{1/3} \qquad \text{(II-23)}$$

and the area

$$A_{cu} = 6V^{2/3} \qquad \text{(II-24)}$$

Therefore, the ratio of the area of the sphere to the area of the cube is

$$\frac{A_s}{A_{cu}} = \frac{4\pi}{6}\left(\frac{3}{4\pi}\right)^{2/3} = 0.804 \qquad \text{(II-25)}$$

These considerations indicate that, if it were feasible to construct thermal batteries in a spherical shape, this would be the optimum configuration from the heat transfer standpoint. There are other restrictions which make this shape impractical, hence the next most efficient shape is that of a right circular cylinder having its diameter equal to its height.

Figure 2 illustrates the temperature histories at the center point of different homogeneous right circular cylinders having equal volumes and different height to diameter ratios, and having initial temperatures of 500°C everywhere except at the surface where the temperature is assumed to be constant at zero degrees. These curves were evaluated from tables presented by Olson and Schulze (23). The parameter shown on the curves is the height to diameter ratio. The volume of all cylinders is that of the cylinder having a height of 3.0 cm (equal to its

diameter). A temperature history for the center point of a sphere having the same volume is also shown. For right circular cylinders of constant volume, Figure 2 indicates that the rate of cooling increases drastically when the height to diameter ratio is made less than the optimum. The rate of cooling also increases when the height to diameter ratio is made greater than the optimum but the effect is less than in the former case.

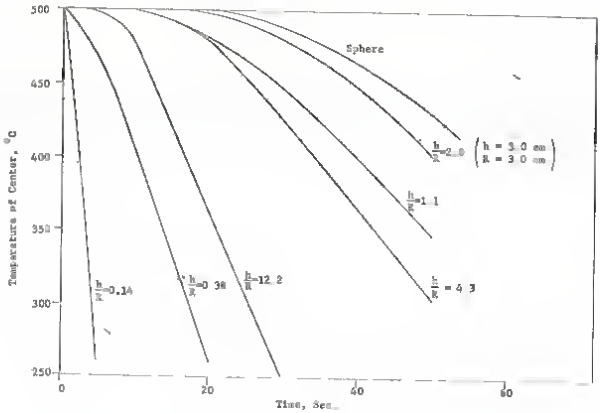

Figure 2 Temperature Histories in Homogeneous Right Circular Cylinders

CHAPTER III

ANALOG COMPUTER MODEL I

A. Description of the Model

The first model developed to simulate a thermal battery consisted of a cylindrical stack of alternating heat generators and cells surrounded by insulation. While the actual number of generators and cells in a real thermal battery may vary, it was assumed that the core was composed of three cylindrical generators and two cells surrounded by top, bottom and lateral insulation. A schematic diagram of the model is shown in Figure 3.

Consideration of the physical dimensions of the elements in the battery led to some assumptions. The very small relative thickness of the elements compared to other dimensions, such as diameter of the cells, heat generators and top insulation, and height for the lateral insulation, suggests that the major portion of the heat transfer is no axial, rather than a radial, process. This suggests that the temperature within each element would be rather uniform, hence it was assumed that each element was "well-stirred", i.e., that its temperature was uniform throughout. This assumption is more valid for some elements than for others. For example, the cells consist (during the operating life of the battery) of molten electrolyte, and since intra-cell chemical and electrochemical reactions may be occurring simultaneously, it appears that the mobility of the ions in the electrolyte provides a relatively

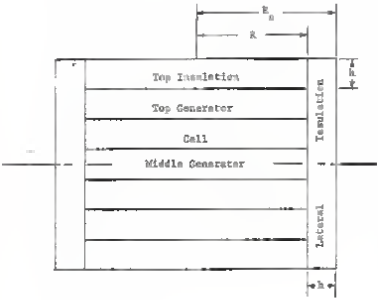

Figure 3 Schematic Diagram of Battery Described by Model I

well-mixed element having an approximately constant temperature. There also exists the possibility that some convection currents might be established, but this is doubtful owing to the small thickness of the cell. The deviation of the heat generators and insulation from this assumption would be of the same order of magnitude because their thermal properties are comparable.

The cylindrical symmetry of the model makes necessary the consideration of only the top half of the unit.

The heat generators achieve their maximum temperature of about 2200°C (47) in a length of time which is negligible compared to the rest of the heat transfer process. Therefore, it was assumed that they reached their maximum temperature instantaneously, and this high temperature becomes the initial driving force of the heat transfer system.

There is a heat of reaction from latte-cell chemical reactions. The experimental data describing this phenomenon are very uncertain. It is known that the heat of reaction increases rapidly at the beginning of the operation, reaches a maximum, and then decays. A triangular shape was assumed for the heat of reaction-time relationship. Both the shape and magnitude of this effect were based on educated guesses of experienced investigators (50), and it is the only factor in this study not based on experimental or computed physical data.

3. Heat Transfer Coefficients

The chief consequence of the assumption of well-mixed elements in the battery is that the heat transfer process which occurs under these conditions becomes one of convection rather than conduction. Because

there can be no temperature gradient through any single element, all of the resistance to heat transfer appears 'lumped' at the interfaces between elements. Therefore, a pseudo-heat transfer coefficient must be calculated by appropriately lumping the heat transfer resistances of two adjacent elements at the interface between them (based, of course, on their thermal conductivities and the mean path traveled by the heat).

The pseudo-heat transfer coefficients were evaluated by considering the two elements to constitute a series arrangement for the resistance to heat flow. For the case of a cell and a heat generator, the coefficient had the following form.

$$\text{Total Resistance} = \text{Resistance of Cell} + \text{Resistance of Generator} \qquad \text{(III-1)}$$

$$\frac{1}{H_{g-c}} = \frac{1}{k_c}\left(\frac{h_c}{2}\right) + \frac{1}{k_g}\left(\frac{h_{tg}}{2}\right) \qquad \text{(III-2)}$$

$$H_{g-c} = \frac{1}{\frac{1}{k_c}\left(\frac{h_c}{2}\right) + \frac{1}{k_g}\left(\frac{h_{tg}}{2}\right)} \qquad \text{(III-3)}$$

where H_{g-c} is the heat transfer coefficient between the heat generator and the cell, and k and h are the thermal conductivities and heights, respectively. The heat transfer coefficients involving the lateral insulation were obtained by calculating the radius equivalent to one-half the volume of the interior element, and considering the mean distance the distance from this radius to the outer radius of the element. The mean distance in the case of the lateral insulation is, of course, one-half of the thickness. Therefore, for a value of the radius of the

element of 1.56, the following heat transfer coefficient was obtained

$$H_{g-1i} = \frac{1}{\frac{1}{k_1}\left(\frac{h_{1i}}{2}\right) + \frac{1}{k_g}(.46)} \qquad \text{(III-4)}$$

All other heat transfer coefficients were computed in a manner similar to those discussed above.

Because of the high initial temperature of the heat generators, radiation rather than convection or conduction is the principal mechanism of heat transfer while the generators are incandescent. A pseudo-convection heat transfer coefficient was calculated for this period based on the laws of radiation. It was arbitrarily decided that 750°C was the temperature where the principal mechanism changed from radiation to "convection". The heat transfer coefficient describing the radiation transfer can be obtained as follows (51):

$$q = A_1 F_{12} \sigma (T_1^4 - T_2^4) \qquad \text{(III-5)}$$

where q is the rate of heat transfer, and A is the area of the heat transfer surface. F is a dimensionless factor to allow for interchange between gray surfaces; σ is the Stefan-Boltzmann constant (4.92×10^{-8} kgcal/m^{2}hr °K^4), and T is the temperature in degrees Kelvin.

$$F_{12} = \frac{1}{\frac{1}{\bar{F}_{12}} + \left(\frac{1}{\epsilon_1} - 1\right) + \frac{A_1}{A_2}\left(\frac{1}{\epsilon_2} - 1\right)} \qquad \text{(III-6)}$$

where $\bar{F}$ is a dimensionless geometrical factor to allow for net radiation between black surfaces including the effect of refractory surfaces, and

ϵ is the dimensionless emissivity

The equivalent heat transfer coefficient is obtained from

$$H_{R-c-E} = \frac{F_{12}\sigma(T_1^4 - T_2^4)}{\Delta T} + H_{E-a} \qquad \text{(III-7)}$$

where T_1 is evaluated as the arithmetic average of the fourth powers of the extreme values of the heat generator temperature during the radiation period and T_2, the cell temperature was evaluated similarly. ΔT was taken as the geometric mean of the extreme values of the temperature differences (52). Detailed computations of all these coefficients are shown in Appendix A

C Development of the Mathematical Model

A differential heat balance around each element (i.e. cell, generator, etc) gives the equations shown in Table 1 with notation having the significance indicated below

H = pseudo-convection heat transfer coefficient, $\frac{cal}{cm^2\,sec\,^\circ C}$

h = height of element, cm(See Figure 3)

R = radius of element, cm(See Figure 3)

R_a = outside radius of assembly, cm(See Figure 3)

T = temperature of element, $^\circ C$

t = time, sec

Subscripts

a = refers to the ambient

c = refers to the cell

g = refers to the generator

TABLE 1

DIFFERENTIAL DIFFERENCE EQUATIONS FOR MATHEMATICAL MODEL 1

Top Insulation

$$-\pi R^2 H_{ti-g}(T_{ti} - T_a) - 2\pi R h_{ti} H_{ti-li}(T_{ti} - T_{li}) - \pi R^2 H_{ti-g}(T_{ti} - T_{tg}) = \rho_i C_{pi} \pi R^2 h_{ti} \frac{dT_{ti}}{dt} \quad \text{(III-8)}$$

Initial Condition For Equation III-8 at $t = 0$ $T_{ti} = T_a$ (III-9)

Top Generator

$$-\pi R^2 H_{ti-g}(T_{tg} - T_{ti}) - 2\pi R h_{tg} H_{g-li}(T_{tg} - T_{li}) - \pi R^2 H_{g-c}(T_{tg} - T_a) = \rho_g C_{pg} \pi R^2 h_{tg} \frac{dT_{tg}}{dt} \quad \text{(III-10)}$$

Initial Condition For Equation III-10 at $t = 0$ $T_{tg} = 2200^\circ C$ (III-11)

Cell

$$-\pi R^2 H_{g-c}(T_a - T_{tg}) - 2\pi R h_c H_{c-li}(T_a - T_{li}) - \pi R^2 H_{g-c}(T_{mg} - T_c) = \rho_a C_{pa} \pi R^2 h_c \frac{dT_c}{dt} \quad \text{(III-12)}$$

Initial Condition For Equation III-12 at $t = 0$ $T_c = T_a$ (III-13)

Middle Generator

$$-\pi R^2 H_{g-c}(T_{mg} - T_a) - 2\pi R h_{\frac{tg}{2}} H_{g-li}(T_{mg} - T_{li}) = \rho_g C_{pg} \pi R^2 h_{\frac{tg}{2}} \frac{dT_{mg}}{dt} \quad \text{(III-14)}$$

Initial Condition For Equation III-14 at $t = 0$ $T_{mg} = 2200^\circ C$ (III-15)

TABLE 1 (Continued)

Lateral Insulation

$$-2\pi R h_{ti} H_{ti-1i}(T_{1i} - T_{ti}) - 2\pi R h_{tg} H_{g-1i}(T_{1i} - T_{tg}) - 2\pi R h_{c} H_{c-1i}(T_{1i} - T_{c}) - 2\pi R h_{\frac{tg}{2}} H_{g-1i}(T_{1i} - T_{mg})$$

$$-2\pi R_{s}(h_{ti} + h_{tg} + h_{c} + h_{\frac{tg}{2}}) H_{1i-s}(T_{1i} - T_{s}) = \rho_{i} C_{pi} 2\pi(R_{s} - R)(h_{ti} + h_{tg} + h_{c} + h_{\frac{tg}{2}}) \frac{dT_{1i}}{dt} \qquad \text{(III-16)}$$

Initial Condition For Equation III-16 at $t = 0$ $T_{1i} = T_{s}$ (III-17)

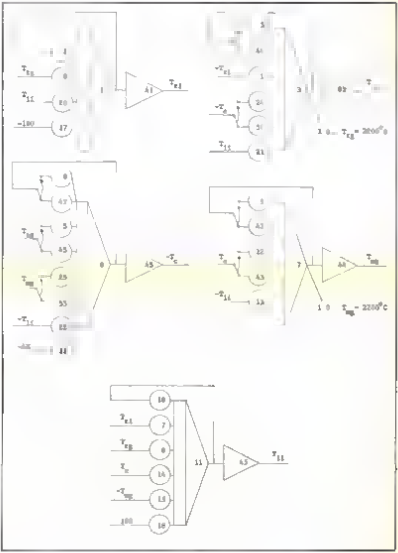

Figure 4

Analog Computer Diagram of Model 1

Subscripts continued

i = refers to the insulation

l = refers to lateral

m = refers to middle i.e. mg refers to middle generators

R = refers to radiation (See equation III-7)

t = refers to top i.e. ti refers to the top insulation

Example

H_{ti-li} refers to the heat transfer coefficient between the top insulation and the lateral insulation.

B Analog Computer Solution

The preceding equations in Table 1 can each be solved for the derivative of temperature with respect to time, and they constitute a system of ordinary first-order linear differential equations which is readily amenable to solution with the aid of an analog computer. The EASE 1032 Analog Computer of the Chemical Engineering Department at the University of Florida was utilized in this investigation.

The basic element of the analog computer is the electronic amplifier which can serve as an integrator or a summer depending on whether a capacitor or a resistor is connected across the amplifier. Many references discuss in detail the theory and operation of analog computers (36,53). The equations describing the model, were programmed on the analog computer, and the analog computer circuit is shown in Figure 4. Table 2 illustrates the algebraic form of the relations between the parameters which contribute to each potentiometer setting

TABLE 2

COEFFICIENTS FOR PROGRAMMED DIFFERENTIAL DIFFERENCE EQUATIONS: MODEL I

Par. No.	Mathematical Expression	Par. Setting
1	$\frac{1}{\rho_i C_{pi} h_{ti}}\left[S_{ti-a} + \frac{2h_{ti}}{R} S_{ti-1i} + S_{ti-g}\right]$	0.663
2	$\frac{S_{ti-g}}{\rho_g C_{pg} h_{tg}}$	0.123
3	$\frac{1}{\rho_g C_{pg} h_{tg}}\left[S_{ti-g} + \frac{2h_{tg}}{R} S_{g-1i} + S_{g-c}\right]$	0.744
4	$\frac{S_{ti-a}}{\rho_i C_{pi} h_{ti}}$	0.286
5	$\frac{S_{g-c}}{\rho_c C_{pc} h_c}$	0.143
6	$\frac{h_{tg} S_{g-1i}}{\rho_i C_{pi}\left(\frac{R}{S} - 1\right)(h_{ti} + 3/2\, h_{tg} + h_a)}$	0.042
7	$\frac{h_{ti} S_{ti-1i}}{\rho_i C_{pi}\left(\frac{R}{S} - 1\right)(h_{ti} + 3/2\, h_{tg} + h_c)}$	0.0319
8	$\frac{1}{\rho_c C_{pc} h_c}\left[S_{g-c} + \frac{2h_c}{R} S_{c-1i} + S_{g-c}\right]$	0.2987
9	$\frac{2}{\rho_g C_{pg} h_{tg}}\left[S_{g-c} + \frac{h_{tg}}{S} S_{g-1i}\right]$	0.126
11	$\frac{\Delta R\, h_c}{100}$	0.0035
12	$\frac{2S}{\rho_g C_{pg} h_{tg}}$	0.123

TABLE 2 (Continued)

Pot. No.	Mathematical Expression	Pot Setting
14	$\dfrac{h_c F_{g-ii}}{\rho_i C_{pi}(\frac{R_g}{R} - 1)(h_{ti} + 3/2\ h_{tg} + h_c)}$	0 1395
15	$\dfrac{(h_{tg}/2)H_{g-ii}}{\rho_i C_{pi}(\frac{R_g}{R} - 1)(h_{ti} + 3/2\ h_{tg} + h_c)}$	0.021
17	$\dfrac{H_{ti-a}T_a}{\rho_i C_{pi} h_{ti}}$	0 0037
18	$\dfrac{R_c/R(H_{ii-a}T_a)}{100\rho_i C_{pi}(\frac{R_g}{R} - 1)}$	0 0063
19	$\dfrac{H_{c-ii}h_c + 3/2\ H_{g-ii}h_{tg} + H_{ti-ii}h_{ti}}{\rho_i C_{pi}(\frac{R_g}{R} - 1)(h_{ti} + 3/2\ h_{tg} + h_c)}$	
	$+ \dfrac{R_c/R(h_{ti} + 3/2\ h_{tg} + h_c)H_{ii-a}}{\rho_i C_{pi}(\frac{R_g}{R} - 1)(h_{ti} + 3/2\ h_{tg} + h_c)}$	0 8644
20	$\dfrac{2H_{ti-ii}}{K\rho_i C_{pi}}$	0.0107
21	$\dfrac{2H_{g-ii}}{K\rho_g C_{pg}}$	0 086
22	$\dfrac{2H_{c-ii}}{K\rho_c C_{pc}}$	0 0048

TABLE 2 (Continued)

Pot No	Mathematical Expression	Pot Setting
23	$\frac{S_{g-1i}}{R\rho_g C_{pg}}$	0 003
24	$\frac{R_{g-c}}{\rho_g C_{pg} h_{ck}}$	0 615
25	$\frac{H_{g-c}}{\rho_c C_{pc} h_c}$	0 143
31	Time Scale	0 050
32	Initial Rate of Heat Generation	0 050
34	Decay Rate of Heat Generation	0 0271
42	$\frac{2}{\rho_g C_{pg} h_{cg}} \left[H_{g-c-R} + \frac{h_{cg}}{R} H_{g-1i} \right]$	0 615
43	$\frac{2H_{g-c-R}}{\rho_g C_{pg} h_{cg}}$	0 615
44	$\frac{1}{\rho_g C_{pg} h_g} \left[H_{ti-g} + \frac{2h_{cg}}{g} R_{g-1i} + H_{g-c-g} \right]$	0 321
45	$\frac{R_{g-c-R}}{\rho_g C_{pc} h_c}$	0 715
49	$\frac{1}{\rho_c C_{pc} h_c} \left[H_{g-c-R} + \frac{2h_g}{R} R_{g-1i} + H_{g-c-R} \right]$	0 143
50	$\frac{S_{g-c-R}}{\rho_g C_{pg} h_{cg}}$	0 306
53	$\frac{H_{g-c-R}}{\rho_c C_{pc} h_c}$	0 715

These factors are, of course, a direct consequence of the form of the system of differential equations.

Table 3 lists the values of the physical parameters for all the materials which constitute the "standard" battery being simulated. These are the values used in obtaining the numbers shown in Table 2 for each potentiometer setting in the simulation of the standard battery. In other words, the values of some of these parameters were changed judiciously to investigate their effect on the performance of the battery.

It has been pointed out earlier that a set of switches was arranged to automatically change the value of the heat transfer coefficient to account for radiation heat transfer at the heat generator-cell interfaces when the heat generator temperature is above 750°C. This temperature was chosen for the change from radiation to convection heat transfer because it seemed reasonable and it gave good agreement with the known activation times of certain thermal batteries. Moreover, it led to realistic cell peak temperatures.

The representation of the intra-cell heat generation by a triangular heat of reaction term also required a number of switches to provide an appropriate simulation on the analog computer. The details of these switching arrangements are shown in Appendix A.

Also a manual switch was installed which permitted the inclusion or exclusion of the heat of reaction due to the electrochemical process in the cells.

TABLE 3

AVERAGE PHYSICAL PROPERTIES AND DIMENSIONS
OF THERMAL BATTERY COMPONENTS: MODEL I

Insulation

ρ, g/cc = 0.193

C_p, $\frac{cal}{g\ ^oC}$ = 0.232

k, $\frac{cal\ cm}{g\ ^oC\ cm^2}$ = 0.0002

h, cm = 0.136

K, cm = 1.56

K_s, cm = 1.72

Generator

ρ, g/cc = 1.25

C_p, $\frac{cal}{g\ ^oC}$ = 0.130

k, $\frac{cal\ cm}{g\ ^oC\ sq\ cm.}$ = 0.0005

h, cm = 0.10

K, cm = 1.56

Cell

ρ, g/cc = 3.48

C_p, $\frac{cal}{g\ ^oC}$ = 0.201

TABLE 3 (Continued)

Cell continued

$$k, \frac{\text{cal cm.}}{\text{g}^{\circ}\text{C sq. cm.}} = 0.10$$

$$h, \text{cm} = 0.10$$

$$R, \text{cm.} = 1.56$$

E Discussion of Results

The great flexibility of the analog computer permitted the investigation of a wide range of parameters and geometrical arrangements which might affect the life of a thermal battery. A summary of the more important results is given in Table 4 and they are discussed below.

The model treated in this work has several limitations and some caution should be exercised in attributing too much significance to small effects. On the other hand, large effects are probably correct and qualitative conclusions based on them should be sound. Probably the most serious limitation of this model is that it is not based on conduction but on pseudo-convection heat transfer coefficients. Temperature gradients within an element are thus precluded, and this is known to be incorrect. However, the temperature gradients within an element do not appear to be large (except perhaps for the first few seconds in the heat generators), and the model appears to simulate the temperature histories of elements in an actual battery rather well (see Figure 5).

It should be noted also that the complexity of the physical models which can be studied on an analog computer is limited by the capacity of the computer, and the time required to obtain meaningful results is greatly increased when the model is made more complex because there are more components and all of them (amplifiers, potentiometers, capacitors, etc.) must perform satisfactorily for the results to be valid. The problem which was here programmed on the

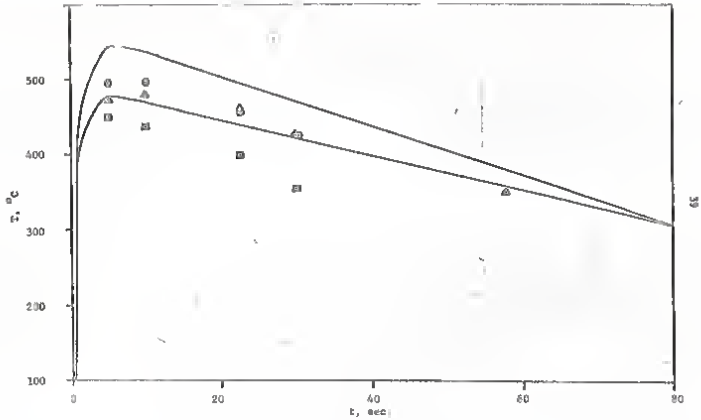

Figure 5 Experimental Versus Computed Results

TABLE 4

EFFECT OF PARAMETERS AND CHANGES ON THE LIFE TO 400°C OF A SIMULATED THERMAL BATTERY

	Heat Sink Temperature				
	-65°F	25°C	160°F	160°Life / -65°Life	25°Life / 25°Std
	Sec.	Sec.	Sec.	Sec	Dimensionless
A. Insulation					
1. Thermal Conductivity					
0.0001	64	87	97	1.52	1.61
0.0002 (Std)	25	48	60	2.40	1.00
0.0003	18.5	32.5	41	2.21	0.66
2. Thickness					
2X*	40	54	65	1.62	1.12
B. Heat Generators					
1. Thickness					
2X		48			1.00
2. Enthalpy					
$\rho = 2X$, $h = 1/2$ X		75			1.57
C Electrochemical Cells					
1. Thickness					
1.2X		54			1.12
1.5X		66 (4 sec actv)			1.38
2X		100 (17 Sec actv)			2.08

* X = times standard value of parameter being varied

TABLE 4 (Continued)

	Heat Sink Temperature				
	-65°F	25°C	160°F	160°Life / -65°Life	25°Life / 25°Std
	Sec.	Sec.	Sec.	Sec	Dimensionless
C Electrochemical Cells (Continued)					
2. Enthalpy (ρC_p)					
1.2X*		38			0.79
0.8X		35			0.73
E Intra-Cell Heat Generation					
1. Level					
Same		30			0.63
Std		48			1.00
1.5X		60			1.25
3X		100			2.08
2. Rise Rate					
0.5X		45			0.94
Std		48			1.00
2X		48			1.00
3. Decay Rate					
0.5X		52			1.08
Std.		48			1.00
1.5X		44			0.92

* X = times standard value of parameter being varied

EASE 1032 Analog Computer represented essentially the limit of the capabilities of the instrument.

1. Temperature Histories in a Standard Simulated Battery

The temperature histories of five elements in the standard simulated thermal battery are shown in Figure 6. These elements are (1) top heat generator, (2) center heat generator, (3) cell, (4) top insulation, (5) lateral insulation.

From Figure 6 it can be seen that both of the heat generators release their heat rapidly to the cell and the top insulation. Within five seconds after activation the temperature of the heat generators is below the cell temperature, but the center heat generator is only slightly cooler than the cell. Thus, it can be said that the cell is heating the generators after the first few seconds.

The cell is shown to reach a temperature of 400°C in less than 0.5 seconds, but little importance should be attached to this because the response of the recorder was not particularly good for times of less than one second. Figure 6 indicates that the cell reaches a peak temperature of about 550°C in approximately five seconds which is in good agreement with experience. All of the curves in Figure 6 are in reasonably good agreement with what one would expect for a heat transfer system of the type under consideration.

2. Effect of Heat Sink Temperature on Cell Temperatures

As one might expect, the temperature history of a cell is strongly dependent on the heat sink temperature. The data summarized in Table 4 indicate that the cell life above 400°C is approximately twice

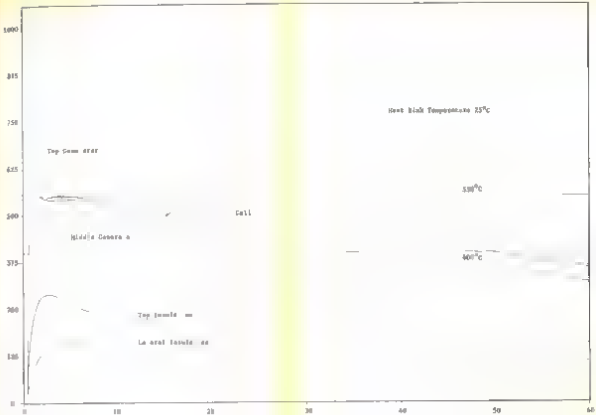

Figure 4 Temperature Histories in Standard Simple Thermal Layer

as great when the heat sink temperature is +160°F instead of -65°F. Room temperature results are intermediate. Figure 7 illustrates the temperature histories for a standard cell at the three heat sink temperatures.

3 Effect of Insulation Parameters on Cell Temperatures

Thermoflex insulation has a thermal conductivity of about 0.0002 cal / cm g^{-1} $°C^{-1}$ cm^{-2}, and this has been adopted as the standard insulation type. The thermal conductivity of asbestos is around 0.0003. In order to assess the effect of a large improvement in insulation properties, one run was made with a hypothetical insulation having a thermal conductivity of 0.0001. These results are tabulated in Table 4, and it may readily be seen that thermal conductivity of the insulation is an important factor in the life of the cell. A comparison of the life above 400°C at a 25°C heat sink temperature shows that a ±50% variation in life might be expected with the sort of variation in thermal conductivity studied. Figures 8 and 9 show the curves for cell temperatures at these conditions.

Table 4 also shows that doubling the insulation thickness (for Thermoflex) results in relatively little increase in life except at a heat sink temperature of -65°F. Where life is now minimal at low heat sink temperatures, increasing the insulation thickness would appear to be a quite promising means of increasing cell life. These curves are shown in Figure 10.

4 Variation of Heat Generator Parameters

Two heat generator parameters were studied: (1) a variation in

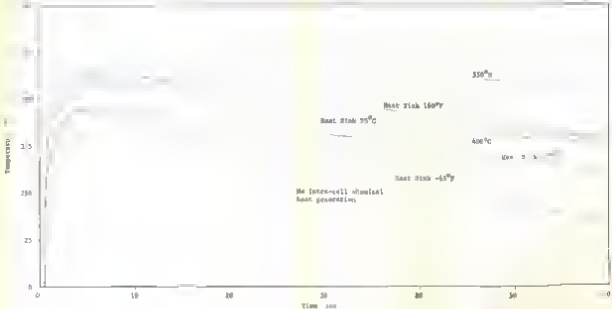

Figure 7 Effect on Cell Temperature of Changing the Temperature of the Heat Sink

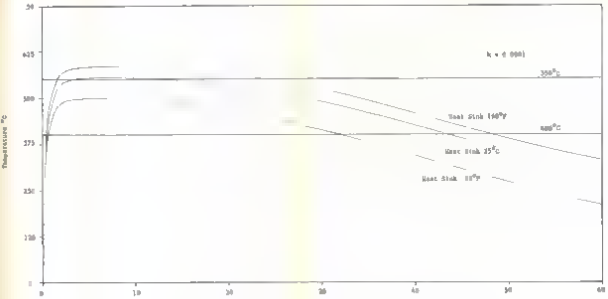

Figure 8 Effect on Cell Temperature of Reducing the Thermal Conductivity of the Insulation

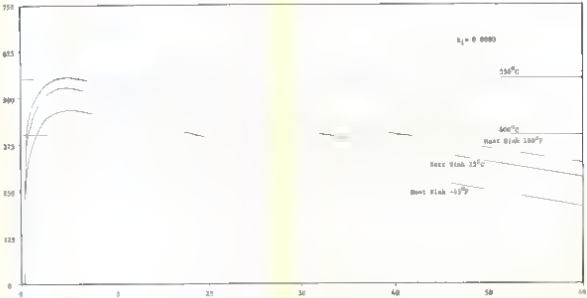

Figure 8 Effect on Cell Temperature of Increasing the Thermal Conductivity of the Insulation

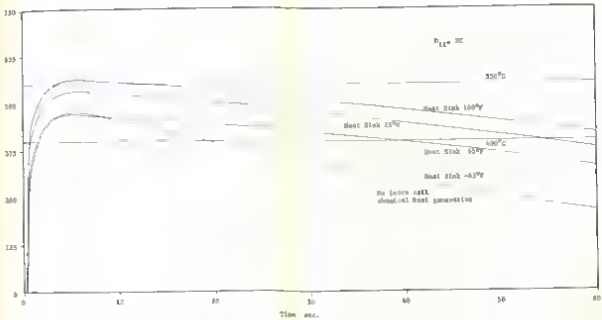

Figure 13 Effect on Cell Temperature of Changing the Thickness of the Insulation

the thickness of the heat generators, and (2) a variation in their enthalpy.

The effect of doubling the thickness of the heat generators is illustrated in Figure 11. The net effect on cell life appears to be quite small. Although doubling the thickness of the heat generator increases the heat available for the cells, the consequent increase in the size of the core requires the same cell to heat a larger volume which more than offsets the gain in heat. It should be recalled that the cells serve as the heat sources after the first few seconds (see Figure 6). Thus there is a slightly higher peak temperature, arrived at later than in the standard arrangement because of the longer heat path in the generator, but the cell cools more rapidly than the standard since cooling starts because the area of the core is larger and thus heat losses are greater. The net effect of the change is essentially zero as far as the cell life above 400°C is concerned.

If the standard heat generator is compressed the heat generation per unit volume of generator increases. In Figure 12 the effect of compressing the heat generator to one-half of its original thickness is portrayed. It may readily be seen that the peak temperature and rise time of the cell are not greatly affected. However, the rate of heat loss of the cell is greatly reduced as compared to the standard arrangement - owing primarily to the reduction in core area - and so increase in cell life over 400°C of about 80% is observed.

5. Variation of Cell Parameters

Three cell parameters were varied: (1) cell thickness, (2) cell

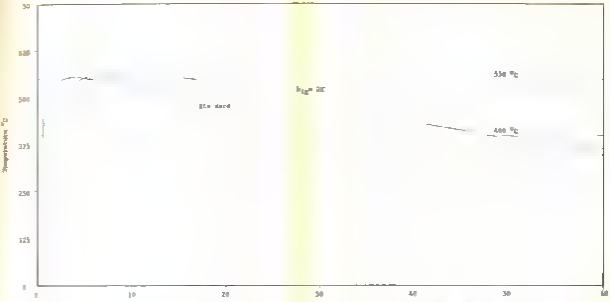

Figure 11 Effect on Cell Temperature of Changing Thickness of Mass Generation

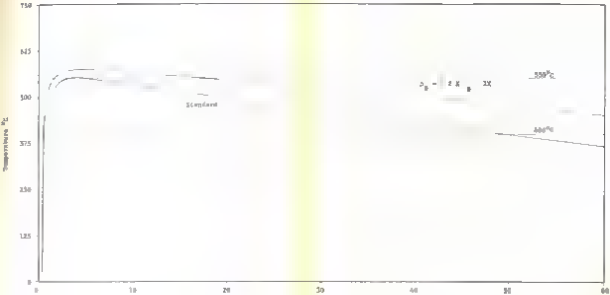

Figure 3 Effect on Cell Temperature of Compressing Heat Generation

enthalpy, and (3) intra-cell chemical heat generation. The third of these parameters is treated in a separate subsection because several factors involved were studied.

Assuming that the standard components of a cell are used regardless of thickness, it is obvious that the enthalpy of a cell is proportional to its thickness. One may also observe that the heat transfer paths are also lengthened for both heating and cooling, and one would expect a thick cell to both heat and cool more slowly than a standard one. The effect of varying cell thickness is illustrated in Figure 13, and one does, indeed, observe these effects. Since the heat input is constant (except for the intra-cell chemical heat generation built in), the peak temperatures decrease as the cell thickness increases, however, the intra-cell heat generation begins to contribute more heavily as cell thickness increases and when the thickness is increased by 50% the peak temperature is actually determined by the intra-cell heat generation. Thus the peak temperatures are reached a fairly long time after activation in these cases.

The activation times of thick cells are also increased, and become prohibitive for very thick cells. It appears that a thickness increase of no more than 50% can be tolerated unless activation times of more than 20 seconds are permissible, or unless other geometric arrangements are used.

It is possible in principle to add to the cell materials which can change its enthalpy. For example, a material having a transition in the temperature range of interest might be added. It is obvious that

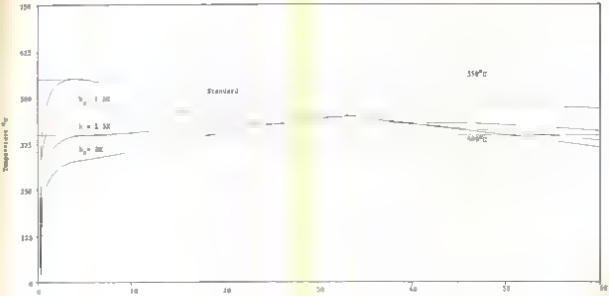

Figure 13 Effect on Grill Temperature of Changing the Th chance of the Ca...

the heat of fusion of the electrolyte in the cell cannot be of any assistance for the performance of thermal batteries must suffer badly when the temperature approaches the freezing point because of the change in the electrolytic conductivity of the electrolyte. Therefore, this factor represents a hypothetical change in parameters which would merit serious investigation if it should appear to contribute strongly to cell life.

In Figure 14 the effect of a ±20% change in cell enthalpy is demonstrated. The most obvious effect is that an peak temperature substantial decrease in the cell enthalpy while maintaining the same heat input from heat generators would result in overheating of the cell. A substantial increase in cell enthalpy with no change in heat input would result in the cell just barely becoming activated. Clearly the only practical approach would be to adjust heat generator input to the enthalpy requirements of the cell.

Since the cells act as the primary heat reservoir after the first few seconds of operation, it is clear that increasing the cell enthalpy should be beneficial everything else being the same. This, in fact, is seen to be the case in Figure 14, where the slopes of the cooling portions of the curves are in proportion to the cell enthalpy. Thus a combination of changes in cell enthalpy, by means of composition or thickness changes, and in the heat generator by similar means would appear to offer possibilities in the way of meeting varying specifications of time of activation and life.

Another possibility appears here, namely construction of duplex cells and heat generators, which have a portion of each made very thin

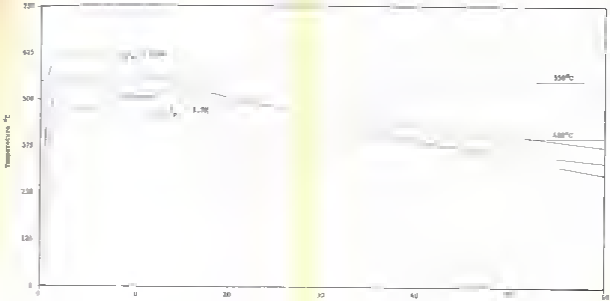

Figure 14 Effect on Cell Temperature of changing the Enthalpy of a c

for fast activation, and a larger portion which activates slowly but serves as a heat reservoir to prolong life. Unfortunately the capacity of the analog computer did not permit a problem of this complexity to be studied.

6. Effect of Rate and Level of Heat Generation by Chemical Reactions in Cells

It has been noted earlier that the reactants in the electrochemical reactions can also react chemically to produce heat but no electricity. While it might appear that any such reaction would be wasteful, it turns out not to be so since the major limitation on cell life appears to be heat losses rather than exhaustion of reactions, and these intra-cell chemical reactions generate heat at a point where it is most effective in keeping the electrolyte molten.

The effect on cell temperature histories of these chemical reactions is illustrated in Figure 15 for a heat sink temperature of 25°C. It is seen that the peak temperature of 550°C is reached at about 4 seconds, and that the life of the cell above 400°C is about 48 seconds when the normal heat generation is used.

A word about the heat generation is in order. The general shape of this function (which is approximate, of course) is also shown in Figure 15. The shape and the average rate of heat input to the system are based on experiments performed earlier at the Energy Conversion Laboratory of the University of Florida, and on educated guesses of experienced investigators familiar with the design and operation of a number of types of thermal batteries. In this study the normal rate of heat generation was chosen to be 15 cal per cm^3 per sec because of the

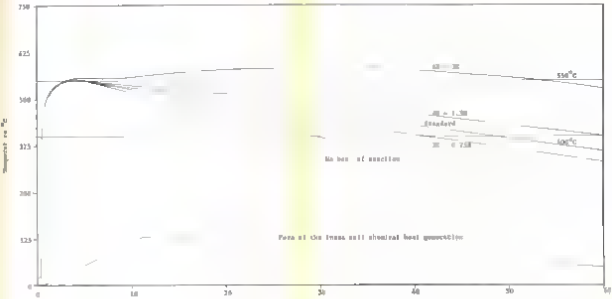

Figure 15 Effect on Cell Temperature of Changing the Magnitude of the Inner Cell Chemical Heat Generation

cell chemistry assumed. The heat generation rates of other cell reactions is covered by the range of heat generation terms used.

From Figure 15 it may be seen that the peak temperature and the time to reach it are not strongly dependent on the value of the cell heat generation term unless very energetic and extensive chemical reaction occurs. A change in the heat generation term of ±50% appears to change the life above 400°C by about ±20% without exceeding allowable peak temperature. Figure 15 also indicates that a heat generating reaction producing heat at approximately three times the rate in the normal situation would lead to a relatively small increase in the peak temperature, but it would result in a delay to reach the peak temperature of approximately 30 seconds and would result in approximately twice the life above 400°C.

Figure 16 indicates the shape of the heat generation functions programmed in these experiments. The peak heat generation rate and the decay rates were held constant and the rise rate varied from one-half to twice the standard rate. The data in Table 4 indicate that this change produced essentially no change in the cell temperature history. Activation times and peak temperatures turned out to be essentially unaffected.

This kind of effect resulted, however, because the heat generation term chosen as a standard is such as to affect only the cooling portion of the temperature history of the rail in any significant way. If, for example, a system employing an intra-cell chemical heat generation rate more than twice as large as the standard should be studied a

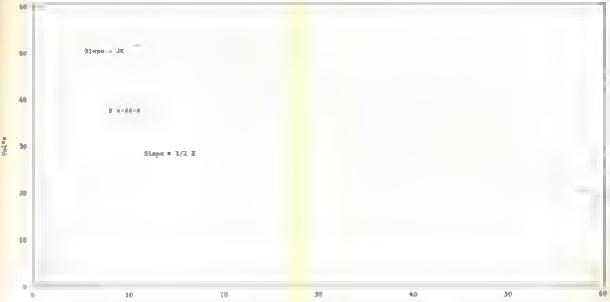

Figure 16 Change of Ia t a Rate of Entry-Cell Chemi al Hea Case [illegible]

much more pronounced effect on the temperature history of the cell would be noted.

Figure 17 illustrates the kinds of changes in decay rate studied. Here the rise rate and peak generation rate were held constant and the decay rate varied from one-half to 1.3 times that of the standard. It is clear from examination of time-temperature curves of a cell (not presented here) and of the data in Table 4 that only a small effect is noted. There is no effect on activation time and peak temperature, but the cooling rate of the cell is affected slightly.

In summary, it does not appear that alternation of either rise or decay rates of the intra-cell chemical heat generation function within broad limits would strongly affect the temperature history of a cell. However, the level of this type of heat generation, i.e., a change in the rate of chemical heat generation per unit volume would have a significant effect.

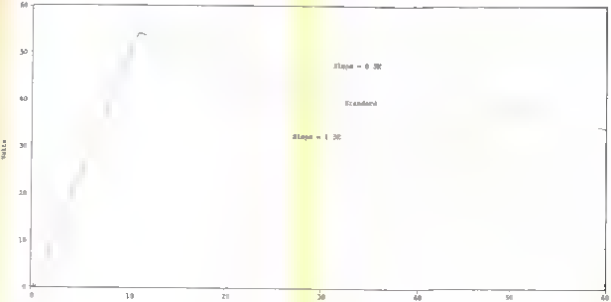

Figure 17 Change of Decay Rate of Inner-Cell Chemical Heat Generation Term

CHAPTER IV

ANALOG COMPUTER MODEL II

A. Description of the Model

The next phase of the investigation concerning dynamic heat transfer in thermal batteries called for a study of the effect of the nature and structure of the insulation on the performance of thermal batteries. It should be obvious that Model I, which was discussed in the preceding chapter is inadequate to simulate an insulation region composed of more than one insulating material.

This model was developed primarily to be able to study the effect of different combinations of insulating materials on the battery performance. In order to accomplish this simulation and at the same time keep the problem within the practical capabilities of the available analog computer (EASE 1032 Analog Computer), a number of simplifying assumptions were made.

The most significant simplifying assumption of this model as compared to Model I is that the cell-generator stack is considered to have a homogeneous core having the average physical properties of the electrochemical cells and heat generators. Furthermore, this homogeneous core is assumed to be well-mixed with no temperature gradients. Therefore, only one ordinary differential equation describes the heat balance considerations in the core.

This model is more complicated than Model I in that the insulation is considered to consist of four elements rather than one (see

Figure 18). This model makes it possible to consider a core surrounded by four successive layers of different thermal characteristics, each, of course, having an internal temperature gradient, and having the thermal resistance lumped at the interfaces as in Model I.

Another important difference between the two models resides in the manner in which the battery activation is achieved. In the case of Model I it was assumed that the heat generators constitute an essentially instantaneous heat source, and, in order to make the set of assumptions consistent, it was postulated that the initial temperature of the heat generator was 2200°C, which is the approximate temperature of the center of the heat generators. The temperature gradient between the heat generator and the cell was the driving force which promoted the heat transfer.

In the case of Model II, where only one element is assumed to simulate the cell-generator stack, it is meaningless to consider core temperatures of the order of 2200°C, first because the enthalpy of the generators does not permit such average core temperatures and secondly because there exists a high-temperature limit of about 550°C above which the electrochemical systems in the cells undergoes undesirable transformations (3). Therefore, after examination of the temperature histories of cell and generators as shown in Figure 5, where it was observed that the temperature of cell and generators was essentially the same only a few seconds after activation and that it remained so for the rest of the operating period, it was decided to assume for the core a heat generation term equivalent in calories to the enthalpy of the

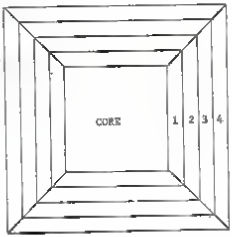

Figure 18 Schematic Diagram of Battery Described by Model II

heat generators of Model I. This heat generation term was assumed to be an exponential decay function which was judged to be an adequate simulation of the sudden energy burst of the heat generators.

Another difference between the two models is that in Model I the boundary between top and lateral insulation was considered to be vertical and in this model, the boundary between the corresponding top and lateral elements in the insulation zone was assumed to be an imaginary surface cutting diagonally from the outer corner of the core to the outer corner of the assembly. This arbitrary shape assumed for the insulation elements has some rather interesting consequences in the form of the coefficients of the differential-difference equations which describe the system. This point will be discussed in more detail later.

One final simplification of this model relative to Model I was the elimination of the heat of reaction term due to the cell. This was done solely because the effect of the intra-cell heat of reaction had been evaluated in Model I, and because its inclusion would have complicated this model without contributing appreciably to the qualitative differentiation between different insulation arrangements.

X Development of the Mathematical Model

It is shown in Appendix X that when the boundary surface between corresponding top and lateral insulation elements is assumed to have the shape illustrated in Figures 18 and B-1b, the volume of the top insulation element is given by

$$V_{Ti} = \frac{\pi h}{3}(R_{i+1}^2 + R_i R_{i+1} + R_i^2) \qquad \text{(III-1)}$$

where V is the volume of the element, h its height, and R is the radius. The common area of contact between the top and lateral elements is given by the expression

$$A_{Tli} = \pi h(R_i + R_{i+1}) \qquad \text{(III-2)}$$

and the volume of the lateral insulation element is given by

$$V_{Li} = \frac{\pi h}{3}(2R_{i+1}^2 + R_i R_{i+1} - R_i^2) + \pi(R_{i+1}^2 - R_i^2)S_i \qquad \text{(III-3)}$$

where S_i is the height of the element as shown in Figure B-1b.

The heat transfer coefficients were calculated in a manner identical to the one utilized in Model 1 that is, by assuming the thermal resistance between two adjacent elements to be lumped at the interface. This resistance was evaluated by consideration of the mean heat path between two adjacent elements and their respective thermal conductivities. The numerical values of the heat transfer coefficients for Run 15 are shown in Appendix B.

The differential-difference equations were developed by heat balance considerations of each of the elements making up the simulated battery. If the following substitutions are utilized for the purpose of simplification, the differential-difference equations which describe the system take the form shown in Table 5.

$$F_i = \frac{\rho_i C_{pi} h_i}{3}(R_{i+1}^2 + R_i R_{i+1} + R_i^2) \qquad \text{(III-4)}$$

and

$$G_i = \frac{\rho_i C_{pi} h_i}{3}(2R_{i+1} - R_i R_{i+1} - R_i^2) + \rho_i C_{pi} S_i (R_{i+1}^2 - R_i^2) \qquad \text{(III-5)}$$

C. Analog Computer Solution

The equations shown in Table 5 were programmed on the analog computer and the circuit is shown in Figure 19.

The potentiometer settings corresponding to Run 15 are listed in Table 6 together with the corresponding mathematical expression for each potentiometer. The values of the physical parameters used in these simulations are shown in Table 7.

It should be noted that Amplifier 17 in the computer diagram represents the exponential decay type of heat generation attributed to the core. This exponential function was designed so that the integral over time of this relation, namely the total amount of heat generated by unit volume of core, resulted in a core peak temperature near the maximum chosen. The value which produced the most realistic core peak temperature (525°C) corresponded to 353 cal /g of heat generator in the core (see Appendix B).

Because of the high initial rate of change of temperature in the core and the nature of the simplifying assumptions of this model, it was realized that the model could not predict these temperatures accurately during the first few seconds of operation. In any case, the primary concern in this study was with the cooling period, and with the effect of changes in the thermal properties of the materials and the geometric arrangement of the assembly on the cooling rate.

D. Discussion of Results

This model is a variation of Model I and it is based on essentially the same assumptions as the latter, therefore, many of the considerations discussed in the preceding chapter are applicable

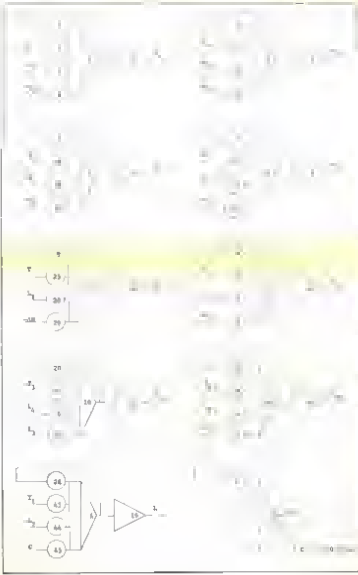

Figure 15

Analog Computer Diagram of Node 1

TABLE 5

DIFFERENTIAL-DIFFERENCE EQUATIONS FOR
MATHEMATICAL MODEL II

Top Element 4

$$-\frac{R_3^2 H_{T4A}}{F_4}(T_4 - A) - \frac{R_4^2 H_{T43}}{F_4}(T_4 - T_3) - \frac{(R_3 + R_4)h_4}{F_4} H_{TL4}(T_4 - L_4) = \frac{dT_4}{dt}$$

Top Element 3

$$-\frac{R_4^2 H_{T43}}{F_3}(T_3 - T_4) - \frac{R_3^2 H_{T32}}{F_3}(T_3 - T_2) - \frac{(R_4 + R_3)h_3}{F_3} H_{TL3}(T_3 - L_3) = \frac{dT_3}{dt}$$

Top Element 2

$$-\frac{R_3^2 H_{T32}}{F_2}(T_2 - T_3) - \frac{R_2^2 H_{T21}}{F_2}(T_2 - T_1) - \frac{(R_3 + R_2)h_2}{F_2} H_{TL2}(T_2 - L_2) = \frac{dT_2}{dt}$$

Top Element 1

$$-\frac{R_2^2 H_{T21}}{F_1}(T_1 - T_2) - \frac{R_1^2 H_{T1C}}{F_1}(T_1 - C) - \frac{(R_2 + R_1)h_1}{F_2} H_{TL1}(T_1 - L_1) = \frac{dT_1}{dt}$$

Core

$$-\frac{H_{T1C}}{\rho_c C_c S_1}(C - T_1) - \frac{2H_{L1C}}{R_1 \rho_c C_{pc}}(C - L_1) - \frac{\Delta H}{\rho_c C_{pc}} = \frac{dC}{dt}$$

Lateral Element 4

$$-\frac{2R_4 S_4 H_{L4C}}{G_4}(L_4 - A) - \frac{2R_4 S_4 H_{L43}}{G_4}(L_4 - L_3) - \frac{(R_3 + R_4)h_4}{G_4} H_{TL4}(L_4 - T_4) = \frac{dL_4}{dt}$$

Lateral Element 3

$$-\frac{2R_4 S_4 H_{L43}}{G_3}(L_3 - L_4) - \frac{2R_3 S_3 H_{L32}}{G_2}(L_3 - L_2) - \frac{(R_4 + R_3)h_3}{G_3} H_{TL3}(L_3 - T_3)$$

$$= \frac{dL_3}{dt}$$

TABLE 5 (Continued)

Lateral Element 2

$$-\frac{2R_3S_3H_{L32}}{G_2}(L_2 - L_3) - \frac{2R_2S_2H_{L21}}{G_2}(L_2 - L_1) - \frac{(R_3 + R_2)h_2}{G_2}H_{TL2}(L_2 - T_2) = \frac{dL_2}{dt}$$

Lateral Element 1

$$-\frac{2R_2S_2H_{L21}}{G_1}(L_1 - L_2) - \frac{2R_1S_1H_{L1C}}{G_1}(L_1 - C) - \frac{(R_2 + R_1)h_1}{G_1}H_{TL1}(L_1 - T_1) = \frac{dL_1}{dt}$$

TABLE 6

COEFFICIENTS FOR PROGRAMMED
DIFFERENTIAL-DIFFERENCE EQUATIONS: MODEL II

Eqn. No	Mathematical Expression	Pot. Setting
1	$\frac{R_5^2 H_{T4A} + R_4^2 H_{T43} + (R_5 + R_4) h_4 H_{TL4}}{F_4}$	26.35
4	$\frac{R_3^2 H_{T4A}}{F_4}$	24.44
5	$\frac{R_4^2 H_{T43}}{F_4}$	1.824
6	$\frac{(R_5 + R_4) h_4 H_{TL4}}{F_4}$	0.086
2	$\frac{R_4^2 H_{T43} + R_3^2 H_{T32} + (R_4 + R_3) h_3 H_{TL3}}{F_3}$	34.31
11	$\frac{R_4^2 H_{T43}}{F_3}$	32.94
16	$\frac{R_3^2 H_{T32}}{F_3}$	1.371
12	$\frac{(R_4 + R_3) h_3 H_{TL3}}{F_3}$	0.0014
3	$\frac{R_3^2 H_{T32} + R_2^2 H_{T21} + (R_3 + R_2) h_2 H_{TL2}}{F_2}$	0.2314
15	$\frac{R_3^2 H_{T32}}{F_2}$	0.1762

TABLE 6 (Continued)

Eqt No	Mathematical Expressions	Eqt Setting
16	$\frac{R_2^2 H_{T21}}{F_2}$	0.0544
17	$\frac{(R_3 + R_2)k_2 H_{TL2}}{F_2}$	0.00875
8	$\frac{R_2^2 H_{T21} + R_1^2 H_{T1C} + (R_2 + R_1)k_1 H_{TL1}}{F_1}$	1.155
22	$\frac{R_2^2 H_{T21}}{F_1}$	0.635
23	$\frac{R_1^2 H_{T1C}}{F_1}$	0.516
24	$\frac{(R_2 + R_1)k_1 H_{TL1}}{F_1}$	0.0040
9	$\frac{H_{T1C}}{F_c C_{pc} S_1} + \frac{2H_{L1C}}{R_1 F_c C_{pc}}$	0.0121
27	ΔH	0.1
25	$\frac{H_{T1C}}{F_c C_{pc} \theta_1}$	0.00357
28	$\frac{2H_{L1C}}{R_1 F_c C_{pc}}$	0.0045
29	$\frac{\Delta H}{F_c C_{pc}}$	0.500
19	$\frac{(R_5 + R_4)k_4 H_{TL4} + 2\theta_5 S_5 H_{L46} + 2\theta_4 S_4 H_{L43}}{C_4}$	26.31

TABLE 6 (Continued)

Pot No	Mathematical Expression	Pot Setting
31	$\frac{(R_5 + R_4)h_4 H_{TL4}}{G_4}$	0.043
32	$\frac{2R_5 S_5 H_{L44}}{G_4}$	24.44
33	$\frac{2R_4 S_4 H_{L43}}{G_4}$	1.824
20	$\frac{(R_4 + R_3)h_3 H_{TL3} + 2R_4 S_4 H_{L43} + 2R_3 S_3 H_{L32}}{G_3}$	34.31
35	$\frac{(R_4 + R_3)h_3 H_{TL3}}{G_3}$	0.0007
38	$\frac{2R_4 S_4 H_{L43}}{G_3}$	32.94
37	$\frac{2R_3 S_3 H_{L32}}{G_3}$	1.371
21	$\frac{(R_3 + R_2)h_2 H_{TL2} + 2R_3 S_3 G_{L32} + 2R_2 S_2 H_{L21}}{G_2}$	0.2310
39	$\frac{(R_3 + R_2)h_2 H_{TL2}}{G_2}$	0.00038
40	$\frac{2R_3 S_3 H_{L32}}{G_2}$	0.1762
41	$\frac{2R_2 S_2 H_{L21}}{G_2}$	0.0544

TABLE 6 (Continued)

Pot No.	Mathematical Expression	Pot. Setting
26	$\frac{(R_2 + R_1)h_1 H_{TL1} + 2R_2 S_2 H_{L21} + 2R_1 S_1 H_{L1C}}{G_1}$	1 155
43	$\frac{(R_2 + R_1)h_1 H_{TL1}}{G_1}$	0 0020
44	$\frac{2R_2 S_2 H_{L21}}{G_1}$	0 635
46	$\frac{2R_1 S_1 H_{L1C}}{G_1}$	0 516

TABLE 7

AVERAGE PHYSICAL PROPERTIES AND DIMENSIONS
OF THERMAL BATTERY COMPONENTS: MODEL II

Core

ρ 2.36 gm/cc

C_p 0.183 cal/gm°C

k 0.35 $\frac{\text{cal} - \text{cm}}{\text{cm}^2\ {}^\circ\text{C sec}}$

Mica

ρ 2.7

C_p 0.206

k 0.001

Asbestos

ρ 1.5

C_p 0.308

k 0.0004

Thermoflex

ρ 0.193

C_p 0.232

k 0.0002

Metal
Steel

ρ 7.9

C_p 0.12

k 0.11

here. The size of the available analog computer was again an important limitation which restricted the complexity that could be built into the model. In spite of this limitation, it was decided to continue with the analog computer study because it was believed that it could lead to qualitative information which would be of value in more precise studies utilizing a digital computer. Thus some valuable qualitative information was obtained which considerably facilitated the development of the digital computer model. The results of the analog simulation of Model II are summarized in Table 8.

1. Geometrical Shape of Insulation Elements

The geometrical shape assumed for the insulation elements in Model II is really no more arbitrary than that assumed for Model I but it has two advantages.

1. Compared to the shape assumed for the insulation elements in Model I, the shape used for the insulation elements in Model II reduced by one the number of elements with which each insulation element was in contact, thus considerably simplifying the differential-difference equations of the system with the obvious consequence of a simplification in the analog computer circuit.

2. The shape assumed for the insulation elements in Model II yields expressions for the area and volume of the corresponding top and lateral insulation elements which illustrate the similarity of the radial and axial modes of heat transfer in a cylindrical structure described by this approximate model (see Appendix B). The similarity lies in the fact that the assumed shape yields values for the area and

TABLE 8

EFFECT OF CHANGES IN THE INSULATION STRUCTURE ON LIFE TO 400°C OF SIMULATED THERMAL BATTERIES

Run No.	Structure Element No.	Material	Life at Heat Sink Temp. of 25°Deg.	25° Life / 25° Std
15	4	Metal (Standard)	52	1.00
	3	Mica		
	2	Asbestos		
	1	Thermoflex		
16	4	Thermoflex	25	0.50
	3	Mica		
	2	Asbestos		
	1	Metal		
17	4	Asbestos (New Stan-	93	1.00
	3	Asbestos dard)		
	2	Thermoflex		
	1	Thermoflex		
18	4	Thermoflex	90	0.95
	3	Thermoflex		
	2	Asbestos		
	1	Asbestos		
19	4	Asbestos	97	1.02
	3	Thermoflex		
	2	Thermoflex		
	1	Thermoflex		
20	4	Thermoflex	130	1.37
	3	Thermoflex		
	2	Thermoflex		
	1	Thermoflex		

volume of a lateral insulation element which are twice the values obtained for these quantities in the corresponding top insulation element. Thus these elements have the same ratio of area to volume and the equations describing the differential heat balance in these elements have very similar coefficients, which is equivalent to very similar potentiometer settings for corresponding potentiometers as shown in Table 6 for the case of potentiometers 1 and 19, 4 and 32, and many others. Figure 23 illustrates the almost identical temperature histories of the corresponding top and lateral insulation elements in Model II as a result of the above discussed similarity in their descriptive equations.

These results provided some justification for the assumption of spherical symmetry utilized in the digital computer model.

2 Simulation of Standard Thermal Battery

The standard thermal battery which, in the framework of this model, consisted of a cylindrical core surrounded in order by Thermoflex insulation, asbestos insulation, a mica layer and a metal case, was simulated and the results are shown in Figure 20. A life above 400°C of 52.5 seconds was indicated. This figure is in reasonable agreement with experimental results.

One significant aspect of this run was that the mica and metal layers did not rise appreciably above the temperature of the heat sink.

In view of these results, the mica and metal layers could be considered extensions of the heat sink. This assumption liberated a section of the analog computer which could be used to simulate in more

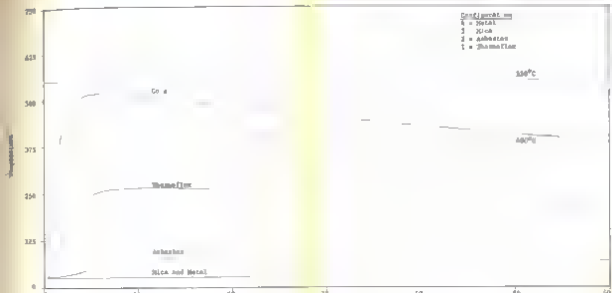

Figure 20 Temperature Histories in 5 Sudded 5 mm Thermal Battery

detail the heat transfer process in other sections of the battery

3. Effect of a Metal Layer Next to the Core on Core Temperature

Some considerations indicated that it might be advantageous from the standpoint of maximization of battery life, to place the metal can next to the core instead of on the outside of the assembly. The intuitive justification of this arrangement was based on the high heat capacity of the metal. It appeared that the metal would absorb the heat given off by the core and act as a buffer between the core and the insulation. The results of a run testing this idea clearly revealed the inefficiency of this arrangement which clearly yielded a lower battery life than the standard as shown in Figure 21. The reason for this result is that the metal layer is essentially an addition of inert material to the core (inert in the sense that there is no heat generation associated with it)which only serves to increase its heat transfer area and hence the rate of heat loss from the core to the insulation.

4. Effect of Varying Insulation Arrangements on Core Temperature

The negligible temperature rise of the outer wire and metal layers discussed before for the case of the standard battery allowed a more precise simulation of the effect of different insulation arrangements on the life of the battery. The number of well-mixed elements used to simulate the insulation space, which in the case of the standard battery is composed of a layer of Thermoflex and a layer of asbestos, was doubled. This allowed for the existence of a step-type temperature gradient in the simulation of an actual layer of homogeneous material

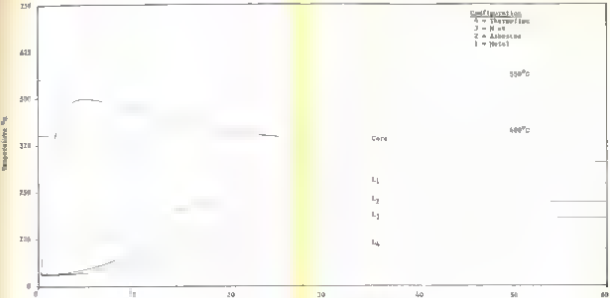

Figure 22 Temperature Rise of the Simple and Thermal Battery with Metal Heat Core

such as Thermaflex. Figure 22 illustrates this effect on the simulation of the standard thermal battery. The results shown in this figure indicate that the mathematical model was very sensitive to this type of change. The standard battery life was almost doubled as a result of inaccuracies introduced by the new mode of simulation. It should be noted that battery life is a very stringent test for agreement between two models because of the low rate of cooling of the battery which makes small changes in the rate of cooling have a large effect on battery life.

The significant discrepancy between the lives of the two simulations of the standard battery is believed to be a consequence of the assumptions of the model. The heat transfer coefficients utilized in the model are calculated on the basis of the thermal resistance of the two adjacent elements. The introduction of extra insulation elements reduces the thickness of the element in contact with the core and makes the value of the core-insulation coefficient more dependent on the core. Therefore, in a sense it may be stated that increasing the number of insulation elements decreases the relative approximation of the core results. Since in this case, the core was being represented by only one element already having by far the greatest volume of all the elements present, the intended improvement in the simulation of the standard battery, actually resulted in a poorer approximation.

In spite of this disagreement between the two simulations of the standard battery, a valid qualitative comparison between different

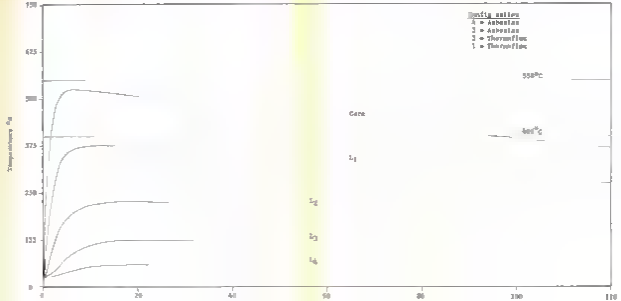

Figure 22 Temperature Histories in Simulated Thermal Battery with Varying Insulation Arrangement

insulation arrangements should exist using, of course, the new standard as the basis for the comparison. Figure 23 shows the effect of interchanging the asbestos and Thermoflex layers to be detrimental to the life of the battery. Figure 24 shows that a slight increase in battery life is obtained when three layers of Thermoflex and only one outer layer of asbestos are utilized. This result indicates the desirability of having as much Thermoflex as possible adjacent to the core. Figure 25 illustrates the obvious arrangement which results as a consequence of the data in Figure 24, this is, an all Thermoflex insulation. In connection with this figure it should be noted that, although it predicts the longest life of all the arrangements tested, the magnitude of the predicted life is clearly in disagreement with the trend established in the preceding figures. The reason for this is probably experimental error in setting the numerous potentiometers in the analog circuit, and the fact that this particular experiment was carried out on a different occasion which means that all the potentiometers had to be set, as opposed to the other three arrangements which were run on the same day. For these runs only a few potentiometers had to be changed to effect the simulation of a particular insulating arrangement.

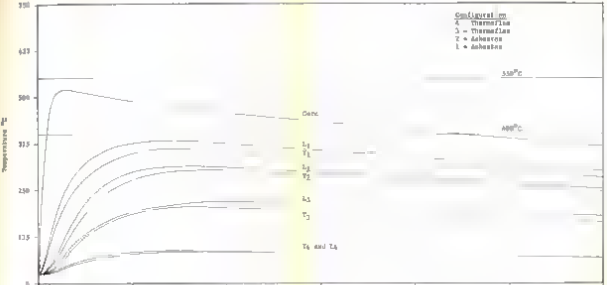

Figure 23 Temperature History as in Simulated Thermal Battery with Varying Insulation Arrangement

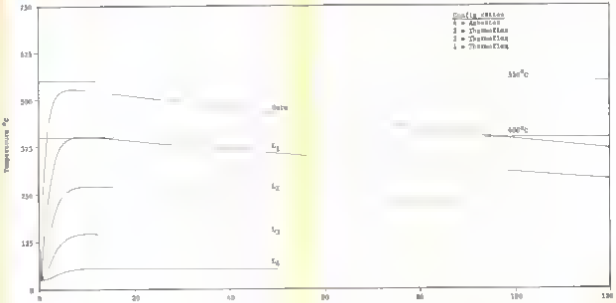

Figure 24 Temperature Histories in Simulated Thermal Battery with Varying Insulation Arrangement

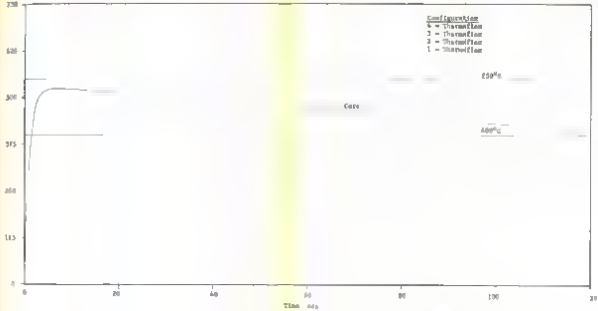

Figure 25 Temperature Histories of Fluids of Thermal Battery with Varying Insulation Arrangement

CHAPTER V

DIGITAL COMPUTER MODEL III

A. Description of the Model

The digital computer model which was programmed on the IBM 709 computer was that of a multi-layered sphere consisting of a well-mixed spherical core surrounded by a core film in which heat conduction is occurring; this, in turn, is surrounded by spherical shells of insulation, and the whole is immersed in an infinite heat sink. This particular physical model was arrived at after careful consideration of the results of the two analog computer models and the requirements of the problem.

One important factor in the use of the digital computer for solution of problems of this type is the matter of the convergence of the approximate (digital) solution to the exact one. If this factor is considered together with the dimensionality of the problem, that is, the number of dimensions involved in the partial differential equation, it may be seen that the amount of effort (time and/or money) necessary to achieve an accurate solution, i.e., asymptotic approach of the digital computer solution to the exact one, becomes prohibitive. Therefore, simplifying assumptions must ordinarily be made which will lead to a solution on the computer, at reasonable expense, and at the same time conserve enough characteristics of the physical model so that the results may be meaningful.

The result of the analog computer study on Model II (a right

circular cylinder with a height equal to the diameter) indicated that the temperature difference between similar points in top and lateral insulation is essentially negligible. In view of these results it appears, then, that the dimensionality can be reduced assuming spherical symmetry without seriously reducing its practicality. The choice of a spherical model reduces the partial differential equation to one containing a single spatial variable and time.

The assumption of a homogeneous core was retained because, it was desired to place the greater emphasis in the study of the insulating materials and configurations as these affect battery life. It should be noted that the period during which the battery is hot enough for operation requires that the electrolyte contained in the cells be in a molten state. Furthermore, there exists during this period a continuous electrochemical reaction with its inherent ionic migration which contributes to convection heat transfer inside the cell. These two facts, together with the very high thermal conductivity of the molten electrolyte, suggest that the temperature gradients in any direction within the cells must be very small. Moreover, since the core is made of alternate disks of heat generators and cells, and the heat generators and the cells are at very nearly the same temperature after the first few seconds of operation, the temperature of most of the core should be essentially independent of position and be dependent on time only. On the other hand, the heat generators in the core provide a significant resistance to heat transfer and within the cells, in the region near the core-insulation interface a significant temperature gradient would

be expected. The foregoing considerations suggested that the core could be considered to consist of two sections, an inner well-mixed section where the temperature was a function of time only, and an outer section consisting of a film where temperature gradients existed. This film concept is implied in all the computations of convective heat transfer which make use of relations such as Newton's cooling law.

The preceding discussion indicates that it would be desirable to simulate heat transfer from the core to the insulation by transfer from a well-mixed element through an imaginary film where heat conduction would be the heat transfer mechanism. The problem of estimating the thickness of this film is a very difficult one, especially from the analytical viewpoint. On the other hand, if the film thickness is used as the simulation parameter, it could be adjusted in such a manner that the performance of a standard battery would be approximated very closely by the mathematical simulation, provided that the same values for all other parameters were used.

This model also includes the effect of intra-cell heat of reaction, and the impulse-type heat input of the generators in the core.

B. Development of the Mathematical Model

On making a thermal energy balance over a spherical shell of thickness Δr within the sphere, the following relations can be obtained:

Thermal energy in at r	$4\pi r^2 q\big\vert_r$	(V-1)
Thermal energy out at $r + \Delta r$	$4\pi(r + \Delta r)^2 q\big\vert_{r + \Delta r}$	(V-2)

Thermal energy generated	$4\pi r^2 \Delta r \Delta H$	(V-3)
Accumulation	$4\pi r^2 \Delta r \rho C_p \frac{\partial T}{\partial t}$	(V-4)

The thermal energy balance equation states that

$$\text{rate of thermal energy in} = \text{rate of thermal energy out} + \text{rate of thermal energy generation} = \text{rate of accumulation} \qquad \text{(V-5)}$$

If equation (V-1) to (V-4) are substituted into equation (V-5) and one takes the limit as Δr approaches zero, the following relation results

$$\frac{\partial T}{\partial t} = \lim_{\Delta r \to 0} \frac{4\pi(r + \Delta r)^2 q\big|_{r+\Delta r} + 4\pi r^2 q\big|_r + 4\pi r^2 \Delta r \Delta H}{4\pi r^2 \Delta r \rho C_p} \qquad \text{(V-6)}$$

hence

$$\frac{\partial T}{\partial t} = \frac{\frac{\partial}{\partial r} r^2 q\big|_r + \Delta H}{\rho C_p} \qquad \text{(V-7)}$$

and since

$$q\big|_r = -k \frac{\partial T}{\partial r} \qquad \text{(V-8)}$$

equation (V-7) becomes

$$\frac{\partial T}{\partial r} = \alpha \left[\frac{\partial^2 T}{\partial r^2} + \frac{2}{r} \frac{\partial T}{\partial r} \right] + \frac{\Delta H}{\rho C_p} \qquad \text{(V-9)}$$

where T is the temperature; t is the time, r is the radius and α is the thermal diffusivity, $\frac{k}{\rho C_p}$ (54).

The mathematical model describing the temperature distribution in a composite sphere consisting of a spherical central core having internal heat generation surrounded by concentric spherical layers of

different materials, takes the following form

for $0 < r < R_1$

$$\frac{\partial T_1}{\partial t} = \alpha_1 \left[\frac{\partial^2 T_1}{\partial r^2} + \frac{2}{r} \frac{\partial T_1}{\partial r} \right] + \frac{\Delta H(t)}{\rho C_p} \tag{V-10}$$

at $r = R_1$, $T = T_2$ and $k_1 \frac{\partial T_1}{\partial r} = k_2 \frac{\partial T_2}{\partial r}$ (V-11)

for $R_1 < r < R_2$

$$\frac{\partial T_2}{\partial t} = \alpha_2 \left[\frac{\partial^2 T_2}{\partial r^2} + \frac{2}{r} \frac{\partial T_2}{\partial r} \right] \tag{V-12}$$

at $r = R_2$, $T_2 = T_3$ and $k_2 \frac{\partial T_2}{\partial r} = k_3 \frac{\partial T_3}{\partial r}$ (V-13)

for $R_2 < r < R_3$

$$\frac{\partial T_3}{\partial t} = \alpha_3 \left[\frac{\partial^2 T_3}{\partial r^2} + \frac{2}{r} \frac{\partial T_3}{\partial r} \right] \tag{V-14}$$

at $r = R_3$, $T_3 = T_A$ (V-15)

In equations (V-10) through (V-15) the subscripts refer to Figure 26

The above equations serve to describe the temperature histories of all of the elements in the system except the well-mixed section of the homogeneous core Since within this section, the temperature at any instant in time is constant throughout the element, the equation describing heat transfer in that element is an ordinary, rather than a partial, differential equation. The form of this equation will be clearer when the finite difference form of the system of equations is examined

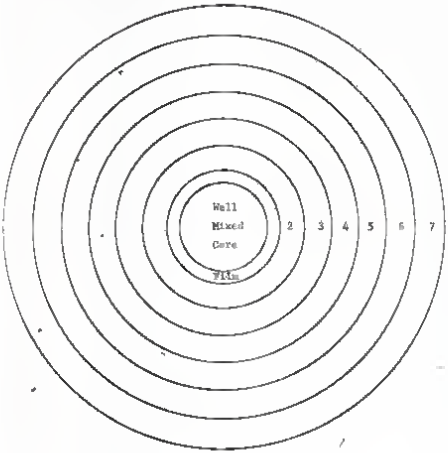

Figure 26 Schematic Diagram of Battery Described by Model III

C. Finite-Differences Approximation

The partial derivatives which appear in equations (V-10) to (V-15) can be approximated by finite difference equations using Taylor's series. In the present case, $T = f(r,t)$; the $f(r,t)$ may be expanded about r for a fixed value of t as follows (41):

$$T(r + \Delta r, t) = T(r,t) + \Delta r \frac{\partial T}{\partial r} + \frac{(\Delta r)^2}{2} \frac{\partial^2 T}{\partial r^2} + \frac{(\Delta r)^3}{6} \frac{\partial^3 T}{\partial r^3} + \cdots \qquad \text{(V-16)}$$

The function $f(r,t)$ can also be expanded as follows:

$$T(r - \Delta r, t) = T(r,t) - \Delta r \frac{\partial T}{\partial r} + \frac{(\Delta r)^2}{2} \frac{\partial^2 T}{\partial r^2} - \frac{\Delta r^3}{6} \frac{\partial^3 T}{\partial r^3} + \cdots \qquad \text{(V-17)}$$

If equations (V-16) and (V-17) are subtracted and terms of the order of $(\Delta r)^3$ are neglected, an approximation of $\partial T/\partial r$ is given by

$$\frac{\partial T}{\partial r} = \frac{T(r + \Delta r, t) - T(r - \Delta r, t)}{2\Delta r} \qquad \text{(V-18)}$$

If equations (V-16) and (V-17) are added and terms of the order of $(\Delta r)^4$ are neglected an approximation of $\partial^2 T/\partial r^2$ is found to be

$$\frac{\partial^2 T}{\partial r^2} = \frac{T(r + \Delta r, t) - 2T(r,t) + T(r - \Delta r, t)}{(\Delta r)^2} \qquad \text{(V-19)}$$

D. Development of the Computer Program

The elements of the idealized spherical thermal battery can be divided into a finite number of sections by dividing the radius into finite increments. Within one of the insulation elements, equations (V-10), (V-12), etc., would take the following form:

$$\frac{dT_r}{dt} = \alpha_{in} \left[\frac{T_{r+\Delta r} - 2T_r + T_{r-\Delta r}}{(\Delta r)^2} + \frac{2}{r} \frac{T_{r+\Delta r} - T_{r-\Delta r}}{2(\Delta r)} \right] \qquad \text{(V-20)}$$

where n is the element number and $R_{n-1} < c < R_n$. This equation applies to all the points within insulation elements if the c corresponding to each element is used.

At the interface points the above equation does not hold because the derivatives would be approximated by points on both sides of the interface, and, since a discontinuity in the temperature profile exists at the interface point, the procedure would not be valid. The equations describing the heat transfer at the interface points are the boundary conditions listed in equations (V-11), (V-13), etc. Since these equations involve a first partial derivative, it is necessary to approximate it with the appropriate finite-difference equation. Equation (V-16) cannot be used because it is based on the assumption that the derivative exists from point j-1 through point j+1. However, for an interface point j the derivative exists up to point j from the element on the left and up to point j from the element on the right. Therefore, the left derivative can be approximated by

$$\frac{\partial T}{\partial r} = \frac{T_c - T_{c-\Delta r}}{\Delta r_n} \qquad \text{(V-21)}$$

and the equation on the right can be expressed similarly. Hence, the equation at an interface point takes the following form

$$k_n \frac{T_c - T_{c-\Delta r}}{\Delta r_n} = k_{n+1} \frac{T_{c+\Delta r} - T_c}{\Delta r_{n+1}} \qquad \text{(V-22)}$$

This equation can be solved for T_j as a function of T_{j+1} and T_{j-1} which are functions of time of the form given in equation (V-20).

The heat generation term, the last term of equation (V-9) is not affected by the differencing technique since it does not involve

any derivatives. Therefore, it remains unchanged in the finite difference form of the equation. The form of the ΔN term is an exponential decay function of time.

Another important assumption which is common to all three models is the consideration of the battery as being in contact with a perfect heat sink. In this model, this assumption affects the form of the boundary condition at the surface of the external element of the battery. Since that interface is in contact with a material whose temperature does not change with time, and its thermal conductivity is essentially infinite, the temperature at that interface must remain constant and hence the time derivative at that point is equal to zero. The heat transfer process in the well-mixed portion of the core requires a particular analysis. Since the temperature within this sphere is a function of time only, a heat balance in the sphere can be expressed in finite difference form as

$$\rho_A C_{pA} V_A \frac{dT_2}{dt} = k_b A \frac{T_3 - T_2}{\Delta r_b} + \Delta H V_A \qquad \text{(V-23)}$$

and $\quad T_1 = T_2 \qquad$ (V-24)

where V_A is the volume of element A. These equations with their corresponding constants were programmed as the DSNIV subroutine of the AMMS program.

The model programmed described the heat transfer in the core which included a well-mixed section where the temperature was a function of time only, and an outer section or film where heat conduction resistance existed. In both sections of the core, the heat generation term which simulates the heat given off by the generators and the intra-cell

chemical reactions was included. Six other elements were included which can be assumed to possess different values of thickness, density, thermal conductivity and heat capacity. The program was modified during the investigation to include the feature that any one of the "insulation" elements (all the elements except the core) may be considered to possess heat generation capabilities. This modification permitted the simulation of a battery where heat generators might be used in place of normal insulating materials in order to provide extra heat to the battery, and thus improve its performance. This point will be discussed more fully in the Discussion of Results.

E. The AMBS Program

The AMBS program is an extension of the Adams-Moulton-Shell (55) routine programmed at the University of Florida by Fairchild, Wengrow and May as a package of FORTRAN subprograms. AMBS has the unique advantage of automatic truncation error control of increment size without requiring any special procedure for restart due to change in increment size.

AMBS requires that the problem be stated as a set of first-order ordinary differential equations with initial conditions specified. In this case, the system of partial differential equations was approximated by ordinary differential equations using appropriate differencing techniques.

The general problem for which the AMBS program was designed consists of solving sets of equations of the form

$$\frac{dx_i}{dt} = f(x_i, t) \qquad \text{(V-25)}$$

Immediately, techniques such as Simpson's Rule or the trapezoidal rule must be discarded because x_i appears on the right hand side of the equations. The simplest constant increment method is Euler's method which can be extended by introducing the concept of predictor and corrector. This is known as the Modified Euler method. A number of predictor-corrector methods have been devised based on Newton's interpolation formula. Those which predict from point n to point n+1 based on derivatives at point n and preceeding points, and which correct the same interval adding the derivative at point n+1, carry the name Adams-Moulton. Because of stability considerations and the possibility of error control, the Adams-Moulton method is the best available constant increment procedure.

Milne (56) has developed similar equations which have lower error for comparable effort but the possibility of instability makes it unsuitable for machine computation. The Runge-Kutta-Gill method (57) has the advantage of requiring no history points, but error control is a significant problem in this method. The constant increment equations are more thoroughly discussed in standard numerical analysis texts (58,59).

The Adams-Moulton-Shell method is a divided difference technique based on Newton's interpolation formula and is an extension by Shell (55) of the Adams-Moulton constant increment method to a non-constant increment method. The advantage of the method can be appreciated where truncation error control is included with the result of frequent changes in interval size. A method requiring constant interval sizes must

generate new starting points after each change in interval size, whereas a method which can utilize non-constant increments can continue after a change of interval size without interruption.

The ABM program consists of a main program and sixteen subprograms, fourteen of which remain unchanged for all problems of the general type discussed. The other two subprograms are called DERIV and INDEV, and they contain the information which is specific to each problem such as the particular form of the differential equations involved and the specification of the input and output requirements of the problem. The program listings used in this study are shown in Appendix D (60).

F Discussion of Results

The digital computer program was subjected to its first test by studying the simulation of a physical model for which an analytical solution can be evaluated readily. This model consisted of a homogeneous sphere having a uniform initial temperature of 500°C everywhere except at its surface, where the initial temperature was 0°C. The analytical and computed temperature profiles are shown in Figure C-1. It may be seen that, with 27 simultaneous equations describing the system, the computed and analytical results agreed within 5% up to values of time of 28 seconds. It was observed that the computed results always predicted a lower temperature than the exact solution, and that the difference between the two solutions increased with time. On the other hand, it should be pointed out that the computer program was not ideally suited to simulate the homogeneous sphere

model because it was developed to simulate a heterogeneous sphere having a well-mixed section in the core where no radial temperature gradients exist. Therefore, a number of changes had to be made in the input data in order to adapt the program to the homogeneous sphere model, such as assuming the radius of the well-mixed section of the core to be zero and assuming all of the insulation layers to be composed of the same material. This assumption produces an inherent loss of precision due to the fact that at each interface point in the model, the equation describing the heat transfer process in the continuity boundary condition between adjacent but supposedly different materials, whereas in the case of a homogeneous sphere the more precise equation involving the second partial derivative would be used. In view of the above factors, the agreement between the approximate and exact solutions can be considered quite satisfactory.

Figure C-1 also illustrates the effect of geometry on the behavior of the homogeneous system. The figure shows a temperature profile of the homogeneous sphere after 50 seconds, and the center point temperatures after 50 seconds of homogeneous right circular cylinders having equal height and diameter, and having (1) a radius and (2) a volume equal to those of the sphere. The temperature of the cylinders was calculated from the tables due to Olson and Schultz (23). It should be noted that the sphere is a more efficient heat reservoir than the cylinder having equal volume owing to the smaller area to volume ratio of the former, and that the center temperatures of these two solids differ by only approximately ten per cent after 50 seconds. This may be consid-

dered another justification for the assumption of spherical symmetry in the simulation of thermal batteries especially because these contain a core where smaller temperature gradients than those encountered in pure heat conduction exist, owing to the molten state of the electrochemical cells and to the ionic migration within them.

1. Simulation of the Standard Thermal Battery

In this model a different approach was used to the battery than had been used in the two analog models. In the analog models, the thermal properties of the materials comprising the battery were incorporated into the model and the value predicted for the life of the thermal battery was accepted. In the case of the spherical model studied on the digital computer, as a consequence of the assumption of a well-mixed section in the core where no temperature gradients and hence no resistance to heat transfer exist, and of a film in the core where the thermal resistance of the core is concentrated, an unknown parameter, namely the thermal resistance of the film, must be considered. It has been pointed out by Jakob (7) that this is the proper approach to analysis of convection heat transfer.

The amount of effort involved in obtaining a very precise solution of the mathematical model under consideration would be prohibitive because of the numerous different alternatives that had to be considered for the purpose of design optimization. In any case, a high degree of accuracy would not be justified because the choice of spherical symmetry was only an approximation of a battery.

In view of the above considerations it was decided to choose the

arbitrary parameter in such a manner that a feasible model would yield results very similar to those given by a standard battery. Specifically, the life of the simulated thermal battery at heat sink temperature of 25°C was arbitrarily made to be 30 seconds.

At the beginning of the investigation, it appeared that there were two arbitrary parameters which resulted from the assumption of a finite film in the core, the thickness of the film and the thermal conductivity of the film. A number of simulations involving different values of these two parameters indicated that within the range of values tested, the same response was obtained for different values of thickness and thermal conductivity of the film if their ratio was the same. This result indicated that essentially only a single thermal resistance parameter had to be chosen arbitrarily.

The form of the heat generation term was chosen to be an exponential decay which would make the core reach 400°C in approximately 0.2 seconds and of such a magnitude that the total heat generated would be equal to the heat given off by the equivalent number of heat generators in the core as determined from calorimetric measurements. The value of the intra-cell heat generation was established to be 10% of the total heat generated by the heat generators. It was again given a triangular form with the maximum heat generation being reached after 15 seconds. The values of the parameters used in the simulation of the standard battery are listed in Table C-1.

This simulation was effected using 27 grid points. The temperature profiles in the battery are shown in Figure 27, and the

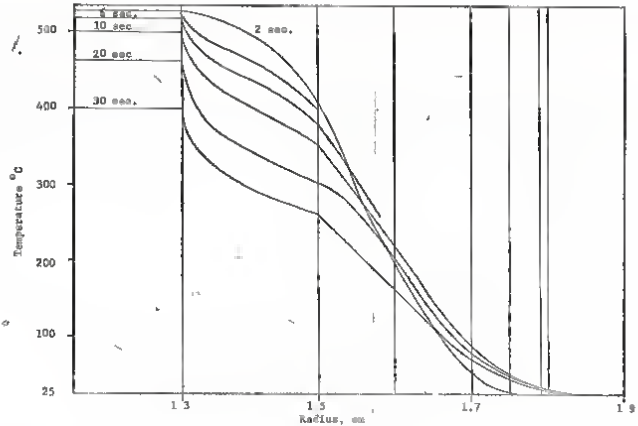

Figure 27 Temperature Profiles in Standard Simulated Thermal Battery

temperature history for the core is illustrated in Figure 28. The numerical results are summarized in Table 9. The life of the battery was dependent on the number of grid points used in the simulation, but since the deviation from the exact solution was estimated to be of about 10%, the number of 27 grid points was chosen in order to keep the problem within the limits of economic feasibility. The film resistance was chosen so that with this number of points the life of the standard battery would coincide with the arbitrarily selected life, i.e., 30 seconds. As will be discussed later, the model proved to be very satisfactory when used in simulating battery performance under other conditions because it predicted lifes above 400°C which agreed reasonably well with experimental results under these new conditions.

2. Effect of Varying Insulation Arrangements on Core Temperature

The experience gained from the analog study greatly reduced the range of possible insulation arrangements which might have yielded an improved battery performance. The all-Thermoflex insulation structure proved to be the optimum available insulating material. The results of this and other insulation arrangements are shown in Figure 28. Table 9 shows that a slight increase in battery life may be obtained if Thermoflex only is used instead of the Thermoflex-asbestos structure. On the other hand, the use of an all-asbestos insulation is seen to be considerably worse than both the standard and the optimum. Similarly an idealized material having the average properties of equal volumes of Thermoflex and asbestos, which was denominated "mixinsulation", also showed a decrease in battery life compared to the standard. In short,

TABLE 5

EFFECT OF PARAMETERS AND CHANGES ON LIFE TO 400°C OF A SIMULATED THERMAL BATTERY

Run No.	Description	Life at Heat Sink temperature of 25°C, sec	25° Life / 25° Std.
22	Standard (Thermoflex-Asbestos Radius of Core=1 50cm)	30 0	1 00
27	All-Thermoflex	32 9	1 09
28	All Asbestos	16 2	0 54
29	Asbestos-Thermoflex	17 0	0 57
30	All Mixinsulation (See Page 104)	20 6	0 68
31	ρ = 0 193, C_p = 0 232,		
	k = 0 0001	51 0	1.70
32	ρ = 1 50, C_p = 0 308,		
	k = 0 0001	24 0	0 80
33	ρ = 15 0, C_p = 0 308,		
	k = 0 0001	16 2	0 54
34	ρ = 150, C_p = 0 308,		
	k = 0.0001	15 0	0 50
35	ρ = 0 015, C_p = 0 308,		
	k = 0.0001	60	2 00

TABLE 9 (Continued)

Run No.	Description	Life at Heat Sink Temperature of 25°C, sec	$\frac{25^{\circ}\text{ Life}}{25^{\circ}\text{ Std}}$
36	Radius of Core = 1.40 All-Thermoflex	32.0	1.06
37	Radius of Core = 1.60 All-Thermoflex	30.6	1.02
38	No Intra-Cell Heat Generation	25.0	0.83
39	ΔH = 2X* (Double Intra-Cell Heat Generation)	37.0	1.23
42	$\rho_s C_{ps}$ = 2X	36.0	1.20
43	$\rho_s C_{ps}$ = 4X	47.0	1.56
44	$\rho_s C_{ps}$ = 2X, ΔH = 2X All-Thermoflex	47.0	1.56
45	Generator Outside Thermoflex (10 sec delay)	55.5	1.85
46	Generator Outside Thermoflex (2 sec delay)	Peak Temp Too High	-
47	Generator ($\rho_s C_{ps}$ = 4X) Outside Thermoflex (2 sec delay)	62.0	2.06
48	Generator ($\rho_s C_{ps}$ = 4X) Outside Asbestos (2 sec delay)	40.0	1.33
49	3 inch diameter battery	122.0	4.05

* X = times standard value of parameter being varied

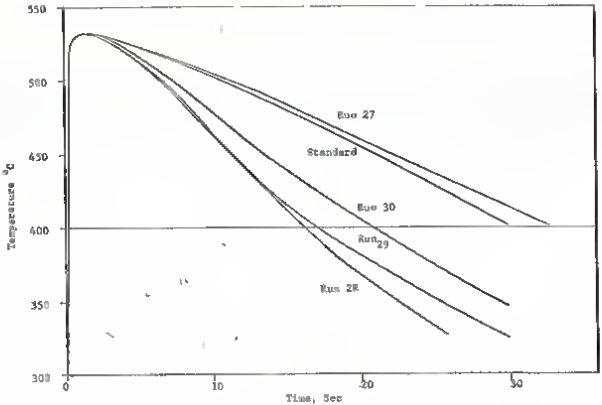

Figure 28 Effect on Cell Temperature of Various Insulation Arrangements

from the standpoint of heat transfer, mixed fiber insulation is less effective than a layer of Thermofiex surrounded by layers of less effective insulation. Reversing the order of the Thermofiex and asbestos layers in the standard battery yielded a lower battery life than the standard. All of the above findings are consistent among themselves, and they substantiate the finding that an all-Thermofiex insulation should give the optimum performance among the available insulating materials.

3. Effect of Idealized Insulating Materials on the Core Temperature

The investigation of the response of battery performance to insulating materials having arbitrary idealized properties was probably the most interesting aspect of the work and probably the most instructive development from an academic standpoint. A number of materials having some thermal properties equal to real materials and having other unrealistic properties were assumed in order to see the effect on battery life of the parameters of the system.

It was found that the arbitrary manner in which the optimization criterion was defined, namely life above 400°C, greatly affected the choice of an optimum idealized insulator. It is believed, and the results shown in Figure 31 seem to confirm it, that the insulator with the lowest thermal diffusivity will yield the longest life above the heat sink temperature, however, if the life above 400°C is considered the criterion, then it is seen that for the values tested, an insulation having low thermal diffusivity will produce a shorter battery life than an insulation having a high thermal diffusivity if both have the same

thermal conductivity. This result can be explained in the following manner. When a high cut-off temperature is chosen as the criterion for battery life, the initial mechanism of heat transfer becomes very significant. This is illustrated in Figure 30 where the temperature at a point in the insulation close to the core is seen to be greater for insulation with a low heat capacity than for insulation with a high heat capacity if both materials have the same thermal conductivity, and the same initial temperature difference exists between the point in the insulation and the core. The higher temperature of the insulation with the low heat capacity produces a smaller temperature gradient between this point and the core, thus reducing the rate of heat loss from the core. It should be noted that as time proceeds the insulation with the lower heat capacity cools more rapidly, and therefore, if the cut-off temperature is chosen low enough, the life above the cut-off temperature will eventually be longer for the material having the higher heat capacity. It was noted that, if the thermal diffusivity is reduced by reducing the thermal conductivity while the density and heat capacity are kept constant, then the battery life is improved regardless of the cut-off temperature.

4. Effect of Core Radius on Core Temperature

The effect of changing the radius of the core on the life of the battery was tested and the results are shown in Figure 32. These results indicate that, though arrived at empirically, the radius of the core had already been optimized in the standard thermal battery. Battery lives lower than that of the standard were obtained for radii of the

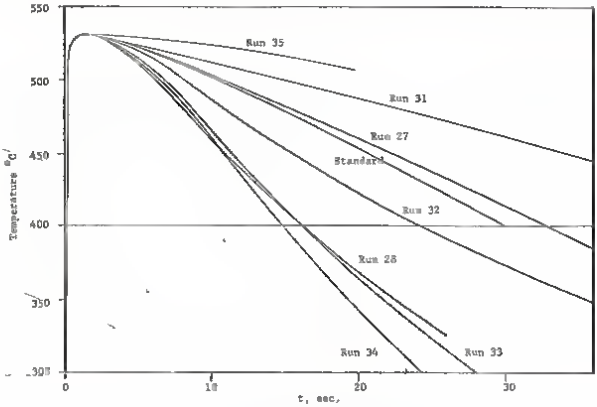

Figure 29 Effect on Cell Temperature of Idealized Changes in the Thermal Properties of the Insulation

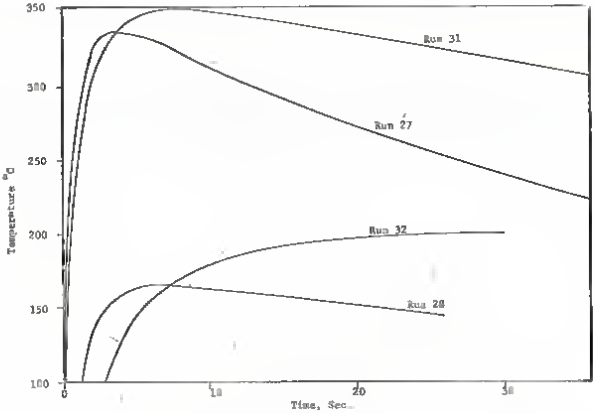

Figure 30 Effect on Insulation Temperature of Idealized Changes in Thermal Properties of the Insulation

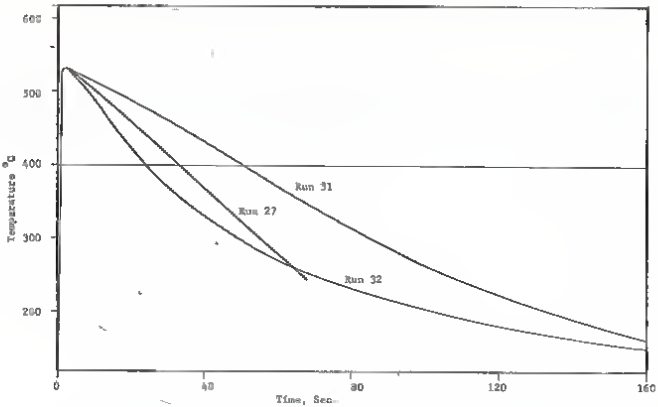

Figure 31 Effect on Cell Temperature of Different Idealized Insulators

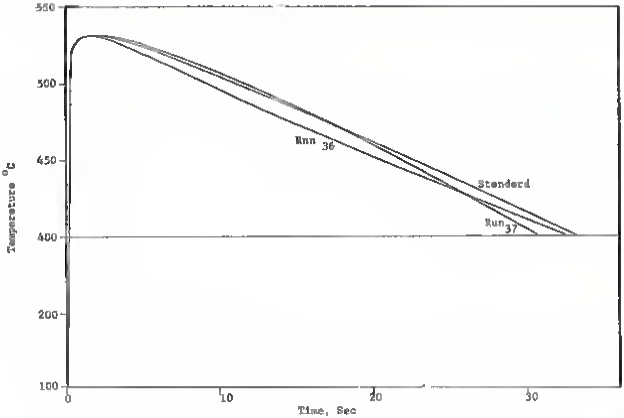

Figure 32 Effect on Cell Temperature of Changes in Core Radius

core both greater and smaller than the standard core radius.

5 Effect of Intra-Cell Heat Generation

The effect of the intra-cell heat generation on the life of the battery was shown to be a significant one. Figure 33 indicates that the side benefit of intra-cell heat generation provides almost a 20% increase in battery life. This figure also shows that another 20% increase could be gained if reacting systems yielding twice the heat of reaction of the standard system could be utilized.

6 Effect of Heat Sink Temperature on Core Temperature

Figure 34 illustrates the effect on the core temperature of a change in the temperature of the external heat sink. The low temperature of -65°F reduces the battery life by 50% while the high temperature of 160°F produces an increase in battery life of about 30% relative, of course, to the life of the standard battery at a heat sink temperature of 25°C. These results including the values obtained for the peak temperatures, are in very close agreement with experimental values obtained under these conditions.

7 Effect of Changes in the Heat Capacity of the Heat Generators on the Core Temperature

The effect of increasing the heat capacity of the heat generators was considered a feasible and beneficial possibility because it permitted a larger quantity of heat in the core without increasing the peak temperature. It was assumed that this change in the heat capacity of the generators did not affect the value for the thermal conductivity of the core. The results are shown in Figure 35. They indicate that

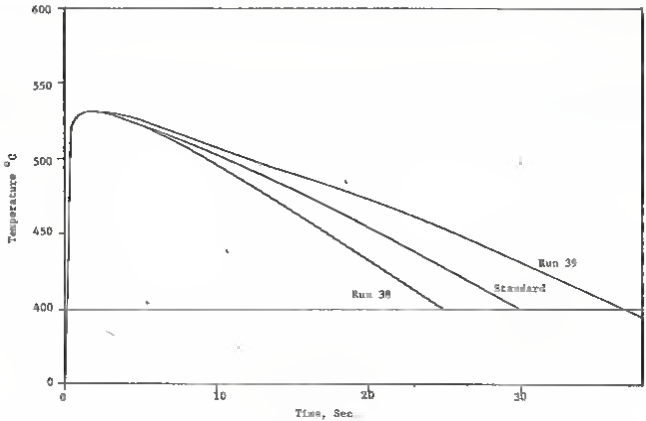

Figure 33 Effect on Cell Temperature of Changes in the Intra-Cell Heat Generation

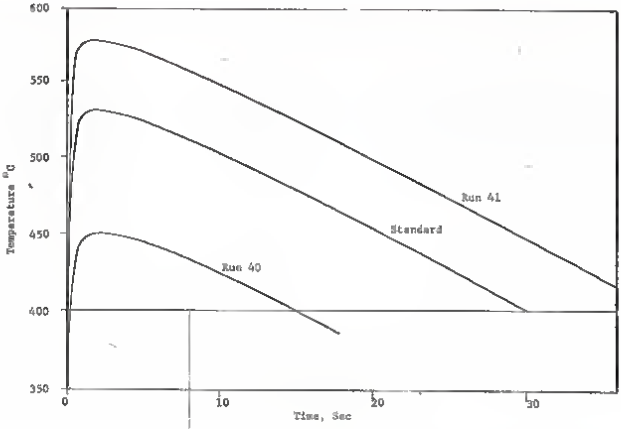

Figure 34 Effect on Cell Temperature of the Heat Sink Temperature

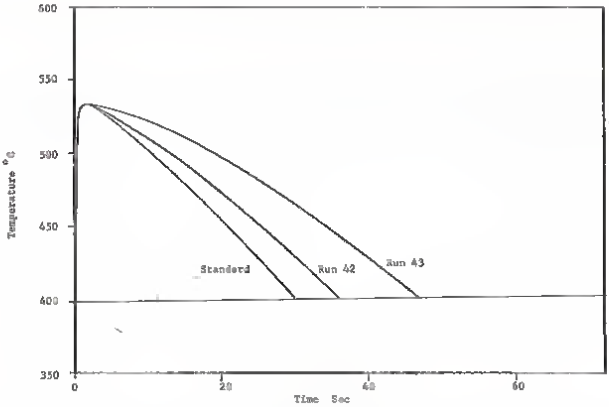

Figure 35 Effect on Cell Temperature of Changes in the Heat Capacity of the Heat Generatore

an increase of 20% above the life of the standard battery could be achieved by doubling the heat capacity (or the density) of the heat generators, and that an increase of 50% could be accomplished if it could be quadrupled.

8. Core Temperature of Improved Thermal Battery

Figure 36 illustrates the effect that some feasible design improvements could have on the life of the battery. It was assumed that an all-Thermoflex layer could be used, that an electrochemical system could be developed which would yield twice the intra-cell heat generation of the standard battery, and that the density or heat capacity of the heat generators could be doubled. The results indicate that an increase in battery life of about 50% could be obtained

9. Effect on Core Temperature of Delayed Heat Generation Within the Insulation

The effect of delayed heat generation within the insulation was found to be very beneficial to battery life. Figure 37 indicates that in some arrangements of this type, the life of the battery could be doubled. This change appears to be more difficult to implement from a design standpoint than those suggested before. The main difficulty appears to be in the manner in which the delayed heat generation is to be achieved. It was found that commonly used heat generators could not be placed in intimate contact with the core because their ignition would increase the temperature of the core above the upper limit. Placing a layer of Thermoflex of about 1 mm in thickness between the core and the heat generator seemed to prevent the core temperature from rising too high and at the same time provided good insulation for the

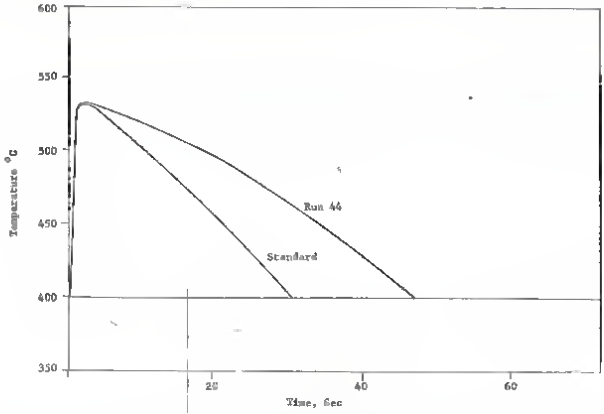

Figure 36 Effect on Cell Temperature of Suggested Design Improvements

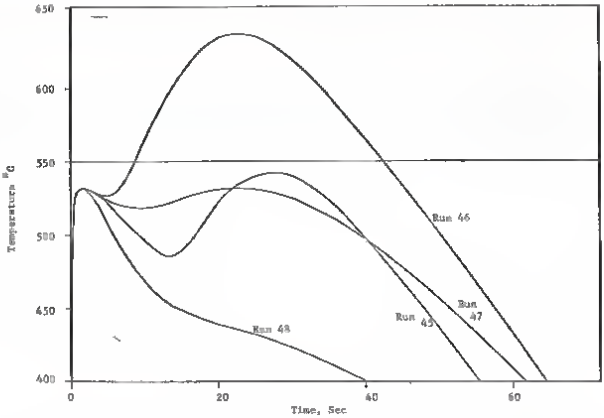

Figure 37 Effect on Cell Temperature of Delayed Heat Generation within the Insulation

core, thus increasing the life of battery considerably.

10. Effect of Change in the Volume of the Battery on Core Temperature

The effect of a change in the volume of the battery on the core temperature constituted an important test of the mathematical model. Figure 38 illustrates the results which again are in reasonable agreement with experimental observations. It should be noted that an increase in the volume of the battery does not change the peak temperature appreciably but it reduces the rate of temperature decay very considerably. This is a consequence of the volume increasing as the third power of the radius while the area increases only as the square of the radius. Therefore, the total amount of heat generated will increase more rapidly (since it is constant per unit volume) than the increase in the rate of heat loss (which is proportional to the area).

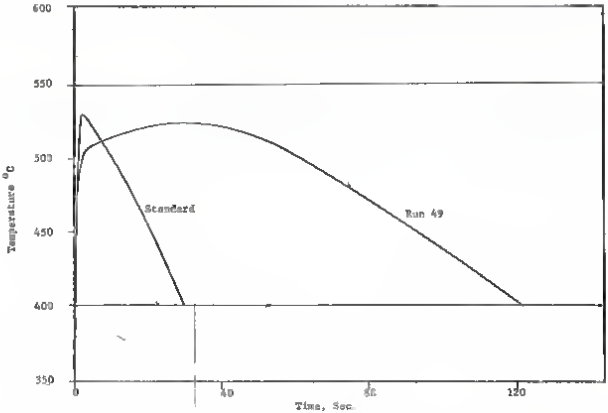

Figure 38 Effect on Cell Temperature of a Change in the Volume of the Battery

CHAPTER VI

CONCLUSIONS AND RECOMMENDATIONS

The objectives of this work were to provide temperature histories for specific locations within a simulated thermal battery and to study the effect of changing the construction configuration and properties of the materials so to optimize battery life and to understand the effects that these changes produce. It was concluded that the analog computer models provided an adequate representation of thermal batteries for drawing qualitative conclusions. They also provided very useful insight into the heat transfer processes that occur in a battery, and this was quite valuable for the development of the digital computer model.

The digital model was a more complete representation of a thermal battery than were the analog models, and it permitted some complex configurations to be simulated.

The results of this investigation indicate that some gain in battery life could be effected if an all-Thermoflex insulation were used instead of the standard Thermoflex-asbestos configuration. It was concluded that the ratio of core volume to insulation volume in the standard battery studied was essentially optimum. The results also indicated the desirability of developing systems which would have higher intra-cell chemical heat generation than the one used in the standard battery. Heat generators having a higher thermal conductivity or density than the standard were shown to be beneficial to battery life.

An examination of the cooling portion of the temperature histories shows that battery life could be extended appreciably if electrochemical systems could be developed which would remain in a molten state below 400°C. It was also shown that placement of heat generators in the insulation section surrounding the core could provide a delayed heat input to the assembly and substantially increased life, but this improvement may not be feasible at this time because of difficulty in controlling the time delay of the heat generator ignition.

It was further concluded that the choice of a cut-off temperature of 480°C as the criterion for battery life strongly influenced the choice of an optimum idealized insulator. For an arbitrary cut-off temperature there exists an ideal material which should have the lowest possible thermal conductivity and value of density and heat capacity which should be low if the cut-off temperature is high and high if the cut-off temperature is low. It should be noted that the lowest value of thermal diffusivity for the insulation does not yield the maximum life above 400°C.

LIST OF SYMBOLS

A	area, cm^2
A	heat sink temperature, ^oC
C	temperature of the core, ^oC
C_p	heat capacity, $\frac{cal}{gm^oC}$
F	defined by equation III-4, dimensionless factor to allow for interchange between gray surfaces
$\bar{F}$	dimensionless factor to allow for interchange between black surfaces
G	defined by equation III-5
h	height of element, cm
H	pseudo-convection heat transfer coefficient, $\frac{cal}{cm^2 sec^o C}$
k	thermal conductivity, $\frac{cal\ cm}{cm^2 sec^o C}$
L	temperature of lateral insulation, ^oC
q	rate of heat transfer, $\frac{cal}{sec}$
Q	rate of heat transfer
R	radius of element, cm
S	height of lateral insulation, cm
t	time, sec.
T	temperature of element, ^oC
V	volume, cm^3

Greek Letters

α	thermal diffusivity
β	defined by equation C-5

Greek Letters (continued)

ϵ	emissivity, dimensionless
ρ	density, g/cm^2
σ	Stefan-Boltzmann Constant

Subscripts

s	refers to the heat sink
A	refers to the heat sink
c	refers to the cell, or to the core
g	refers to the generator
i	refers to the insulation or to the ith element
j	refers to the jth element
l	refers to lateral
L	refers to lateral
m	refers to middle, i.e., mg refers to middle generators
r	refers to radius
R	refers to radiation
t	refers to top
T	refers to top
1	refers to element number 1
2	refers to element number 2
3	refers to element number 3
4	refers to element number 4

LITERATURE CITED

1 Goodrich, R. E., and Evans, R. G., J. Electrochem. Soc., 99, p. 207c (1952).

2. Vinal, G. W., "Primary Batteries," John Wiley & Sons, Inc., New York (1930).

3 Selis, S. M., et al, J. Electrochem. Soc., 110, p. 469 (1963)

4 McKee, H. E., Proc. 10th Annual Battery Res. and Dev. Conf., p. 25, New Jersey (1956)

5 Johnson, L. E., Ind. Eng. Chem., 52, p. 868 (1960)

6 Hill, R. A. W., Trans. Farad. Soc., 53, p. 1136 (1957)

7. Jakob, M., "Heat Transfer", vol. I, John Wiley and Sons, Inc., New York, p. 393 (1949).

8. Biot, J. B., Bibliotecque Britannique, 27, p. 310 (1804).

9. Fourier, J. B. J., "Theorie Analitique de la Chaleur", Paris (1822).

10. Newton, I., Phil. Trans. Roy. Soc. London, 22, p. 824 (1701).

11. Stefan, J., Sitzungsber. K. Kais. Akad. D. Wiess. Wien. Math.-Naturwiss. Klasse, 79, p. 391 (1879)

12 Boltzmann, L., Wiedemanns Annalen, 22, p. 291 (1884)

13. Carslaw, H. S., and Jaeger, J. C., "Heat Conduction In Solids", Second Ed. Oxford (1959)

14. McAdams, W. S., "Heat Transmission", Third Ed., McGraw-Hill, New York (1954)

15. Anthony, M. L., General Discussion on Heat Transfer, Inst. Mech. Engrs. (London) and Am. Soc. of Mech. Engrs. (1951)

16. Newcomb, T. P., British J. Appl. Phys., 9, p. 370 (1958)

17. Wasserman, S., J. Aero. Science, 24, p. 524 (1957)

18. Slade, P., J. Aero Science, 25, p. 523 (1958).

19. Friedman, M. E., Trans. Am. Inst. Mech. Engr., 80, p. 633 (1958)

20 Yang, K. T., J Appl. Mech , 25, p 146 (1958)

21. Surney, S P , and Lurie, J Ind Eng Chem , 15, p 1170 (1925)

22. Groeber, J., Zeitschr d. Ver deutsch. Ing , 69, p 705 (1925)

23. Olson, F C W., and Schultz, O T., Ind Eng Chem , 34, p 874 (1942)

24 Newman, A. B., Ind. Eng Chem., 38, p 545 (1936)

25. Heisler, M P., Trans. Am. Soc Mech Engrs., 69, p. 227 (1947)

26 Rosenhow, W M , Trans Am. Inst Mech Engrs , 68, p. 195 (1946)

27. Paschkis, V , and Hilnka, J. W., Trans Am. Inst Mech Engrs , 79, p. 1742 (1957)

28. Binder, L., Dissertation, Techn. Hochschule Muenchen, Munich (1911)

29 Schmidt, E., Forsch Gebiete Ing., 13, p 177 (1942).

30. Nessi, A., and Nisselin, L , "Methodes graphiques pour l'etude des installations de chauffage", Dunod, Paris (1929)

31 Patton, T C., Trans Am. Inst Mech Engrs., 66, p 990 (1944)

32. Longwell, P A., A I.Ch.E Journal 4, p 53 (1958)

33. Langmuir, I., Adams S Q., and Meikle, G. S., Trans Am. Electro Chem. Soc., 24, p 53 (1913)

34. Benkon, C L., Dissertation, Sachs Bergakademie Frieberg, Triltsch and Huther, Berlin (1936)

35. Paschkis, V., and Baker, B D , Trans Am Inst Mech Engrs , 64, p 105 (1942)

36. Karplus, S. J , and Sarnke, W W , 'Analog Methods", McGraw-Hill New York (1959)

37 Emmons, S. W., Trans. Am. Soc Mech Engrs., 65, p. 607 (1943)

38 Southwell, S V , "Relaxation Methods in Engineering Science", Oxford University Press, New York (1940)

39 Allen, S N de G., "Relaxation Methods", McGraw-Hill, New York (1954)

40 Duclaberre, C M , Trans Am Soc Mech Engrs 67, p. 703 (1945)

41. Mickley, H. S., Sherwood, J. K., and Reed, C. E., "Applied Mathematics in Chemical Engineering", Second Ed. McGraw-Hill, New York (1957)

42. Hildebrand, F. E., J. Math. Phys., 31, p. 35 (1952)

43. Evans, G. W., et al, J. Math. Phys., 34, p. 267 (1956)

44. Brian, P. L. T., A.I.Ch.E. Journal 7, p. 367 (1961).

45. Douglas, J., Jr., and Peaceman, D.W., A.I.Ch.E. Journal 1, p. 505 (1955).

46. Yaverskv, P. M., et al, Ind. Eng. Chem., 51, p. 833 (1959)

47. Dickert, S. P., M. S. Thesis, U. of Fla., Gainesville, Fla. (1960)

48. Horne, R. A., and Richardson, E. L., Proc. 18th Annual Battery Res. and Dev. Conf., p. 75, New Jersey (1964)

49. Forsyth, A. R., "Calculus of Variations", Dover Publications, Inc., New York (1960)

50. Walker, R. E., Jr., and Chipley, E. L., private communication, (Dec., 1964)

51. Perry, J. E., "Chemical Engineers' Handbook", Third Ed., O. 488, McGraw-Hill, New York (1950)

52. Brown, G. G., "Unit Operations", John Wiley & Sons, Inc., New York, (1956)

53. Johnson, C. L., "Analog Computer Techniques", McGraw-Hill, New York, (1956)

54. Bird, R. B., Stewart, W. E., and Lightfoot, E. N., "Transport Phenomena", John Wiley and Sons, Inc., New York (1960)

55. Shell, D. L., General Electric Company Technical Information Series No. DF 58AGT679, G.E. Co., Cincinnati, Ohio.

56. Milne, W. E., "Numerical Calculus," Princeton University Press, New Jersey (1949)

57. Gill, P., Proc. Cambr. Phil. Soc. 47, Part 1, (1951)

58. Lapidus, L., "Digital Computation for Chemical Engineers", McGraw-Hill, New York (1962)

59. Hamming, R. W., "Numerical Methods for Scientists and Engineers", McGraw-Hill, New York (1962)

60. Pelechild, E. T., Wengraw, E. R., and May, P. P., "AMSS: Numerical Integration of Differential Equations with the Adams-Moulton-Shell Method", Chem. Eng. Dept., U. of Fla. Gainesville, Fla. (1965)

APPENDICES

APPENDIX A

DETAILS OF ANALOG MODEL I

COMPUTATION OF HEAT TRANSFER COEFFICIENTS

The following heat transfer coefficients yield the values for the potentiometer settings listed in Table 1 (based on the data given in Table 2).

$$H_{ti-s} = \left[\frac{1}{0.0002}\ \frac{0.156}{2}\right]^{-1} = 0.00256$$

$$H_{ti-li} = \left[\frac{0.46}{0.0002} + \frac{1}{0.0002}\ \frac{0.156}{2}\right]^{-1} = 0.000372$$

$$H_{ti-g} = \left[\frac{1}{0.0002}\ \frac{0.156}{2} + \frac{1}{0.0005}\ \frac{0.1}{2}\right]^{-1} = 0.002$$

$$H_{g-li} = \left[\frac{1}{0.0002}\ \frac{0.156}{2} + \frac{0.46}{0.0005}\right]^{-1} = 0.000763$$

$$H_{g-c} = \left[\frac{1}{0.0005}\ \frac{0.1}{2} + \frac{1}{0.1ft}\ \frac{0.1}{2}\right]^{-1} = 0.01$$

$$H_{c-li} = \left[\frac{1}{0.0002}\ \frac{0.156}{2} + \frac{.46}{1ft}\right]^{-1} = 0.00254$$

$$H_{li-s} = H_{ti-s}$$

Note: The value of 0.46 is the radius of the circle having an area equal to one-half of the circle whose radius is 1.56.

TABLE A-1

SUMMARY OF RUNS

Run No.	Description	Results
1	Standard	Tabulated in Table 3, Shown in Figures 5, 6 and 7
2	$k_L = 1/2\ X$	Tabulated in Table 3, Shown in Figure 8
3	$k_1 = 1.5X$	Tabulated in Table 3, Shown in Figure 9
4	$h_{t1} = 2X$	Tabulated in Table 3, Shown in Figure 10
5	$h_{tg} = 2X$	Tabulated in Table 3, Shown in Figure 11
6	$\rho_g = 2X$, $h_{tg} = 1/2\ X$	Tabulated in Table 3, Shown in Figure 12
7	$h_c = 1\ 2X$	Tabulated in Table 3, Shown in Figure 13
8	$h_c = 1.5X$	Tabulated in Table 3, Shown in Figure 13
9	$h_c = 2X$	Tabulated in Table 3, Shown in Figure 13
10	$\rho_a Q_{pc} = 0.5X$	Tabulated in Table 3, Shown in Figure 14

Run No.	Description	Results
11	$\rho_c C_{pc} = 1$ 2X	Tabulated in Table 3, Shown in Figure 14
12	Change Magnitude of Intra-cell Heat Generation	Tabulated in Table 3, Shown in Figure 15
13	Change Initial Rate of Intra-cell Heat Generation	Tabulated in Table 3, Shown in Figure 16
14	Change Decay Rate of Intra-cell Heat Generation	Tabulated in Table 3; Shown in Figure 17

TABLE A-2

SUMMARY OF POTENTIOMETER SETTINGS

Run No.	1	2	3	4	5
Pot. No.					
1	0.663	0.3583	0.974	0.328	0.700
2	0.123	0.075	0.184	0.132	0.076
3	0.744	0.692	0.804	0.748	0.235
4	0.266	0.163	0.398	0.143	0.324
5	0.163	0.145	0.143	0.143	0.0715
6	0.062	0.0378	0.0565	0.022	0.067
7	0.0319	0.0152	0.015	0.015	0.0256
8	0.2907	0.288	0.292	0.292	0.148
9	0.126	0.130	0.132	0.138	0.064
11	0.00346	0.0034	0.0034	0.0034	0.00346
12	0.123	0.123	0.123	0.123	0.0615
14	0.1395	0.070	0.208	0.069	0.1395
15	0.021	0.0176	0.0254	0.0067	0.017
17	0.00366	0.0019	0.0054	0.0018	0.00366
18	0.0063	0.0031	0.0095	0.0063	0.0063
19	0.8644	0.451	1.280	0.745	0.8591
20	0.0107	0.0053	0.014	0.005	0.0107
21	0.006	0.0056	0.008	0.0062	0.003
22	0.00465	0.00234	0.0069	0.0046	0.0058
23	0.003	0.0030	0.00435	0.0034	0.0015
24	0.615	0.615	0.615	0.615	0.153
25	0.143	0.143	0.143	0.143	0.0715
31	0.050	0.050	0.050	0.050	0.050
32	0.050	0.050	0.050	0.050	0.050
34	0.0071	0.0071	0.0071	0.0071	0.0071
42	0.615	0.615	0.615	0.615	0.615
43	0.615	0.615	0.615	0.615	0.615
44	0.321	0.321	0.321	0.321	0.312
45	0.715	0.714	0.714	0.714	0.715
49	0.143	0.143	0.143	0.143	0.143
50	0.308	0.308	0.308	0.308	0.308
53	0.715	0.714	0.714	0.714	0.715

TABLE A2 (Continued)

Run No.	6	7	8	9	10
Fat No.					
1	0.621	0.700	0.700	0.663	0.663
2	0.105	0.076	0.076	0.123	0.123
3	1.608	0.235	0.235	0.744	0.744
4	0.243	0.324	0.324	0.286	0.286
5	0.286	0.0948	0.119	0.0715	0.179
6	0.024	0.0374	0.040	0.0337	0.042
7	0.0364	0.0284	0.0304	0.0256	0.0319
8	0.577	0.194	0.243	0.164	0.364
9	0.247	0.064	0.064	0.126	0.126
11	0.00366	0.0052	0.00615	0.007	0.00346
12	0.246	0.0615	0.0615	0.123	0.123
14	0.159	0.186	0.159	0.224	0.1395
15	0.012	0.018	0.020	0.0166	0.021
17	0.00366	0.00366	0.00366	0.00366	0.00366
18	0.0063	0.0063	0.0063	0.0063	0.0063
19	0.8614	0.300	0.879	0.5301	0.8544
20	0.0107	0.0107	0.0107	0.0107	0.0107
21	0.003	0.003	0.003	0.006	0.006
22	0.0058	0.0058	0.0058	0.0058	0.0058
23	0.0015	0.0015	0.0015	0.003	0.003
24	1.30	0.153	0.153	0.615	0.615
25	0.286	0.948	0.119	0.0715	0.179
31	0.050	0.050	0.050	0.050	0.050
32	0.050	0.050	0.050	0.050	0.050
34	0.0071	0.0071	0.0071	0.0071	0.0071
42	0.615	0.615	0.615	0.615	0.615
43	0.615	0.615	0.615	0.615	0.615
44	0.321	0.321	0.321	0.321	0.321
45	0.715	0.472	0.596	0.357	0.895
49	0.143	0.0948	0.119	0.0719	0.179
50	0.308	0.308	0.308	0.308	0.308
53	0.715	0.672	0.594	0.357	0.895

TABLE A-2 (Continued)

Run No. 11

Pot. No.	
1	0.663
2	0.123
3	0.744
4	0.286
5	0.119
6	0.042
7	0.0319
8	0.242
9	0.126
11	0.00346
12	0.123
14	0.1395
15	0.021
17	0.00366
18	0.0063
19	0.8644
20	0.0107
21	0.006
22	0.0039
23	0.003
24	0.615
25	0.119
31	0.050
32	0.050
34	0.0071
42	0.615
43	0.615
44	0.321
45	0.595
49	0.119
50	0.308
53	0.595

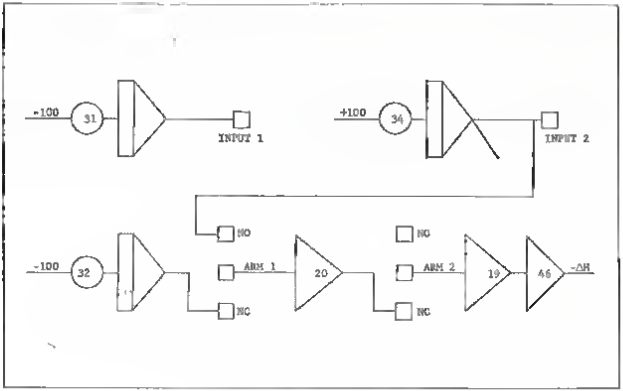

Figure A-2 Analog Circuit of Heat of Reaction Term

APPENDIX B

DETAILS OF ANALOG MODEL II

AREA AND VOLUME OF THE INSULATION ELEMENTS OF MODEL II

The lateral area and volume of the cap insulation elements assumed in Model II can be evaluated by the methods of elementary calculus. The equation of the straight line shown in Figure B-1a is

$$y = \frac{h}{(R_2 - R_1)} (R - R_1) \tag{B-1}$$

This line can be rotated around the y axis to yield the shape of the insulation element. The area of the element is given by

$$A_T = \int_{A_1}^{A_2} dA = \int_{y_1}^{y_2} 2\pi R\,dy = \int_{R_1}^{R_2} \frac{2\pi R h}{R_2 - R_1} \tag{B-2}$$

Therefore, the area is

$$A_T = \frac{2\pi h}{R_2 - R_1} \frac{R_2^2 - R_1^2}{2} = \pi h(R_2 + R_1) \tag{B-3}$$

The volume of a cap element is given by

$$V_T = \int_{V_1}^{V_2} dV = \int_{y_1}^{y_2} \pi R^2\,dy = \int_{R_1}^{R_2} \frac{\pi R^2 h}{R_2 - R_1}\,dR \tag{B-4}$$

which becomes

$$V_T = \frac{\pi h(R_2^3 - R_1^3)}{3(R_2 - R_1)} = \frac{\pi h}{3}(R_2^2 + R_1 R_2 + R_1^2) \tag{B-5}$$

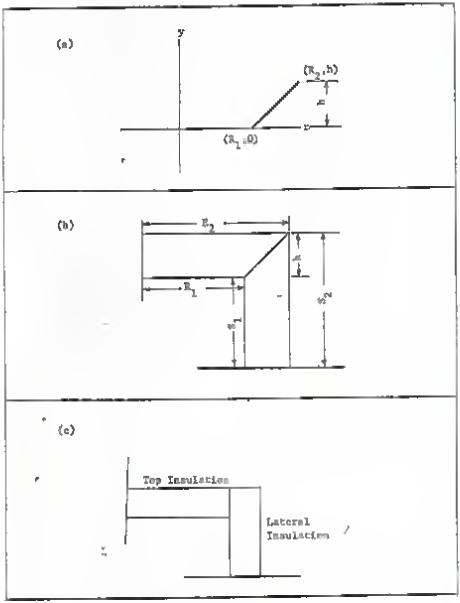

Figure B-1 Details of the Shape of Insulation Elements

The volume of a lateral insulation element can now be expressed as

$$V_L = \pi R_2^2 - \frac{\pi h}{3}(R_2^2 + R_1 R_2 + R_1^2) + \pi(R_2^2 - R_1^2)\delta_1 \qquad (B\text{-}6)$$

where δ_1 is defined in Figure B-D. This expression simplifies to

$$V_L = \frac{\pi h}{3}(2R_2^2 - R_1 R_2 - R_1^2) + \pi(R_2^2 - R_1^2)\delta_1 \qquad (B\text{-}7)$$

It should be noted that the dimensions of the model are such that $\delta_1 = R_1$ and $h = \delta_2 - R_1$. When these expressions are substituted into equation(B-7)it becomes

$$V_L = \frac{\pi(R_2 - R_1)}{3}(2R_2^2 - R_1 R_2 - R_1^2) + \pi R_1(R_2^2 - R_1^2) \qquad (B\text{-}8)$$

or

$$V_L = \frac{\pi(R_2 - R_1)}{3}(2R_2^2 - R_1 \delta_2 - R_1^2) + R_1(R_2 + R_1) \qquad (B\text{-}9)$$

which yields upon simplification

$$V_L = \frac{2\pi h}{3}(R_2^2 + R_1 R_2 + R_1^2) \qquad (B\text{-}10)$$

Equation(B-10)illustrates the fact that for these dimensions and this model the volume of a lateral insulation element is twice the volume of the corresponding top insulation element. This circumstance thus offers a simplification in the calculation of the potentiometer settings, furthermore, it reduces the number of elements with which a given element of lateral insulation may be center. This is illustrated in Figure B-1c where it is seen that the element of lateral insulation is an alternate structure has two faces in contact with the heat sink, thus giving a more complicated system of equations.

COMPUTATION OF HEAT TRANSFER COEFFICIENTS

The following equations for heat transfer coefficients yield the values for the potentiometer settings listed in Table 6 based on the data given in Table 7.

$$R_5 = 1.90$$

Element 4 Metal $\quad R_4 = 1.80$

Element 3 Mica $\quad R_3 = 1.79$

Element 2 Asbestos $\quad R_2 = 1.69$

Element 1 Thermoflex $\quad R_1 = 1.59$

$$H_{T44} = H_{L44} = \left[\frac{1}{.110}\ .05\right]^{-1} = 2.20$$

$$H_{T43} = H_{L43} = \left[\frac{1}{.110}\ .05 + \frac{1}{.001}\ .005\right]^{-1} = .183$$

$$H_{T32} = H_{L32} = \left[\frac{1}{.001}\ .005 + \frac{1}{.0004}\ .05\right]^{-1} = .0077$$

$$H_{T21} = H_{L21} = \left[\frac{1}{.0004}\ .05 + \frac{1}{.0002}\ .05\right]^{-1} = .00267$$

$$H_{T10} = \left[\frac{1}{.0002}\ .05 + \frac{1}{(.005)}\ .795\right]^{-1} = .00245$$

$$H_{TL4} = \left[\frac{1}{.110}\ (.530 + .925)\right]^{-1} = .0756$$

$$H_{TL3} = \left[\frac{1}{.001}\ (.527 + .897)\right]^{-1} = .0007$$

$$H_{TL2} = \left[\frac{1}{.0004}\ (.500 + .870)\right]^{-1} = .0003$$

$$H_{LL1} = \left[\frac{1}{.0002} \left(.470 + .820 \right) \right]^{-1} = .00015$$

$$H_{LLC} = \left[\frac{1}{.0002} \; .05 + \frac{1}{(.005)} \; .445 \right]^{-1} = .00292$$

TABLE B-1

SUMMARY OF RUNS

Run No.	Insulation Structure	Results
15	4 Metal 3 Mica 2 Asbestos (Standard) 1 Thermoflex	Tabulated in Table 8 Shown in Figure 20
16	4 Thermoflex 3 Mica 2 Asbestos 1 Metal	Tabulated in Table 8 Shown in Figure 21
17	4 Asbestos 3 Asbestos 2 Thermoflex (Standard) 1 Thermoflex	Tabulated in Table 8 Shown in Figure 22
18	4 Thermoflex 3 Thermoflex 2 Asbestos 1 Asbestos	Tabulated in Table 8 Shown in Figure 23
19	4 Asbestos 3 Thermoflex 2 Thermoflex 1 Thermoflex	Tabulated in Table 8 Shown in Figure 24
20	4 Thermoflex 3 Thermoflex 2 Thermoflex 1 Thermoflex	Tabulated in Table 8 Shown in Figure 25

TABLE 8-2

SUMMARY OF POTENTIOMETER SETTINGS

Run No	15	16	17	18	19
Pot No.					
1	26.35	2.635	1.066	5.40	0.934
4	24.44	1.40	0.710	5.665	0.710
5	1.824	1.23	0.355	1.73	0.223
6	0.086	0.0054	0.00068	0.002	0.00068
2	34.31	2.077	0.587	4.20	4.24
11	32.96	0.705	0.360	1.86	2.48
10	1.371	1.371	0.226	2.34	1.76
12	0.0014	0.0014	0.00076	0.0037	0.0039
3	0.2314	0.340	4.244	0.571	3.626
15	0.1762	0.1762	2.48	0.240	1.86
16	0.0546	0.163	1.76	0.331	1.76
17	0.00075	0.00075	0.0041	0.00077	0.0041
8	1.155	0.249	3.384	0.547	3.384
22	0.635	0.0895	1.85	0.357	1.85
25	0.516	0.0620	1.53	0.190	1.53
24	0.0040	0.0972	0.0044	0.00085	0.0044
9	0.0121	0.0246	0.0118	0.01608	0.0118
23	0.00357	0.00912	0.00513	0.00658	0.00513
28	0.0085	0.0155	0.00667	0.0095	0.00667
29	0.500	0.500	0.500	0.500	0.500
19	26.31	2.635	1.085	5.40	0.933
31	0.043	0.0027	0.0003	0.001	0.00034
32	24.44	1.40	0.710	5.665	0.710
35	1.824	1.23	0.355	1.73	0.223
20	34.31	2.077	0.366	4.20	4.24
33	0.0007	0.0007	0.0004	0.0001	0.002
36	32.94	0.705	0.360	1.86	2.48
37	1.371	1.371	0.226	2.34	1.78
21	0.2310	0.339	4.242	0.571	5.62
39	0.00038	0.00038	0.002	0.0004	0.002
40	0.1762	0.1762	2.48	0.240	1.86
41	0.0546	0.163	1.76	0.331	1.76
26	1.153	0.198	3.842	0.628	5.842
63	0.0020	0.0436	0.0022	0.0004	0.0022
44	0.635	0.0895	1.85	0.357	1.85
46	0.516	0.0620	1.99	0.271	1.99

TABLE B-2 (Continued)

Run No	20
Fat No	
1	5 40
4	3 665
5	1 73
6	0 002
2	3 61
11	1 86
10	1 75
12	0 0037
3	3 624
15	1 86
16	1 76
17	0 0041
6	3 384
22	1 85
23	1 53
24	0 0044
9	0 0118
25	0 00513
28	0 00667
29	0 5
19	5 40
31	0 001
32	3 665
33	1 73
20	3 61
35	0 002
36	1 86
37	1 75
21	3 624
39	0 008
40	1 86
41	1 76
26	3 54
43	0 002
44	1 85
46	1 99

COMPUTATION OF FIRST ORDER TRANSFER FUNCTION
USED TO SIMULATE HEAT GENERATORS

Pot. 27 = 0.1 and Pot. 29 = 0.5

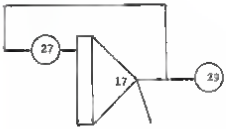

The amplifier circuit represents the following function

$$J = -\frac{dJ}{dt} \qquad (B-11)$$

$$\frac{dJ}{J} = -dt \qquad (B-12)$$

$$\ln J = -t + c, \quad J = ce^{-t} \qquad (B-13)$$

$$\text{at } t = 0 \quad J = -40 \qquad (B-14)$$

$$J = -40e^{-t} \quad \text{volts} \qquad (B-15)$$

$$\text{Since 1 volt} = 25^{\circ} \quad J = -1025e^{-t} \qquad (B-16)$$

$$\text{Since Pot. 29} = 0.5, \ \frac{\Delta H}{\rho C_p} \int_0^{\infty} 512e^{-t}\,(12.6\text{sec}) = 12.6(512) \qquad (B-17)$$

and hence the total heat given off by the core is given by

$$\Delta H = (.432)12.6(512) = 2785 \text{ cal} \qquad (B-18)$$

COMPUTATION OF HEAT GIVEN OFF BY CORE

Model I

Volume of Gen. = $\pi(1.56)^2(.15) = 1.15$ cc

Heat Given Off by Gen. = 1.25 (.130)(1.15)(2200-25) = 406 cal

Volume of Cell = $\pi(1.56)^2(.1) = .765$ cc

Weight of Cell = 3.48(.765) = 2.67 gms

Heat Per Unit Volume of Core in the First 5 sec = 213 cal/cc

Heat Per Unit Volume of Core From 5 to 80 sec = 120 cal/cc

Heat Per Unit Volume of Gen. in first 5 sec. = 333 cal/cc
283 cal/gm

Model II

Volume of Core = $\pi(1.59)^2(1.59) = 12.6$ cc

Heat Given Off by Core = 2785 cal

Heat Per Unit Volume of Core in the First 5 sec = 221 cal/cc

Heat Per Unit Weight of Gen. in First 5 sec. = 442 cal/cc
333 cal/gm

This result is a consequence of assuming equal generators and cell volumes in Model II whereas there is 50% more generators than cell volumes in Model I. It should be noted that on the basis of core volume, the amount of heat given off is essentially the same (213 and 221 cal/cc).

APPENDIX C

DETAILS OF DIGITAL MODEL III

SIMULATION OF CONDUCTION HEAT TRANSFER IN A HOMOGENEOUS SPHERE

In order to test the validity of the finite difference approximation to the partial differential equations describing heat conduction in a composite sphere, the computer program was used to simulate a system for which the analytical solution was known.

The model consisted of a homogeneous sphere having an initial temperature equal to 500°C everywhere except at the surface where the temperature was constant at zero degrees. The analytical solution for this model is presented by Carslaw and Jaeger (13).

The results for both the approximate and exact solutions are shown in Figure C-1.

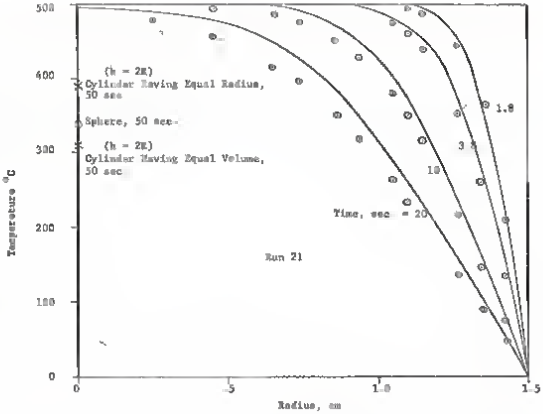

Figure C-1. Analytical Versus Computed Results for the Cooling of a Homogeneous Sphere

TABLE G-1

DATA USED IN SIMULATION OF STANDARD THERMAL BATTERY

The computation simultaneously solves 27 ordinary differential equations

Material	Radius	Density	Thermal Cond.	Heat Capacity
Core	1.50	2.36	0.00056	0.183
Thermoflam	1.60	2.193	0.0002	0.232
Thermoflam	1.70	2.193	0.0002	0.232
Asbestos	1.75	1.50	0.0004	0.308
Asbestos	1.79	1.50	0.0004	0.308
Mica	1.80	2.70	0.031	0.206
Metal	1.90	7.90	0.110	0.120

ΔH is represented by

$$\Delta H = 2185.0e^{-10.0t} + 0.050t \qquad \text{for } t < 15.0$$

and

$$\Delta H = 2185.0e^{-10.0(15.0)} + 0.050(15.0) - 0.817(t-15.0)$$

for $t > 15.0$

The well-mixed portion of the core has a radius of 1.323 cm.

TABLE C-2

SUMMARY OF RUNS

Run No	Description	Results
21	Carslow and Jaeger p. 234 (13)	Shown in Figure
22	Standard (20 points) (Thermoflex-asbestos)	Tabulated in Table 9 Shown in Figure 27
23	10 grid points	
24	30 grid points	
25	30 grid points, AMS 4	
26	40 grid points	
27	All-Thermoflex	Tabulated in Table 9 Shown in Figure 28
28	All-asbestos	Tabulated in Table 9 Shown in Figure 28
29	Asbestos-Thermoflex	Tabulated in Table 9 Shown in Figure 28
30	Mixinsulation	Tabulated in Table 9 Shown in Figure 28
31	All-Thermoflex k = 0 0001	Tabulated in Table 9 Shown in Figures 29 and 31
32	All-asbestos k = 0 0001	Tabulated in Table 9 Shown in Figures 29 and 31
33	All-asbestos k = 0 0001, β = 15	Tabulated in Table 9 Shown in Figure 29
34	All-asbestos k = 0 0001, β = 150	Tabulated in Table 9 Shown in Figure 29

TABLE C-2 (Continued)

Run No.	Description	Results
35	All-asbestos $k = 0.0001$, $\rho = 0.015$	Tabulated in Table 9 Shown in Figure 29
36	Radius of core = 1.40	Tabulated in Table 9 Shown in Figure 32
37	Radius of core = 1.60	Tabulated in Table 9 Shown in Figure 32
38	No heat of reaction	Tabulated in Table 9 Shown in Figure 33
39	$\Delta H = 2X$ (double intracell chemical heat generation)	Tabulated in Table 9 Shown in Figure 33
40	Heat sink temperature = -65°F	Shown in Figure 34
41	Heat sink temperature = 160°F	Shown in Figure 34
42	${}_BC_{PB} = 2X$	Tabulated in Table 9 Shown in Figure 35
43	${}_BC_{PB} = 4X$	Tabulated in Table 9 Shown in Figure 35
44	${}_BC_{PB} = 2X$ $k = 2X$ All-Thermoflex	Tabulated in Table 9 Shown in Figure 36
45	Generator outside Thermoflex (10 Sec delay)	Tabulated in Table 9 Shown in Figure 37
46	Generator outside Thermoflex (2 Sec delay)	Tabulated in Table 9 Shown in Figure 37
47	Generator (${}_BC_{PB} = 4X$) outside Thermoflex (2 Sec delay)	Tabulated in Table 9 Shown in Figure 37
48	Generator (${}_BC_{PB} = 4X$) outside asbestos (2 Sec delay)	Tabulated in Table 9 Shown in Figure 37
49	3-inch battery diameter	Tabulated in Table 9 Shown in Figure 38

MATHEMATICAL ILLUSTRATION OF THE SIMILARITY BETWEEN THE FINITE DIFFERENCE APPROXIMATION AND THE APPROXIMATION BASED ON WELL-MIXED (LUMPED PARAMETER) ELEMENTS

The equation which describes the unsteady-state heat transfer by conduction in a homogeneous body in one-dimensional Cartesian coordinates is given by

$$\frac{\partial T}{\partial t} = \alpha \frac{\partial^2 T}{\partial x^2} \qquad (C\text{-}1)$$

where $\alpha = k/\rho C_p$

The three-point central difference approximation of this partial derivative is given by

$$\frac{d^2 T}{dx^2} = \frac{T_{j+1} - 2T_j + T_{j-1}}{(\Delta x)^2} \qquad (C\text{-}2)$$

hence equation C-1 takes the form

$$\frac{dT_j}{dt} = \frac{\alpha}{(\Delta x)^2} \left[T_{j+1} - 2T_j + T_{j-1} \right] \qquad (C\text{-}3)$$

The heat transfer may be assumed to occur by transfer from one well-mixed element to an adjacent one having the thermal resistance lumped at the interface as shown in the following diagram

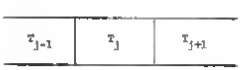

A heat balance on element j gives the following relation

$$AH(T_{j-1} - T_j) - AH(T_j - T_{j+1}) = \rho C_p A\Delta x \frac{dT_j}{dt} \qquad (C\text{-}4)$$

and this equation can be rewritten in the following form

$$\frac{dT_j}{dt} = \frac{\beta}{(\Delta x)^2}\left[T_{j+1} - 2T_j + T_{j-1}\right] \qquad (C\text{-}5)$$

where $\beta = \frac{H\Delta x}{\rho C_p}$

If equations (C-3) and (C-5) are compared, it is seen that if H is calculated by the relation $H = k/\Delta x$ the two equations are identical

In the case of spherical coordinates, the finite difference form of the heat transfer equation is given by

$$\frac{dT_i}{dt} = \alpha \frac{T_{i+1} - 2T_i + T_{i-1}}{\Delta R^2} + \frac{2}{R}\frac{T_{i+1} - T_{i-1}}{\Delta R} \qquad (C\text{-}6)$$

If $R = j\Delta R$ equation (C-6) reduces to

$$\frac{dT_j}{dt} = \frac{\alpha}{j\Delta R^2}\left[(j+1)T_{j+1} - 2jT_j + (j-1)T_{j-1}\right] \qquad (C\text{-}7)$$

The well-mixed (lumped resistance) approximation takes the following form

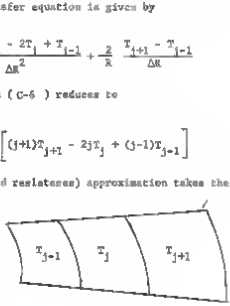

$$4\pi R_{j-1}^2 E(T_{j-1} - T_j) + 4\pi R_j^2 E(T_j - T_{j+1}) = \rho C_p 4\pi R_j^2 \Delta R \frac{dT_j}{dt} \qquad (C\text{-}8)$$

It should be noted that the expression for the volume of the element is a good approximation only for small values of ΔR

$$\frac{dT_j}{dt} = \frac{E}{j\Delta R^2}\left[jT_{j+1} + (2j - 1)T_j + (j - 1)T_{j-1}\right] \qquad (C\text{-}9)$$

Therefore, equations (C-7) and (C-9) are very similar, and it should be obvious that they approach the same limit as the number of grid points is increased, i.e., as the volume of the element approaches zero. It should also be noted, however, that for small values of j the difference between the two equations may be significant. This is a consequence of the form of the partial differential equations in spherical coordinates.

APPENDIX D

DETAILS OF THE COMPUTER PROGRAM

TABLE D-1

MNEMONICS OF 10DRV AND DERIV

ALPHA	α, Thermal Diffusivity
AVGT	Average Temperature of Element
B2	Auxiliary Constant
B3	Auxiliary Constant
C	Constants of Differential Equations
CP	Heat Capacity
DELR	Heat Generation of the Core
DELRG	Heat Generation of Generator Surrounding the Core
FJ	Floating Point Values of J1, J2, etc
HRG	Constant in Heat Generation of Core
INDEX	Parameter Indicating Whether a Heat Generator Exists in the Insulation
J1	Highest Grid Point Number of Element 1
J2	Highest Grid Point Number of Element 2
J3	Highest Grid Point Number of Element 3
J4	Highest Grid Point Number of Element 4
J5	Highest Grid Point Number of Element 5
J6	Highest Grid Point Number of Element 6
J7	Highest Grid Point Number of Element 7
JDCORE	Parameter Indicating Whether an Artificial Profile Will be Used to Initiate Run Instead of the Core Heat Generation

TABLE D-1 (Continued)

N	Number of Grid Points in Each Element
NAME	Material Making up Each Element
NELG	Element Number Which Becomes a Heat Generator
NFREQ1	Frequency of Output in Element 1
NFREQ1	Frequency of Output in Element 2
NFREQ3	Frequency of Output in Element 3
NFREQ4	Frequency of Output in Element 4
NFREQ5	Frequency of Output in Element 5
NFREQ6	Frequency of Output in Element 6
NFREQ7	Frequency of Output in Element 7
NPOINT	Highest Grid Point Number in the Assembly
R	Radius
RC	Radius of the Well-Mixed Section of the Core
RHO	Density
T	Time
TBREAK	Time at Which the Intra-Cell Heat Generation Term Begins to Decay
TEMP	Temperature
TEMPD	Derivative of the Temperature
THRCON	Thermal Conductivity
TKON	Coefficient of Exponent in Core Heat Generation Term
T&T	Coefficient of Exponent in Generator Heat Generation Term
SLOPE1	Initial Slope of Intra-Cell Heat Generation Term

TABLE B-1 (Continued)

SLOPEZ	Decay Slope of Intra-Cell Heat Generator Term
SUM	Sum of Grid Point Temperature Within an Element

Figure D-1 Flow Diagram for the AM#S Program

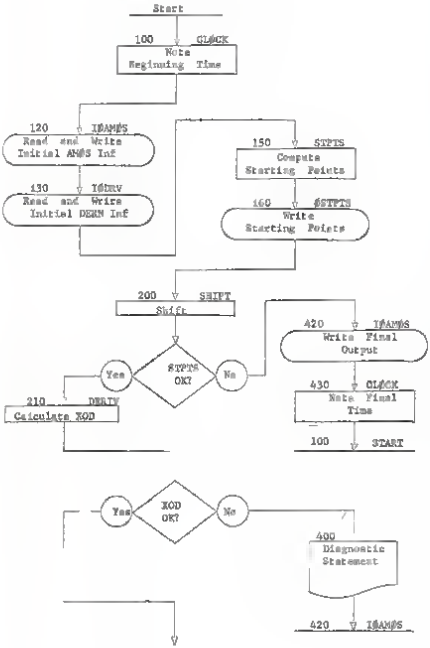

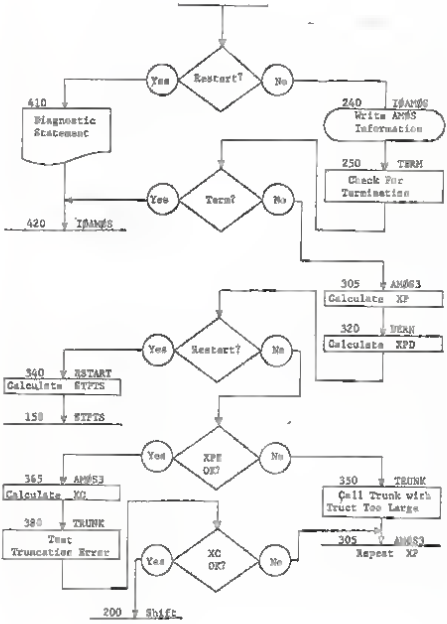
Restart?
Yes
No
410
Diagnostic Statement
240
IØAMØS
Write AMØS Information
250
TERM
Check For Termination
Term?
Yes
No
420
IØAMØS
305
AMØS3
Calculate XP
320
DERN
Calculate XPD
Restart?
Yes
No
340
RSTART
Calculate STPTS
150
STPTS
XPE OK?
Yes
No
365
AMØS3
Calculate XC
380
TRUNK
Test Truncation Error
350
TRUNK
Call Trunk with Truct Too Large
305
AMØS3
Repeat XP
XC OK?
Yes
No
200
Shift

```
C                    MAIN AND SUBROUTINE SUBPROGRAMS
C
C        XXX MAIN    THE SUPERVISORY PROGRAM
C       1XXX IOAMOS  HANDLES I/O FOR THE NUMERICAL ROUTINE
C                      JIOA1 = 1, INITIAL I/O
C                      JIOA1 = 2, NORMAL OUTPUT
C                      JIOA1 = 3, FINAL OUTPUT INCLUDING PUNCH OPTION
C                      JIOA1 = 4, MACHINE CLOCK OUTPUT
C       2XXX IODRV   HANDLES I/O FOR THE DIFFERENTIAL EQUATIONS
C                      JIOD1 = 1, INITIAL I/O
C                      JIOD1 = 2, NORMAL OUTPUT
C                      JIOD1 = 3, FINAL OUTPUT
C                      JIOD1 = 4, PUNCH OUTPUT IF OPTED
C       3XXX USTPTS  HANDLES OUTPUT FOR STARTING POINTS
C       5XXX SLTUP   INITIALIZATION
C                      JSU1 = 1, IMMEDIATE INITIAL SETUP
C                      JSU1 = 2, SETUP AFTER INPUT READ
C       6XXX RSTART  SUPERVISORY PROGRAM FOR RESTARTING
C      10XXX AMUS4   5 POINT INTERPOLATION PROGRAM
C      11XXX AMUS1   THE 1 POINT AMOS EQUATIONS
C      12XXX AMUS2   THE 2 POINT AMOS EQUATIONS
C      13XXX AMUS3   THE 3 POINT AMOS EQUATIONS
C      14XXX AMUS4   THE 4 POINT AMOS EQUATIONS
C      15XXX AMUS5   THE 5 POINT AMOS EQUATIONS
C                      JAS1 = 1, PREDICTOR
C                      JAS1 = 2, CORRECTOR
C      17XXX TERM    THE TERMINATION CRITERIA
C                      JTM1 = 1, CONTINUE
C                      JTM1 = 2, TERMINATE
C      18XXX SHIFT   THE SHIFTING ROUTINE
C      19XXX TRUNK   TEST TRUNCATION ERROR AND ADJUST INCREMENT SIZE
C                      JTR1 = 1, ACCEPT COMPUTED VALUES
C                      JTR1 = 2, REJECT COMPUTED VALUES
C                      JTR2 = 1, NORMAL ENTRANCE
C                      JTR2 = 2, ENTER WITH TRUNCT TOO LARGE
C       2XXXX DERIV  COMPUTES DERIVATIVES
```

```
C                    JOV1 = 1, SETUP ENTRANCE
C                    JOV1 = 2, NORMAL ENTRANCE
C                    JOV2 = 1, ACCEPTABLE EXIT
C                    JOV2 = 2, UNACCEPTABLE EXIT
C                    JOV3 = 1, ACCEPTABLE EXIT
C                    JOV3 = 2, RESTART COMMAND
C      3XXXX STPTS   COMPUTES STARTING POINTS
C                    JSP1 = 1, ACCEPTABLE EXIT
C                    JSP1 = 2, UNACCEPTABLE EXIT
C            CLOCK   ADDRESSES MACHINE CLOCK
```

```
C                         MNEMONICS
C
C     AMOS$ (J$,I)            SUBROUTINE FOR THE $ POINT AMOS INTEGRATION
C     AMOSW (X,I)             SUBROUTINE FOR THE 5 POINT INTERPOLATION
C     CLRT                    MACHINE CLOCK TIME
C     CLOCK (Z, CLRT, DATE)   SUBROUTINE TO ADDRESS MACHINE CLOCK
C     DATE                    THE DATE
C     DERIV (X, Y, XD, JDV1, JDV2, JDV3)    SUBROUTINE TO COMPUTE
C                             DERIVATIVES
C     FGONE                   FACTOR BY WHICH TIME INCREMENT IS INCREASED
C     FINCR                   FLOATING POINT INCR
C     FSONE                   FACTOR BY WHICH TIME INCREMENT IS DECREASED
C     H$                      TIME INCREMENT FROM POINT -$ TO POINT -$+1
C     HR$                     TIME FROM POINT -$-1 TO POINT -$+1
C     HRW                     TIME INCREMENT FROM POINT -1 TO POINT W
C     HL$                     TIME FROM POINT -$-2 TO POINT -$+1
C     HLW                     TIME INCREMENT FROM POINT -2 TO POINT W
C     HH$                     TIME FROM POINT -$-3 TO POINT -$+1
C     HHW                     TIME INCREMENT FROM POINT -3 TO POINT W
C     HOEST                   SUGGESTED INITIAL TIME INCREMENT
C     HONEW                   NEW TIME INCREMENT DETERMINED BY SUBROUTINE
C                             TRUNK
C     HW                      TIME INCREMENT FROM POINT  0 TO POINT W
C     I                       FIRST SUBSCRIPT FOR ARRAYS
C     IDENTIFI                ALPHANUMERIC INFORMATION ARRAY
C     IMAX                    MAXIMUM VALUE OF I
C     INCPL1                  INCREMENT NUMBER PLUS ONE
C     INCPL2                  INCREMENT NUMBER PLUS TWO
C     INCR                    INCREMENT NUMBER
C     INCRO                   DUMMY INCREMENT NUMBER IN SUBROUTINE USTPTS
C     IOAMOS (JIO,I)          SUBROUTINE TO HANDLE I/O FOR AMOS
C     IODRV (X, Y, JIODIF     SUBROUTINE TO HANDLE I/O FOR THE
C                             DIFFERENTIAL EQUATIONS
C     J                       SECOND SUBSCRIPT FOR ARRAYS
C     JASI                    ARGUMENT IN SUBROUTINE AMOS$
C     JAMOS                   DEGREE OF AMOS$
```

C	JDIAG	CONTROLS DIAGNOSTIC OUTPUT
C	JDVS	ARGUMENTS IN SUBROUTINE DERIV
C	JIDAI	ARGUMENT IN SUBROUTINE IDAMOS
C	JIDDI	ARGUMENT IN SUBROUTINE IDORV
C	JMAX	MAXIMUM VALUE OF J
C	JOSTPT	CONTROLS STARTING POINTS OUTPUT
C	JPUNOT	CONTROLS PUNCH OUTPUT
C	JSPI	ARGUMENT IN SUBROUTINE STPTS
C	JSUI	ARGUMENT IN SUBROUTINE SETUP
C	JTESTT	REMEMBERS PREVIOUS PATH THROUGH SUBROUTINE
C		TRUNK
C	JTM1	ARGUMENT IN SUBROUTINE TERM
C	JTP5	LOGICAL DESIGNATION OF INPUT TAPE
C	JTP6	LOGICAL DESIGNATION OF OUTPUT TAPE
C	JTR3	ARGUMENTS IN SUBROUTINE TRUNK
C	K	THIRD SUBSCRIPT FOR ARRAYS
C	KMAX	MAXIMUM VALUE OF K
C	LOOP	CONTROLS CORRECTOR LOOP IN SUBROUTINE STPTS
C	NCORR	NUMBER OF UTILIZATIONS OF THE CORRECTOR
C		EQUATIONS
C	NDRV	NUMBER OF UTILIZATIONS OF SUBROUTINE DERIV
C	NEQ	NUMBER OF EQUATIONS
C	NPRED	NUMBER OF UTILIZATIONS OF THE PREDICTOR
C		EQUATIONS
C	OSTPTS	SUBROUTINE TO HANDLE OUTPUT FOR THE
C		STARTING POINTS
C	P4	CONSTANTS IN AMOS EQUATIONS
C	RSTART	SUBROUTINE TO SUPERVISE RESTART
C	SETUP (JSUII	SUBROUTINE FOR INITIALIZATION
C	SHIFT	SUBROUTINE FOR SHIFTING
C	STPTS (JSPII	SUBROUTINE TO COMPUTE STARTING POINTS
C	T	TIME AT POINT 1
C	TU	DUMMY TIME IN SUBROUTINE OSTPTS
C	TERM (JTMII	SUBROUTINE CONTAINING TERMINATION CRITERIA
C	TERMT	TERMINATION CRITERIA FOR TIME
C	TIME	TIME AT POINT 0

```
C       TLOWER                  LOWER LIMIT FOR TRUNCATI[illegible]
C       TMBEG                   BEGINNING MACHINE TIME
C       TMEND                   ENDING MACHINE TIME
C       TMPAB                   TOTAL MACHINE TIME
C       TPERIN                  MACHINE TIME PER INCREMENT
C       TRESOL                  RESOLUTION OF WRIOT
C       TRUC                    CORRECTOR TRUNCATION CONSTANT
C       TRUEP                   TRUC + TRUP
C       TRUNC(I,J,K)            TRUNCATION ERROR
C       TRUNCK                  TRUC / (TRUC + TRUP)
C       TRUMCT                  LARGEST UP TRUNC(I,J,K)
C       TRUNK (JTR1, JTR2)      SUBROUTINE TO TEST TRUNCATION ERROR AND
C                               ADJUST INCREMENT SIZE
C       TRUP                    PREDICTOR TRUNCATION CONSTANT
C       TUPPER                  UPPER LIMIT FOR TRUNCATION ERROR
C       TW                      TIME AT INTERPOLATION FOR OUTPUT OR RESTART
C       WRTINE                  TIME BETWEEN OUTPUTS
C       WRTOT                   TIME AT WHICH OUTPUT OCCURS
C       XS(I,J,K)               THE DEPENDENT VARIABLE AT POINT -S
C       XSD(I,J,K)              DERIVATIVE OF XS(I,J,K)
C       XC(I,J,K)               CORRECTED VALUE OF DEPENDENT VARIABLE AT
C                               POINT I
C       XKS                     CONSTANTS IN AMOS EQUATIONS
C       XMIN                    TERMINATION CRITERIA FOR DEPENDENT VARIABLE
C       XP(I,J,K)               PREDICTED VALUE OF DEPENDENT VARIABLE AT
C                               POINT I
C       XPD(I,J,K)              DERIVATIVE OF XP(I,J,K)
C       XW(I,J,K)               ARGUMENT IN AMOSW, DEPENDENT VARIABLE
C                               COMPUTED FOR OUTPUT OR RESTART
```

```
C                    INPUT DATA CARDS
C
C     CARD 1      72 COLUMNS OF ALPHANUMERIC IDENTIFICATION
C
C     CARD 2      IMAX, JMAX, KMAX, IANOS, TUPPER, TLOWER, HDEST
C                 FORMAT (4I10, 3E10.2)
C
C     CARD 3      TIME, INCR, WRTIME, TRESUL, TERMT, XHIN
C                 FORMAT (E20.7, I10, 4E10.3 )
C
C     CARD 4      JDIAG, JPUNCH, JOSTPT
C                 FORMAT (5I10)
```

```
C
C                    MODEL III
C
C
C
C
      XC, XP, XPD
      DIMENSION IDENT(12), TRUNC(10, 30, 3), XD(10, 30, 3),
      COMMON IDENT, TRUNC, XD, X1, X2, X3, X4, XDD, X10, X20, X30, X40,
     1          X11(0, 30, 3), X21(0, 30, 3), X31(0, 30, 3),
     2          X41(0, 30, 3), XDD(10, 30, 3), X10(10, 30, 3),
     3          X20(10, 30, 3), X30(10, 30, 3), X40(10, 30, 3),
     4          XL(10, 30, 3), XP(10, 30, 3), XPD(10, 30, 3)
      COMMON /CON / PIMCR, PSOXF, H0, H1, H2, H3, H4, HRO, HR1, HR2,
     1        HN3, HNW, HL0, HL1, HL2, HLW, HMO, HR1, HNW, HOEST, HONEW,
     3        JMAX, JOSTPT, JPUNOT, JTEST, JTP5, JTP6, R, KMAX, NCORX,
     4        NORV, NEO, NPRED, P1, P2, P3, P4, P5, T, TO, TERMT, TIME,
     2        HW, L, IMAX, INCPL1, INCPL2, INCR, INCRD, J, JAMOS, JDIAG,
     5        TLOWER, TMAEL, TMEND, TMPRW, TPERIN, TRESOL, TRUC, TRUCP,
     6        TRUNOR, TXUNCT, TRUP, TUPACR, TW, WRTIME, WRTOT, XR1, XK2,
     7        XK3, XK4, XK5, XM1X
10 FORMAT (96H0SUBROUTINE DERIV HAS REQUESTED ANOS TO REDUCE INCREMEN
   1T SIZE, THIS IS NOT A RESONABLE REQUEST. / 87H0JAMOS IS PROGRAMMED
   2 TO TERMINATE THIS PROBLEM AND GO ON TO THE NEXT SET OF DATA CARDS
   3.)
20 FORMAT (95H0SUBROUTINE DERIV HAS REQUESTED ANOS TO RESTART AT A TI
   1ME IT HAD PREVIOUSLY ACCEPTED. /105H0THIS IS INCONSISTENT, THEREFO
   2RE ANOS HAS TERMINATED THIS PROBLEM AND GONE TO THE NEXT SET OF DA
   3TA CARDS.)
100 CALL CLOCK (2, TMBEG, DATE)
110 CALL SETUP (1)
120 CALL IOAMOS (1)
125 JAMOS = JAMOS
130 CALL IOURV (X4, TIME, 1)
```

```
140 CALL SETUP (2)
150 CALL STPIS (JSP1)
160 CALL OSTPTS
200 CALL SHIFT
205 GO TO (210, 420), JSP1
210 CALL DERIV (40, TIME, XOD, 2, JDV2, JDV3)
215 NDRV = NDRV + 1
225 GO TO (235, 400), JDV2
235 GO TO (240, 410), JDV3
240 CALL DAMOS (2)
250 CALL TERM (JTM1)
255 GO TO (300, 420), JTM1
300 GO TO (301, 303, 305, 307, 309), JAMOS
301 CALL AMOS1 (1)
302 GO TO 310
303 CALL AMOS2 (1)
304 GO TO 310
305 CALL AMOS3 (1)
306 GO TO 310
307 CALL AMOS4 (1)
308 GO TO 310
309 CALL AMOS 5 (1)
310 NPRED = NPRED + 1
315 I = IIML + NO
320 CALL DERIV (AP, T, XPO, 2, JDV2, JDV3)
325 NDRV = NDRV + 1
335 GO TO (345, 340), JDV3
340 CALL RSTART
341 GO TO 150
345 GO TO (360, 350), JDV2
350 CALL TRUNK (JTR1, 2)
355 GO TO 300
360 GO TO (361, 363, 365, 367, 369), JAMOS
361 CALL AMOS1 (2)
362 GO TO 370
363 CALL AMOS2 (2)
```

```
364 GO TO 370
365 CALL AMOS3 (1)
366 GO TO 370
367 CALL AMOS4 (2)
368 GO TO 370
369 CALL AMOS5 (2)
370 NCORR = NCORR + 1
380 CALL TRUNK (JTRL, 1)
390 GO TO (200, 300), JTRL
400 WRITE OUTPUT TAPE JTP6, [illegible]
405 GO TO 420
410 WRITE OUTPUT TAPE JTP6, [illegible]
420 CALL IOAMOS (3)
430 CALL CLOCK (2, TMEND, [illegible])
440 CALL IOAMOS (4)
450 GO TO 100
    END
```

```
1000 SUBROUTINE IDAMOS (JIDAI)
     COMMON IDE(4), TRUNC, X0, X1, X2, X3, X4, X00, X10, X20, X30, X40,
     1       XC, XP, XPU
      DIMENSION IDEN(112), TRUNC(10, 30, 31, X0(10, 30, 31,
     1          X1(10, 30, 31, X2(10, 30, 31, X3(10, 30, 31,
     2          X4(10, 30, 31, X00(10, 30, 31, X10(10, 30, 31,
     3          X20(10, 30, 31, X30(10, 30, 31, X40(10, 30, 31,
     4          XC(10, 30, 31, XP(10, 30, 31, XPU(10, 30, 31
      COMMON FGONE, FINCR, ESONL, HO, H1, H2, H3, H4, HKO, HK1, HK2,
     1       HK3, HKM, HLO, HL1, HL2, HLM, HMO, HM1, HMM, HDEST, HONEW,
     2       HW, I, IMAX, INCPL1, INCPL2, INCR, INCRD, J, JAMOS, JDIAG,
     3       JMAX, JOSTET, JPUNOT, JTESTT, JTP5, JTP6, K, KMAX, NCORR,
     4       NDRV, NEQ, NERED, E1, E2, E3, P4, P5, T, T0, TERMT, TIME,
     5       TLOWER, IMBEG, THEAD, TMFAR, TPERIN, TREADL, TRUC, TRUCF,
     6       TRUNCK, TRUNCT, TRUP, TOPPER, TW, WRTIME, WRTOT, XK1, XK2,
     7       XK3, XK4, XK5, XMIN
1100 FORMAT (12A4/ 4I10, 3E10.2// E20.9, I10, 4E10.3/ 5I10)
1200 FORMAT (1H1, 23X, 12A4 //// 40HOTHIS COMPUTATION SIMULTANEOUSLY SO
     1LVES , I3,  33H ORDINARY DIFFERENTIAL EQUATIONS. /32HOTHE NUMERICA
     2L ROUTINE UTILIZES , I1,37H POINT ADAMS-MOULTON-SHELL EQUATIONS. /
     345HOUEPER AND LOWER TRUNCATION ERROR LIMITS ARE , E8.2, 5H AND ,
     4E8.2,1H. /41HOTHE SUGGESTED INITIAL TIME INCREMENT IS ,E8.2, 1H./
     535HOOUTPUT IS WRITTEN AT INTERVALS OF , E8.2, 15H PLUS OR MINUS ,
     6 E8.2, 5H, GENERATED WITH A 5 POINT INTERPOLATION POLYNOMIAL. /
     742HOLOMPUTATION TERMINATES WHEN TIME EXCEEDS , E8.2,35H OR WHEN EV
     8ERY X CHANGES LESS THAN , E8.2, 20H IN FOUR INCREMENTS.)
1210 FORMAT (1H0   TIME = , E10.4, 19H, DURING INCREMENT I6,
     1 9H ISIZE = , E10.4, 2H1.)
1215 FORMAT (1H0   TIME = , E10.4, 19H,          INCREMENT I6,
     1 9H ISIZE = , E10.4, 2H1.)
1220 FORMAT (2X/40HTHIS COMPUTATION REQUIRED , I6, 50H APPLICATIONS OF TH
     1E AMOS PREDICTOR EQUATIONS AND , I6,13H APPLICATIONS / 59H0 OF THE
     2 CORRECTOR EQUATIONS.  SUBROUTINE DERIV WAS CALLED , I6, 7H TIMES.
     3/1H0, F7.3, 49H HOURS OF MACHINE TIME WAS REQUIRED TO CALCULATE ,
     4 I6, 16H INCREMENTS, OR , F10.6, 21H HOURS PER INCREMENT.)
1230 FORMAT (1HP, 12A6, 8X/ 1HP, 4I10, 3E10.2,10X/ 1HP, E20.9, I10,
```

```
    1 4E10.3, 10X / 1HP, 5I10, 30X )
1500 GO TO (1600, 1700, 1800, 1900), JIOA1
1600 READ INPUT TAPE JTP5, 1100, (IDCATIJ)I, JI = 1, 121, IMAX, JMAX,
    1 KMAX, JAMUS, TUPPER, TLOWER, HOEST, TIME, INCR, WRTIME, TRESUL,
    2 TERMT, XMIN, JDIAG, JPUNOT, JOSTPT
1610 NEQ = IMAX * JMAX * KMAX
1620 WRITE OUTPUT TAPE JTP6, 1200, (IDENTIJ)I, JI = 1, 121, NEQ, JAMUS,
    1 TUPPER, TLOWER, HOEST, WRITIME, TRESUL, TERMT, XMIN
1650 RETURN
1700 IF(TIME -(WRTOT + TRESUL)) 1710, 1710, 1719
1710 IF (TIME- WRTOT - TRESUL) 1799, 1730, 1730
1719 TH   WRTOT
1720 CALL AMOSH (XP)
1721 WRITE OUTPUT TAPE JTP6, 1210, WRTOT, INCR, HI
1722 CALL IODRV (XP, IW, 2)
1729 GO TO 1740
1730 WRITE OUTPUT TAPE JTP6, 1215, TIME, INCR, HI
1735 CALL IODRV (XO, TIME, 2)
1740 WRTOT = WRTOT + WRTIME
1750 IF (JIOA1 - 2) 1799, 1700, 1799
1799 RETURN
1800 GO TO (1810, 1830), JPUNO1
1810 WRITE OUTPUT TAPE JTP6, 1230, (IDENTIJ)I, JI = 1, 121, IMAX, JMAX,
    1 KMAX, JAMUS, TUPPER, TLOWER, HOEST, TIME, INCR, WRTIME, TRESUL,
    2 TERMT, XMIN, JDIAG, JPUNOT, JOSTPT
1820 CALL IODRV (XO, TIME, 4)
1830 CALL IODRV (XO, TIME, 3)
1840 GO TO 1730
1900 TMPRD = TMCID - TMBEG
1901 FINCR = INCR
1902 TPERIN = TMPRD/FINCR
1910 WRITE OUTPUT TAPE JTP6, [illegible]
    1  TPERIN
1999 RETURN
     END
```

```
3000 SUBROUTINE OSIPIS
     COMMON IDENT, IRUNC, X0, X1, X2, X3, X4, X00, X10, X20, X3[illegible],
    1        XC, XP, XPD
     DIMENSION IDENT(12), TRUNC(10, 30, 3), X0(10, 30, 3),
    1         X1(10, 30, 3), X2(10, 30, 3), X3(10, 30, 3),
    2         X4(10, 30, 3), X00(10, 30, 3), X10(10, 30, 3),
    3         X20(10, 30, 3), X30(10, 30, 3), X40(10, 30, 3),
    4         XC(10, 30, 3), XP(10, 30, 3), XPD(10, 30, 3)
     COMMON FGONE, FINCR, FSONE, H0, H1, H2, H3, H4, HK0, HK1, HK2,
    1        HK3, HKN, HLD, HL1, HL2, HLN, HMO, HM1, HMW, HOEST, HONEW,
    2        HW, I, IMAX, IMCPL1, IMCPL2, INCR, INCRO, J, JAMOS, JOIAG,
    3        JMAX, JOSTPT, JPUNOT, JTESTT, JTP5, JTP6, K, KMAX, NCORR,
    4        NORV, NEQ, NPREU, P1, P2, P3, P4, P5, T, TD, TERMT, TIME,
    5        TLOWER, TMZEG, TMENO, TMPAR, TPERIN, TRESOL, TRUC, TRUCP,
    6        TRUNCR, TRUNCT, TRUP, TUPPER, TW, WRITIME, WRIOT, XK1, XK2,
    7        XK3, XK4, XKW, XNI4
3010 FORMAT ( 1H0, 30A, 6H * * *, 7X, 19HTHE STARTING POINTS, 7X,
    1  6H * * * )
3020 FORMAT (1H0    TIME = , F10.4, 19H,          INCREMENT I6,
    1 9H (SIPE - , I10.4, 2H).)
3000 GO TO ( 3400, 3100), JOSTPT
3100 WRITE OUTPUT TAPE JTP5, 3010
3200 TD = TIME - 3.*H0
3210 INCRO = INCR - 3
3220 WRITE OUTPUT TAPE JTP6, 3020, TD, INCRO, H0
3230 CALL IODRV ( X3, TO, 2)
3240 TD = TD + H0
3250 INCRO = INCRO + 1
3260 WRITE OUTPUT TAPE JTP6, 3020, TD, INCRO, H0
3270 CALL IODRV ( X2, TO, 2)
3280 TD = TD + H0
3290 INCRO = INCRO + 1
3300 WRITE OUTPUT TAPE JTP6, 3020, TD, INCRO, H0
3310 CALL IODRV ( X1, TO, 2)
3320 TD = TD + H0
3330 INCRO = INCRO + 1
```

```
3340 WRITE OUTPUT TAPE JTP6, 3020, TD, INCRD, HD
3350 CALL IOURV ( XO, TD, 2)
3360 TD = TD + HD
3370 INCRD = INCRD + 1
3380 WRITE OUTPUT TAPE JTP6, 3020, TD, INCRD, HD
3390 CALL IOURV ( XC, TD, 2)
3400 RETURN
     END
```

```
5000 SUBROUTINE SETUP (JSUB)
     COMMON IDENT, TRUNC, X0, X1, X2, X3, X4, X00, X10, X20, X30, X40,
     1        XC, XP, XPD
      DIMENSION IDENT(12), TRUNC(10, 30, 3), X0(10, 30, 3),
     2          X1(10, 30, 3), X2(10, 30, 3), X3(10, 30, 3),
     3          X4(10, 30, 3), X00(10, 30, 3), X10(10, 30, 3),
     3          X20(10, 30, 3), X30(10, 30, 3), X40(10, 30, 3),
     4          XC(10, 30, 3), XP(10, 30, 3), XPD(10, 30, 3)
      COMMON FSONE, FINCR, FSONC, H0, H1, H2, H3, H4, HR0, HR1, HR2,
     1       HK3, HKN, HLO, HLL, HL2, HLN, HMO, HM1, HMN, HDEST, HONEW,
     2       H4, I, IMAX, INCPL1, INCPL2, INCR, INCRO, J, JAMOS, JDIAG,
     3       JMAX, JOSIPT, JPUNOT, JTESTT, JTP5, JTP6, K, KMAX, NCORR,
     4       NORV, NCQ, NPRED, P1, P2, P3, P4, P5, T, TO, TERMT, TIME,
     5       TLOWCR, TMDEC, TMEND, THPRB, TPERIN, TRESOL, TRUC, TRUCP,
     6       TRUNCK, TRUNLT, TRUP, TUPPER, TW, WRTINE, WRTOT, XK1, XK2,
     7       XK3, XK4, XK5, XMIN
5100 GO TO (5200, 5300), JSUI
5200 JTP5 = 5
5201 JTP6 = 6
5210 JTLSTI   3
5211 FSONC = 0.0
5212 FSONE   2.0
5213 NORV = 0
5214 NPRED = 0
5215 NCORR = 0
5240 RETURN
5300 H0 = H0 SI
5301 WRTOT = WRTINE + TIME
5310 RETURN
     END
```

```
6000 SUBROUTINE PSTAR1
     COMMON IDENT, TRUNC, XD, X1, X2, X3, X4, XDD, X1D, X2D, X3D, X4D,
    1        XC, XP, XPD
     DIMENSION IDENT(12), TRUNC(10, 30, 3), XD(10, 30, 3),
    1        X1(10, 30, 3), X2(10, 30, 3), X3(10, 30, 3),
    2        X4(10, 30, 3), XDD(10, 30, 3), X1D(10, 30, 3),
    3        X2D(10, 30, 3), X3D(10, 30, 3), X4D(10, 30, 3),
    4        XC(10, 30, 3), XP(10, 30, 3), XPD(10, 30, 3)
     COMMON FCONE, FINCR, FSONE, H0, H1, H2, H3, H4, HKD, HK1, HK2,
    1       HK3, HKW, HL0, HL1, HL2, HLW, HHO, HH1, HHW, HDEST, HDNEW,
    2       H0, I, IMAX, INCPL1, INCPL2, INCR, INCRD, J, JAMOS, JDIAG,
    3       JHAX, JOSTPT, JPUNOT, JTESTT, JTP5, JTP6, K, KMAX, NCURR,
    4       NDRV, NEQ, NPNEQ, P1, P2, P3, P4, P5, T, TD, TERMT, TIME,
    5       TLOWER, TMBEG, TMEND, TMPAB, TPERIN, TRESOL, TRUC, TRUCP,
    6       TRUMAX, TRUNCT, TRUP, TUPPER, TW, WRTIME, WRTOT, XK1, XK2,
    7       XK3, XK4, XK5, XMIN
6100 FORMAT (4HDIFF , E10.4,6H HAS CAUSED SUBROUTINE DERIV TO REQUEST
    1 ARGS TO RESTART AT TIME = , E10.4,1H. / 5HDAMOS, I1, 15H HAS COMPLE
    2TED , I6, 25H INCREMENTS, THROUGH TIME , E10.4,1H.)
6110 FORMAT (11H0    TIME = , E10.4,19H,  AFTER INCREMENT I6,
    1 9H STEP = , E10.4, 2H).
6140 TD = TW
6160 IF ( TD  - WRTOT) 6180, 6170, 6170
6170 TW = WRTOT
6171 CALL AMOSW (XP)
6172 WRITE OUTPUT TAPE JTP6, 6110, WRTOT, INCR, H1
6173 CALL IDDRV (XP, WRTOT, Z)
6174 WRTOT = WRTOT + WRTIME
6175 GO TO 6160
6180 TW = TD
6200 CALL AMOSW (XP)
6300 CALL DERIV (XP, TW, XPD, Z, JDV2, JDV3)
6400 WRITE OUTPUT TAPE JTP5, 6100, T, TW, JAMOS, INCR, TIME
6500 CALL IDDRV (XP, TW, Z)
6600 INCR = INCR + 1
6610 NDRV = NDRV + 1
```

```
6620 11[illegible] = 12
6630 10 = FOLST
6641 DO 6650  K = 1, KMAX
6642 DO 6650  J = 1, JMAX
6643 DO 6650  I = 1, IMAX
6650 X4I(I,J,K) = XPI(I,J,K)
6655 FGONE = 2.0
6656 FSUIE = 0.5
6657 JTCSTT = 3
6700 RETURN
     END
```

```
10000 SUBROUTINE AMOSW (XW)
      COMMON IDENT, TRUNC, X0, X1, X2, X3, X4, X0D, X1D, X2D, X3D, X4D,
     1        XE, XP, XPD
      DIMENSION IDENT(12), TRUNC(10, 30, 3), X0(10, 30, 3),
     1          X1(10, 30, 3), X2(10, 30, 3), X3(10, 30, 3),
     2          X4(10, 30, 3), X0D(10, 30, 3), X1D(10, 30, 3),
     3          X2D(10, 30, 3), X3D(10, 30, 3), X4D(10, 30, 3),
     4          XE(10, 30, 3), XP(10, 30, 3), XPD(10, 30, 3)
      COMMON FGONE, FINCR, FSOME, H0, H1, H2, H3, H4, HK0, HK1, HK2,
     1       HK3, HKW, HLO, HL1, HL2, HLW, HMO, HM1, HMW, HOES1, HONEW,
     2       HW, I, IMAX, INCPL1, INCPL2, INCR, INCRD, J, JAMOS, JOIAO,
     3       JMAX, JUSTPT, JPUNOT, JTCSTT, JTP5, JTP6, K, KMAX, NCOAR,
     4       NURV, NEO, NPPEO, P1, P2, P3, P4, P5, T, TD, TERMT, TIME,
     5       TLOWCR, TMBEG, TMEND, TMPRD, TPERIN, TRESOL, TRUC, TRUCP,
     6       TRUNCK, TRUNCT, TRUP, TUPPER, TW, WRTIME, WRTOT, XK1, XK2,
     7       XK3, XK4, XK5, XMIN
      DIMENSION XW(10,30,3)
10100 HW = TW - TIME
10101 HKW = HW + H1
10102 HLW = HK1 + H2
10103 HMW = HLW + H3
10104 P2 = HW * HKW
10105 P3 = P2 * HLW
10106 P4 = P3 * HMW
10201 XW = 1.0 + (((P4/HM1 + P3)/HL1 + P2)/HK1 + HW)/H1
10202 XK2 = (((P4/HL2 + P3)/HK2 + P2)/HW + HW) /H1
10203 XK3 = (((P4/HK3 + P3)/H3 + P2)/(H2*H1 1)
10204 XK4 = (P4/H4 + P3)/(H3*HK2*HL1)
10205 XK5 = P4/(H4*(K3*HL2*HM1)
10220 DO 10240 K = 1, KMAX
10221 DO 10240 J = 1, JMAX
10222 DO 10240 I = 1, IMAX
10240 XW(I,J,K) = XW1 * X0(I),J,K) - XK2 * X1(I,J,K) + XK3 * X2(I,J,K)
     1          -XK4 * X3(I),J,K) + XK5 * X4(I,J,K)
10250 RETURN
      END
```

```
11000 SUBROUTINE ARDSI (J,I)
      COMMON IDEN1, TRUNC, X0, X1, X2, X3, X4, X0D, X1D, X2D, X3D, X4D,
     1       XC, XP, XPD
      DIMENSION IDEN(1112), TRUNC(10, 30, 31, X0(10, 30, 31,
     1          X1(10, 30, 31, X2(10, 30, 31, X3(10, 30, 31,
     2          X4(10, 30, 31, X0D(10, 30, 31, X1D(10, 30, 31,
     3          X2D(10, 30, 31, X3D(10, 30, 31, X4D(10, 30, 31,
     4          XC(10, 30, 31, XP(10, 30, 31, XPD(10, 30, 31
      COMMON FGONE, FINCR, FSONE, H0, H1, H2, H3, H4, HK0, HK1, HK2,
     1       HK3, HKW, HL0, HL1, HL2, HLW, HN0, HN1, HNW, HOEST, HONEW,
     2       IBW, I, IMAX, INCPL, INCPL2, INCR, INCRO, J, JAMOS, JDIAG,
     3       JMAX, JUSTPT, JPUNOT, JTEST, JTP5, JTP6, K, KMAX, NCORA,
     4       NORV, NEQ, NPRED, P1, P2, P3, P4, P5, T, T9, TERM1, TIME,
     5       TLOWER, INBEG, TMEND, INPRE, TPERIN, TRESOL, TRUC, TRUCP,
     6       TRUNCK, TRUNCT, TRUP, TUPPER, TW, WATIME, WATOT, XR1, XR2,
     7       XK3, XK4, XK5, XMIN
11100 GO TO (11200, 11300, 1211
11200 DO 11240 K = 1, KMAX
11201 DO 11240 J = 1, JMAX
11202 DO 11240 I = 1, IMAX
11240 XP(I,J,K) = X0(I,J,K) + H0*X0D(I,J,K)
11250 RETURN
11300 DO 11340 K = 1, KMAX
11301 DO 11340 J = 1, JMAX
11302 DO 11340 I = 1, IMAX
11340 X0(I,J,K) = X0(I,J,K) + H0*XPD(I,J,K)
11400 INDRCK = 0
11500 RETURN
      END
```

```
12000 SUBROUTINE AMOS2 (JA21)
      COMMON IDEGT, TAUNC, X0, X1, X2, X3, X4, X00, X10, X20, X30, X40,
     1       XC, XP, XPD
      DIMENSION IULN1(12), TRUNC(10, 30, 31, X0(10, 30, 31,
     1          X1(10, 30, 31, X2(10, 30, 31, X3(10, 30, 31,
     2          X4(10, 30, 31, X00(10, 30, 31, X10(10, 30, 31,
     3          X20(10, 30, 31, X30(10, 30, 31, X40(10, 30, 31,
     4          XC(10, 30, 31, XP(10, 30, 31, XPD(10, 30, 31
      COMMON FGUNE, FINCR, FSONC, H0, H1, H2, H3, H4, HK0, HK1, HK2,
     1       HK3, HKW, HLO, HL1, HL2, HLW, HMO, HM1, HMW, HOEST, HONEW,
     2       HW, I, IMAX, INCPL1, INCPL2, INCR, IICRO, J, JAMOS, JO1AG,
     3       JMAX, JOSTPT, JPUNOT, JTESIT, JTP5, JTP4, K, KMAX, NCORR,
     4       NDAY, NEQ, NPREO, P1, P2, P3, P4, P5, T, TD, TERMT, TIME,
     5       TLDWCR, TMBEGR, TMEND, TMPRB, TPERIN, TRESOL, TRUC, TRUCP,
     6       TRUNCK, TRUNCT, TRUP, TUPPER, TW, WRTIME, WRITOT, XK1, XK2,
     7       XK3, XK4, XK5, XMIN
12100 GO TO (12200, 12300), JA21
12200 P2 = 0.5*H0*(0/H1
12201 XK1 = H0 + P2
12210 DO 12240 K = 1, KMAX
12211 DO 12240 J = 1, JMAX
12212 DO 12240 I = 1, IMAX
12240 X0(I,J,K) = X0(I,J,K) + XP1*X00(I,J,K) - P2*X10(I,J,K)
12290 RETURN
12300 P1 = 0.5*H0
12310 DO 12340 K = 1, KMAX
12311 DO 12340 J = 1, JMAX
12312 DO 12340 I = 1, IMAX
12340 X0(I,J,K) = X0(I,J,K) + P1*(XP0(I,J,K) + X00(I,J,K))
12400 TRUNCK = 0.3333333333333*H0/HK0
12500 RETURN
      END
```

```
13000 SUBROUTINE AMOS3 (JA31)
      COMMON IDENT, IRUNG, X0, X1, X2, X3, X4, X00, X10, X20, X30, X40,
     1       XC, XP, XPD
      DIMENSION IDENT(12), TRUNG(10, 30, 31), X0(10, 30, 31),
     1          X1(10, 30, 31, X2(10, 30, 31, X3(10, 30, 31,
     2          X4(10, 30, 31, X00(10, 30, 31, X10(10, 30, 31,
     3          X20(10, 30, 31, X30(10, 30, 31, X40(10, 30, 31,
     4          XC(10, 30, 31, XP(10, 30, 31, XPD(10, 30, 31
      COMMON FGONE, FINCR, FSONE, H0, H1, H2, H3, H4, HK0, HK1, HK2,
     1       HK3, HKN, HLO, HL1, HL2, HLN, HMO, HM1, HMN, HOEST, HONEW,
     2       HN, I, IMAX, INCFL1, INCFL2, IMCR, INCRD, J, JAMOS, JO1AG,
     3       JMAX, JOSIPT, JPUNOT, JTESTT, JTP5, JTP6, K, KMAX, NCORR,
     4       NORV, NCQ, NPRED, P1, P2, P3, P4, P5, T, T0, TERMT, TIME,
     5       TLONGR, TMBEG, TMEND, TMFRB, TPERIN, TRESOL, TAUC, TAUCP,
     6       TRUNCK, TPUNCT, TRUP, TUPPER, IW, WRTIME, WRTOUT, XK1, XK2,
     7       XK3, XK4, XK5, XP1(
13050 GO TO (13100, 13301, JA31
13100 P2 = H0*H0
13101 P3 = P2*H0*(0.3333333)
13102 P2 = P2*0.5
13201 XP1 = H0 + (P2*(H1+HK1) +P3)/(H1*HK1)
13202 XK2 = (P2*HK1 +P3)/(H1*H2)
13203 XK3 = (P2*HL +P3)/(H2*HK1)
13220 DO 13240  K = 1, KMAX
13221 DO 13240  J = 1, JMAX
13222 DO 13240  I = 1, IMAX
13240 XP(I,J,K) = X0(I,J,K) + XK1*X00(I,J,K) - XK2*X10(I,J,K)
     1          + XK3*X20(I,J,K)
13250 RETURN
13301 XK1 = (P2*H1 +P3)/(H0*HK0)
13302 XK2 = (P2*(H1-H0) +P3)/(H0*H1) - H0
13303 XK3 = (P2*(-H0) +P3)/(H1*HK0)
13320 DO 13340  K = 1, KMAX
13321 DO 13340  J = 1, JMAX
13322 DO 13340  I = 1, IMAX
13340 XC(I,J,K) = X0(I,J,K) + XK1*XPD(I,J,K)   XK2*XP(I,J,K)
```

```
     1            + XK3*X10(I,J,K)
13400 TRUNCF - (HO*(HKO+H1))/(HLO*(2.0*H1+4.0*HKO))
13500 RETURN
      END
```

```
14000 SUBROUTINE MOS4 (JA41)
      COMMON (DEHI, IKUNC, X0, X1, X2, X3, X4, X00, X10, X20, X30, X40,
     1        XC, XP, XPD
      DIMENSION IDENT(12), TKUNC(10, 30, 31, X0(10, 30, 31,
     1          X1(10, 30, 31, X2(10, 30, 31, X3(10, 30, 31,
     2          X4(10, 30, 31, X00(10, 30, 31, X10(10, 30, 31,
     3          X20(10, 30, 31, X30(10, 30, 31, X40(10, 30, 31,
     4          XC(10, 30, 31, XP(10, 30, 31, XPD(10, 30, 31
      COMMON FUONE, FINCK, FSUNE, HO, H1, H2, H3, H4, HKO, HK1, HK2,
     1        HK3, HKW, HLO, HL1, HL2, HLW, HMO, HM1, JMW, HDEST, HDNEW,
     2        HW, L, LMAX, INCPL1, INCPL2, INCR, INCRD, J, JAMOS, JOIAG,
     3        JMAX, JOSTPT, JPUNOT, JTEST, JTP5, JTP6, K, KMAX, NCORR,
     4        NDRV, NEQ, NPRED, P1, P2, P3, P4, P5, T, TD, TEMT, TIME,
     5        TLOWER, TMBEG, TMEND, TMPR8, TPERIN, TRESOL, TKUC, TRUCP,
     6        TRUNCK, TRUNCT, TRUP, TUPPER, TW, WRITIME, WRTOT, XK1, XK2,
     7        XK3, XK4, XK5, XKIH
14050 GO TO (14100, 14301), JA41
14100 P2 = HU+HO
14101 P3 = P2*HU
14102 P4 = P3*HO*0.25
14103 P3 = P3*0.33333333
14104 P2 = P2*0.5
14201 XK1 = HU + (P2*(HI*HK1+HI*HL1+HK1*HL1) +P3*(HI*HK1+HL1) +P4)/
     1          (HI*HK1*HL1)
14202 XK2 = (P2*HK1*HL1 +P3*(HK1+HL1) +P4)/(HI*HL2*HK2)
14203 XK3 = (P2*HI*HL1 +P3*(HI+HL1) +P4)/(HI2*HI*HK1)
14204 XK4 = (P2*HI*HK1 +P3*(HI+HK1) +P4)/(HI*HK2*HL1)
14220 DO 14240  K = 1, KMAX
14221 DO 14240  J = 1, JMAX
14222 DO 14240  I = 1, IMAX
14240 AP(I,J,K) = X0(I,J,K) + XK1*X00(I,J,K) - XK2*X10(I,J,K)
     1          +XK3*X20(I,J,K) - XK4*X30(I,J,K)
14250 RETURN
14301 XK1 = (P2*HI*(HO +P3*(HI+HK1) +P4)/(HO*HK0*HL0)
14302 XK2 = (P2*(HI*HK1-HO*HK1-HO*HI) +P3*(HI-HO*HK1) + P4)/
     1          (HO*HI*HK1) - HO
```

```
14303 XK3 = (-P2*HO*HK1 +P3*(HK1-HO) +P4)/(H1*H2*HKO)
14304 XK4 = (-P2*HO*HI +P3*(H(-HO) +P4)/(H2*HK1*HLD)
14320 DO (4340  K = 1, KMAX
14321 DO 14340  J = 1, JMAX
14322 DO 14340  I = 1, IMAX
14340 XO(I,J,K) = XO(I,J,K) + XK(*XPD(I,J,K) - XK2*XOL(I,J,K)
     1              +XP3*XID(I,J,K) - XK4*X2D(I,J,K)
14400 TRUCP = HMO*(0.5*HL*HK1 + HO*(HL*HK1/3.0 + 0.25*HI))
14401 TRUC   P3*(0.15 + (P2*(HL*HK1) + HO*HI*HK1)/6.0
14402 TRUNCK = TRUC/TRUCP
14500 RETURN
      END
```

```
15000 SUBROUTINE ABOSS (JA51)
      COMMON DEAT, TRUNC, Y0, X1, X2, X3, X4, X0H, X1D, X2D, X[illegible],
     1       XC, XF, XPD
      DIMENSION IDENT(12), TRUNC(10, 30, 3), X0(10, 30, 3),
     1          X1(10, 30, 3), X2(10, 30, 3), X3(10, 30, 3),
     2          X4(10, 30, 3), X0D(10, 30, 3), X1D(10, 30, 3)
     3          X2D(10, 30, 3), X3D(10, 30, 3), X4D(10, 30, 3),
     4          XC(10, 30, 3), XP(10, 30, 3), XPD(10, 30, 3)
      COMMON FGONE, FINCR, FSONE, HO, H1, H2, H3, H4, HKO, HK1, HK2,
     1       HK3, HKW, HLO, HL1, HL2, HLW, HMO, HM1, HMW, HOEST, HONEW,
     2       DN, I, IMAX, INCPL1, INCPL2, INCR, INCRD, J, JAMOS, JDIAG,
     3       JMAX, JOSTPT, JPUNOT, JTEST1, JTP5, JTP6, K, KMAX, NCDAR,
     4       NDRV, NEQ, NLRED, P1, P2, P3, P4, P5, T, T0, TERHT, TIME,
     5       TLOWER, TMBEG, TMEND, TPRAB, TPERIN, TRESOL, TRUC, TRUCP,
     6       TRUNCK, TRUNCT, TRUP, TUPPER, TW, WRTIME, WRTOT, XK1, XK2,
     7       XK3, XK4, XK5, XM1
15050 GO TO (15100, 15200), JA51
15100 P2 = HO*HO
15101 P3 = P2*HO
15102 P4 = P3*HO
15103 P5 = P4*(D*O-2
15104 P6 = P4*(D-2)
15105 P3 = P3/3.0
15106 P2 = P2/2.0
15110 P10 = H1*HK1
15111 P11 = HL1*HM1
15112 P12 = P10+P11
15113 P13 = P10+HL1
15120 P20 = H1*HK1
15121 P21 = H1*HL1
15122 P22 = H1*HP1
15123 P23 = HK1*HL1
15124 P24 = HK1*HP1
15125 P25 = HL1*HM1
15126 P26 = P20+P21+P23
15130 P30 = P20*HL1
```

```
1 131 P31 = P2*HM1
15132 P32 = P21*HL1
15133 P33 = P23*HM1
15201 XK1 = HO + (P2*(P30+P31+P32+P33) +P3*(P24+P22+P24+P25)
     1      +P4*(P10+P11) +P5(/(P20+P25)
15202 XK2 = (P2*P33 +P3*(P23+P24+P25( +P4*(HK1+P11( +P5(/(H1*H2+HK2+HL2)
15203 XK3 = (P2*P32 +P3*(P21+P22+P25( +P4*(H1+P11( +P5(/(H2+H3+HK1+HK3(
15204 XK4 = (P2*P31 +P3*(P20+P22+P24( +P4*(P10+HM1( +P5(/(H3+H4+HK2+HL1)
15205 XK5 = (P2*P30 +P3*(P20+P21+P23( +P4*(P10+HL1(+P5)/(H4+HK3+HL2+HM1)
15220 DO 15240  K = 1, KMAX
15221 DO 15240  J = 1, JMAX
15222 DO 15240  I = 1, IMAX
15240 XP(I,J,K) = XO(I,J,K( + XK1*XOD(I,J,K( - XK2*XID(I,J,K)
     1              +XK3*X2D(I,J,K) - XK4*X3D(I,J,K( + XK5*X4D(I,J,K)
15250 RETURN
15260 P60 = -HO*M1
15261 P61 = -HO*H1(
15262 P62 = -HO*HL1
15263 P63 = H1*HK1
15264 P64 =P60+P61+P63
15270 P70 = P60*HK1
15271 P71 = P60*HL2
15272 P72 = P61*HK1
15280 P80 = -HO*HL1
15301 XK1 = (P2*P30 +P3*P26 +P4*P13 +P5(/(HO*HO+HL0+HK0(
15302 XK2 = (P2*(P30+P70+P71+P72) +P3*(P64+P62+P21+P23(
     1      +P4*(P10+P80( +P5(/(HO*P30( - HO
15303 XK3 = (P2*P72 +P3*(P61+P62+P23( +P4*(P80+HK1( +P5)/(H1+H2+HK0+HK2)
15304 XK4 = (P2*P71 +P3*(P60+P62+P21( +P4*(P80+H1( +P5(/(H2+H3+HK1+HL0)
15305 XK5 = (P2*P70 +P3*(P60+P61+P20( +P4*(P10-HO( +P5(/(H3+HK2+HL1+HM0(
15320 DO 15340  K = 1, KMAX
15321 DO 15340  J = 1, JMAX
15322 DO 15340  I = 1, IMAX
15340 XC(I,J,K)   XO(I,J,K( + XK1*XPD(I,J,K( - XK2*XOD(I,J,K)
     1              +XK3*X1D(I,J,K)   XK4*X2D(I,J,K( + XK5*X3D(I,J,K(
15400 TAUCP = (HO+HM1(*(P2*P30 +P3*P26 +P4*P13 +P5(
```

```
15401 TRUC  = P3*H0/6.0 + [illegible] 2* (T[illegible]*T26/3.0 +P3*P30*D [illegible]
15402 TRUNCK = TRUC/TRUCI
15500 RETURN
      END
```

```
17000 SUBROUTINE TRUN (JTRH)
      COMMON TIEMI, TRUNC, X0, X1, X2, X3, X4, [illegible]
     1        XC, XP, XPO
      DIMENSION IDENT(12), TRUNF(10, 30, 3), X0(10, 30, 3),
     1          X1(10, 30, 3), X2(10, 30, 3), X3(10, 30, 3),
     2          X4(10, 30, 3), X0D(10, 30, 3), X1D(10, 30, 3),
     3          X2D(10, 30, 3), X3D(10, 30, 3), X4D(10, 30, 3),
     4          XC(10, 30, 3), XP(10, 30, 3), XPO(10, 30, 3)
      COMMON FGUNC, FINCR, FSUNC, H0, H1, H2, H3, H4, HK0, HK1, HK2,
     1       HK3, HK4, HLJ, HL1, HL2, HLW, HMO, HM1, HM4, HOEST, HONEW,
     2       HW, I, IMAX, INCPL1, INCPL2, INCR, INCRD, J, JAMOS, JDIAG,
     3       JMAX, JOSTPT, JPUNOT, JTESTT, JTP5, JTP6, K, KMAX, NCURR,
     4       NDUY, NEQ, NPRED, P1, P2, P3, P4, P5, T, TD, TERMT, TIME,
     5       TLUNCA, TMBEG, TMEND, TMPRD, TPERIN, TRESOL, TRUC, TRUCP,
     6       TRUNCN, TRUNCT, TSUP, TUPPER, TW, WRTIME, WRTOT, XK1, XK2,
     7       XK3, XK4, XK5, XMIN
1T030 FORMAT 145H0COMPUTATION TERMINATES BECAUSE TIME EXCEEDS , E10.4,1H
     1.)
17060 FORMAT 155H0COMPUTATION TERMINATES BECAUSE EVERY X CHANGES LESS IN
     1AN ,E10.-, 20H IN FOUR INCREMENTS.)
17100 IF(TIME - TERMT) 17300,17200, 17200
17200 WRITE OUTPUT TAPE JTP6, 17050, TERMT
17201 JTM1 = 2
17210 RETURN
17300 DO 17330 K = 1, KMAX
17301 DO 17330 J = 1, JMAX
17302 DO 17330 I = 1, IMAX
17310 IF (ABSF(X0(I,J,K)) - X4(I,J,K)) - XMIN) 17330, 17600, 17600
17330 CONTINUE
17340 WRITE OUTPUT TAPE JTP6, 17040, XMIN
17360 GO TO 17201
17600 JTM1 = 1
17610 RETURN
      END
```

```
18000 SUBROUTINE SHIFT
      COMMON IDENT, TRUNC, X0, X1, X2, X3, X4, X0D, X1D, X2D, X3D, X4D,
     1       XC, XP, XTD
      DIMENSION IDENT(12), TRUNC(10, 30, 3), X0(10, 30, 3),
     1          X1(10, 30, 3), X2(10, 30, 3), X3(10, 30, 3),
     2          X4(10, 30, 3), X0D(10, 30, 3), X1D(10, 30, 3),
     3          X2D(10, 30, 3), X3D(10, 30, 3), X4D(10, 30, 3),
     4          XC(10, 30, 3), XP(10, 30, 3), XPD(10, 30, 3)
      COMMON FGONE, FINCR, FSONE, H0, H1, H2, H3, H4, HK0, HK1, HK2,
     1       HK3, HKW, HLO, HL1, HL2, HLW, HMO, HM1, HMW, HOEST, HONEW,
     2       HW, I, IMAX, INCPL1, INCPL2, INCP, INCRD, J, JAMDS, JDIAG,
     3       JMAX, JOSTPT, JPUNOT, JTESTT, JTPS, JTPW, K, KMAX, NCORR,
     4       NDAV, NEQ, NPREQ, P1, P2, P3, P4, P5, T, T0, TERMT, TIME,
     5       TLOWER, TMBEG, TMEND, TMPRN, TPERIN, TRESOL, TRUC, TRUCP,
     6       TRUNCK, TRUNCT, TRUP, TUPPER, TW, WATIME, WRTOT, XX1, XX2,
     7       XX3, XX4, XX5, XX10
18100 DO 18330 K = 1, KMAX
18101 DO 18330 J = 1, JMAX
18102 DO 18330 I = 1, IMAX
18200 X0(I,J,K) = X3(I,J,K)
18210 X3(I,J,K) = X2(I,J,K)
18220 X2(I,J,K) = X1(I,J,K)
18230 X1(I,J,K) = X0(I,J,K)
18240 X0D(I,J,K) = X3D(I,J,K)
18300 X4D(I,J,K) = X3D(I,J,K)
18310 X3D(I,J,K) = X2D(I,J,K)
18320 X2D(I,J,K) = X1D(I,J,K)
18330 X1D(I,J,K) = X0D(I,J,K)
18400 TIME = TIME + H0
18410 H4 = H3
18420 H3 = H2
18430 H2 = H1
18440 H1 = H0
18450 H0 = HW
18510 HK3 = HK2
18520 HK2 = HK1
```

```
18530 HK1 = HK0
18540 HK0 = H0 [illegible]
18610 HL2 = HL1
18620 HL1 = HL0
18630 HL0 = HK0 [illegible]
18710 HM1 = HM0
18720 HM0 = HL [illegible]
18730 IMCR = I [illegible]
18800 RETUR
      END
```

```
19000 SUBROUTINE TRUNK (JIRI, JI[illegible]
      COMMON IDENT, TRUNC, X0, X1, X2, X3, X4, X0J, X1J, X2J, [illegible],
     1        XC, XP, XPO
      DIMENSION IDENT(121, TRUNC(10, 30, 31, X0(10, 30, 3),
     1          X1(10, 30, 3), X2(10, 30, 3), X3(10, 30, 3),
     2          X4(10, 30, 3), X0J(10, 30, 3), X1J(10, 30, 3),
     3          X2J(10, 30, 3), X3J(10, 30, 3), X4J(10, 30, 3),
     4          XC(10, 30, 3), XP(10, 30, 3), XPO(10, 30, 3)
      COMMON FCONF, FINCR, FSONC, HD, H1, H2, H3, H4, HKO, HK1, HP2,
     1        HA3, HKW, HLO, HL1, HL2, HLW, HMO, HM1, HMW, HOEST, HONEW,
     2        H4, I, IMAX, INCPL1, INCPL2, INCR, INCRO, J, JAMOS, JOIAG,
     3        JMAX, JOSTPT, JPUNOT, JTESTT, JTP5, JTP4, K, KMAX, NLOKR,
     4        NORV, NEQ, NPRED, P1, P2, P3, P4, P5, T, TD, TERMT, TIME,
     5        TLOWER, TABEL, TRESO, TNPRS, TPERIN, TRESOL, TRUC, TRUCP,
     6        TRUNCK, TRUNCT, TRUP, TUPPER, TW, WRITME, WRTOT, XK1, XK2,
     7        XK3, XK4, XK5, XK6
19010 FORMAT ( 9H AT TIME , E12.6, 12H, INCREMENT , I6, 9H ISIZE = ,
     1 E12.6, 13H, INCREMENT , I6, 9H ISIZE = , E12.6, 17H IS REJECTED
     2 AND / 6X, 11HCHANGED BY , E12.5, 11H TO SIZE = , E12.5, 1H.)
19020 FORMAT ( 9HOAT TIME , E12.6, 12H, INCREMENT , I6, 9H ISIZE = ,
     1 E12.6, 13H, INCREMENT , I6, 9H ISIZE = , E12.6, 17H IS
     2 / 6X, 11HCHANGED BY , E12.5, 11H TO SIZE = , E12.6, 1H.)
19090 GO TO (19100, 194001, JIRZ
19100 TRUNCT = 0.0
19110 DO 19120 K = 1, KMAX
19111 DO 19120 J = 1, JMAX
19112 DO 19120 I = 1, IMAX
19113 TRUNC(I,J,K) = TRUNC(K)*(XP(I,J,K) - XC(I,J,K))
19120 TRUNCT = MAX1(TRUNCT, ABS(TRUNC(I,J,K)))
19200 IF (TLOWER - TRUNCT) 19210, 19500, 19500
19210 IF (TUPPER - TRUNCT) 19400, 19400, 19300
19300 JTEST1 = 3
19301 HONEW = HD
19310 DO 19317 K = 1, KMAX
19311 DO 19317 J = 1, JMAX
19312 DO 19317 I = 1, IMAX
```

```
19317 XC(I,J,K) = XC(I,J,K) + TRUE(I,J,K)
19330 JTRI   I
19332 RETURN
19400 HONEW = FSONE * HO
19401 GO TO (19402, 19401, JDIAG
19402 INCPLL = INCR + 1
19403 WRITE OUTPUT TAPE JIF6, 19010, TIME, INCR, H1, INCPLL, HO, FSONE,
     1                                                    HONEW
19410 GO TO (19420, 19430, 19440),JTESTT
19420 FSONE =FSONE * FSONE
19421 GO TO 19440
19430 FSONE   SQRTF(FSONE)
19440 JTESTT = 1
19479 JTRI = 2
19480 HO = HONEW
19481 HKO = HO + H1
19482 HLO   HKO + H2
19483 HMO = HLO + H3
19484 RETURN
19500 HONEW = FGONE * HO
19501 GO TO (19502, 19510), JDIAG
19502 INCPLZ = INCR + 2
19503 WRITE OUTPUT TAPE JIF6, 19020, TIME, INCR, H1, INCPLZ, HO, FGONE,
     1                                                    HONEW
19510 GO TO (19520, 19530,19540), JTESTT
19520 FSONE = SQRTF(FSONE)
19522 GO TO 19540
19530 FGONE = FGONE * FGONE
19540 JTESTT = 2
19600 GO TO 19310
      END
```

```
30000 SUBROUTIN  [illegible] IS [illegible]
      COMMON IDENT, IRUNC, X0, X1, X2, X3  X4, X0D, X1[illegible]
     1       XC, XP, XPD
      DIMENSION IDENT(12), TRUNC(10, 30, 31, X0(10, [illegible]
     1          X1(10, 30, 31, X2(10, 30, 31, X3(10, 30, [illegible]
     2          X4(10, 30, 31, X0D(10, 30, 31, X1D(10, 30, 31,
     3          X2D(10, 30, 31, X3D(10, 30, 31, X4D(10, 30, 31,
     4          XP(10, 30, 31, XPD(10, 30, 31, XPD(10, 30, 31
      COMMON EGUNS, EINCR, FSONE, H0, H1, H2, H3, H4, HK0, HK1, HK2,
     1       HK3, HKW, HLU, HL1, HL2, HLW, HMO, HH1, HHH, HOEST, HONEH,
     2       HW, I, IMAX, INCPL1, INCPL2, INCR, INCRD, J, JAMOS, JOIAG,
     3       JMAX, JOSIPT, JPUNOT, JTEST, JTPS, JIPS, K, KMAX, NCORR,
     4       NDRV, NEQ, NPREQ, P1, P2, P3, P4, P5, T, T0, TERMT, TIME,
     5       TLOWER, THSEG, TM-HD, TMPRB, TPERIN, TRESOL, TRUC, TAUCP,
     6       TRUNCR, TRUNCT, TPUP, TUPPER, TH, WRIINC, WRIOT, XK1, XK2,
     7       XK3, XK4, XK5, XMIN
30010 FORMAT (43HJSTARTING POINTS REJECTED, HO SET TO H0/4.0)
30020 FORMAT (39HJSUBROUTINE DERIV HAS REQUESTED AMOS TO REDUCE INCREMEN
     1T SIZE WITHIN THE RANGE OF SUBROUTINE STPTS.)
30030 FORMAT (35HJSUBROUTINE DERIV HAS REQUESTED AMOS TO RESTART WITHIN
     1THE RANGE OF SUBROUTINE STPTS.)
30040 FORMAT (13H AMOS IS NOT PROGRAMMED TO RESTART THIS REQUESTED)
30105 T = TIME
30110 CALL DERIV (X4, T, X4D, 1, JDV2, JDV3)
30111 NDRV = NDRV + 1
30120 GO TO (30125, 32200), JDV2
30125 GO TO (30130, 32300), JDV3
30130 DO 30140  K   1, KMAX
30131 DO 30140  J - 1, JMAX
30132 DO 30140  I - 1, IMAX
30140 X3I(I,J,K) - X4(I,J,K) + H0*X4D(I,J,K)
30205 T = T + H0
30210 CALL DERIV (X3, T, X3D, 2, JDV2, JDV3)
30220 GO TO (30225, 32200), JDV2
30225 GO TO (30230, 32300), JDV3
30230 DO 30240  K -1, KMAX
```

```
30231 DO 30240  J= 1, JMAX
30232 DO 30240  I = 1, IMAX
30240 X2I(I,J,K) = X3I(I,J,K) + HO*(1,5*X3D(I,J,K)   0.5*X4D(I,J,K)
30305 T = T + HO
30310 CALL DERIV (X2, T, X2D, 2, JOV2, JOV3)
30320 GO TO (30325, 32200), JHV2
30325 GO TO (30330, 32300), JOV3
30330 DO 30340  K= 1, KMAX
30331 DO 30340  J= 1, JMAX
30332 DO 30340  I = 1, IMAX
30340 X1I(I,J,K) = X2I(I,J,K) + HO*(1,916666667*X2D(I,J,K) +[illegible]
    1                 *X3D(I,J,K) + 0.416666667*X4D(I,J,K))
30405 T = T + HO
30410 CALL DERIV (X1, T, X1D, 2, JOV2, JOV3)
30420 GO TO (30425, 32200), JOV2
30425 GO TO (30430, 32300), JOV3
30430 DO 30440  K  1, KMAX
30431 DO 30440  J= 1, JMAX
30432 DO 30440  I  1, IMAX
30440 X0I(I,J,K) = X1I(I,J,K) + HO*(2.291666667*X1D(I,J,K) [illegible]
    1                 *X2D(I,J,K) + 1.541666667*X3D(I,J,K)
    2                 -0.3750*X4D(I,J,K))
30500 LOOP - 1
30505 T - T + HO
30510 CALL DERIV (X0, T, X0D, 2, JOV2, JOV3)
30520 GO TO (30525, 32200), JOV2
30525 GO TO (30530, 32300), JOV3
30530 DO 30540  K = 1, KMAX
30531 DO 30540  J = 1, JMAX
30532 DO 30540  I = 1, IMAX
30540 X3I(I,J,K) = X4I(I,J,K) + HO*(-0.025390889*X0D(I,J,K)
    1                 +0.147222222*X1D(I,J,K) -0.366666667*X2D(I,J,K)
    2                 +0.897222222*X3D(I,J,K) +0.348611111*X4D(I,J,K))
31145 T   TIME + HO
31150 CALL DERIV (X3, T, X3D, 2, JOV2, JOV3)
31220 GO TO (31525, 32200), JOV2
```

```
31230 GO TO 31230, 32300), JOV3
31230 DO 31240  K = 1, KMAX
31231 DO 31240  J = 1, JMAX
31232 DO 31240  I = 1, IMAX
31240 X2(I,J,K) = Z(I,J,K) + [illegible]
     1            0.1027777[illegible]
     2           +0.4005[illegible]
31305 T = T + HO
31310 CALL DERIV (X2, T, X2D, 2, [illegible]
31320 GO TO (31325, 32200), JOV2
31325 GO TO (31330, 32300), JOV3
31330 DO 31340  K = 1, KMAX
31331 DO 31340  J = 1, JMAX
31332 DO 31340  I = 1, IMAX
31340 X3(I,J,K) = X2(I,J,K) + HO*( 0.0263888889*X0D(I,J,K)
     1            +0.4009555556*X1D(I,J,K) +0.6333333333*X2D(I,J,K)
     2            -0.1027777778*X3D(I,J,K) +0.0152777777778*X4D(I,J,K))
31405 T = T + HO
31410 CALL DERIV (X3, T, X3D, 2, JOV2, JOV3)
31420 GO TO (31425, 32200), JOV2
31425 GO TO (31430, 32300), JOV3
31430 DO 31440  K = 1, KMAX
31431 DO 31440  J = 1, JMAX
31432 DO 31440  I = 1, IMAX
31440 X4D(I,J,K) = X3D(I,J,K) + HO*(0.3486111111*X0D(I,J,K)
     1            +0.8372222222*X1D(I,J,K) -0.3666666666*X2D(I,J,K)
     2            +0.1472222222*X3D(I,J,K) -0.0263888889*X4D(I,J,K))
31441 GO TO (31450, 31505), LOOP
31450 LOOP = LOOP + 1
31451 GO TO 30505
31505 T = T + HO
31510 CALL DERIV (X0, T, X0D, 2, JOV2, JOV3)
31520 GO TO (31525, 32200), JOV2
31525 GO TO (31530, 32300), JOV3
31530 DO 31540  K = 1, KMAX
31531 DO 31540  J = 1, JMAX
```

```
31532 DO 31540  I   1, IMAX
31540 XP(I,J,K)   X0(I,J,K) + H0*(2.640277777*X0(I,J,K)
     1            -3.052777778*X1(I,J,K) +3.633333333*X2(I,J,K)
     2            -1.769444444*X3(I,J,K) +0.3486111111*X4(I,J,K))
31605 T = T + H0
31610 CALL DERIV (XP, T, XP0, Z, JDV2, JDV3)
31611 NDRV = NDRV + 13
31620 GO TO (31622, 322001, JDV2
31625 GO TO (31630, 323001, JDV3
31630 DO 31640  K = 1, KMAX
31631 DO 31640  J = 1, JMAX
31632 DO 31640  I = 1, IMAX
31640 X(I,J,K) = X0(I,J,K) + H0*(0.3486111111*XP0(I,J,K)
     1            +0.8972222222*X0(I,J,K) -0.3555666667*X1(I,J,K)
     2            +0.1672222222*X2(I,J,K)  0.0243888889*X3(I,J,K))
31730 DO 31740  K = 1, KMAX
31731 DO 31740  J = 1, JMAX
31732 DO 31740  I = 1, IMAX
31734 TRUNC(I,J,K)   0.0557[illegible]*(XP(I,J,K) -X(I,J,K))
31735 TRUNCT =  AMAX1(TRUNC(I,J,K))
31736 IF (TRUNCT - TOPPER)  31740, 32100, 32100
31740 CONTINUE
31830 DO 31840  K = 1, KMAX
31831 DO 31840  J = 1, JMAX
31832 DO 31840  I = 1, IMAX
31840 X(I,J,K) = X(I,J,K) + TRUNC(I,J,K)
32000 TIME = T - H0
32001 H4 = H0
32002 H3   H0
32003 H2 = H0
32004 H1 = H0
32005 GIVEN = H0
32010 HK3 = H0 + H0
32011 HK2 = HK3
32012 HK1 = HK2
32013 HK0 = HK1
```

```
32020 HL2 = HN0 + H0
32021 HL1 = HL2
32022 HL0 = HL1
32030 HN1 = HL0 + H0
32031 HN0 = HN1
3 040 INCR = IN[illegible]
3.050 JSP1 = 1
32090 RETURN
32100 H0 = 0.2[illegible] 0
32101 1   TIME
32102 GO TO (32103, 30130),JDIAG
32103 WRITE OUTPUT TAPE JTP6, 30010
32104 GO TO 30130
32200 JSP1 = 2
32201 WRITE OUTPUT TAPE JTP6, 30020
32202 WRITE OUTPUT TAPE JTP6, 30040
32203 RETURN
32300 JSP1 = 2
32301 WRITE OUTPUT TAP  JTP6, 10030
32302 WRITE OUTPUT TAPE JTP6, 1[illegible]
32303 RETURN
      END
```

```
10 SUBROUTINE CLOCK (J, TM, NT)
11 TM = J + 1
12 NT = TM + 1
13 RETURN
   END
```

```
C     DYNAMIC HEAT TRANSFER WITH HEAT GENERATION IN A SPHERE
C
 2000 SUBROUTINE JOURV (TEMP, T, J1001)
      COMMON IDEAT, TAUNC, X0, X1, X2, X3, X4, X0D, X1D, X2D, X3D, X4D,
     1       XC, XP, XPD
      DIMENSION IHENT(12), THMC(10, 30, 3), X0(10, 30, 3),
     1          X1(10, 30, 3), X2(10, 30, 3), X3(10, 30, 3),
     2          X4(10, 30, 3), X0D(10, 30, 3), X1D(10, 30, 3),
     3          X2D(10, 30, 3), X3D(10, 30, 3), X4D(10, 30, 3),
     4          XC(10, 30, 3), XP(10, 30, 3), XPD(10, 30, 3)
      COMMON FCONE, TINCR, FSONE, H0, H1, H2, H3, H4, HK0, HK1, HK2,
     1       HK3, HKN, HLO, HL1, HL2, HLN, HMO, HM1, HMN, NOEST, NOREW,
     2       HH, I, IMAX, INCPL1, INCPL2, INCR, INCRD, J, JAMOS, JOIAG,
     3       JMAX, JOSIPT, JPUMOT, JTEST1, JTP5, JTP6, K, KMAX, NCORR,
     4       NDRV, NEQ, NPRCD, P1, P2, P3, P4, P5, T, TD, TERMT, TIME,
     5       TLOWER, TNRCG, TUEND, TMPRB, TPERIN, TRESOL, TRUC, TRUCP,
     6       TRUNCR, TRUNCT, TRUP, TUPPER, TW, WRITINE, WRTGT, XK1, XK2,
     7       XK3, XK4, XK9, XHIN
      COMMON NANC, N, R, THRCON, CP, RHO, FJ, AVGT, DELR, ALPHA, VOL1,
     1       VOL2, CPOAR, TCOAR, ALPOAR, C, DELH, HDLG,
     2       NFREQ1, NFREQ2, NFREQ3, NFREQ4 , NFREQ5 , NFREQ6, NFREQ7,
     3       J1,J2,J3,J4,J5,J6,J7, NPOINT, ISRLAK,TKON,SLOPE1,SLOPE2,RC
     4       ,JOCORL,INDEX,NELG,N2,IST,N3

      DIMENSION  NANDE(2,7),N(7),R(7), TIRCON(7), CP(7), RHO(7),
     1           FJ(7), AVGT(7), DELR(7), ALPHA(7), VOL1(7), VOL2(7),
     2           CPOAR(7,7), TCOAR(7,7), ALPOAR(7,7), C(900,5),
     3           TEMP(900), TEMPO(900), SUN(7)

 2101 FORMAT (14A5/ 7I10/ 7F10.3/ 7E10.3/ 7E10.3/ 7E10.3)
 2102 FORMAT (7I10)
 2103 FORMAT (25H THE CORE IS COMPOSED OF , 2A5,22H  POSITION TEMPERATUR
     1E)
 2104 FORMAT (40X, I4, 4X, F10.3)
 2105 FORMAT (25H THE SECOND ELEMENT IS    ,2A5, 22H  POSITION TEMPERATUR
     1E)
```

```
2106 FORMAT (2X, I=1 (1I10 [illegible] I [illegible] 2X POSITION TEMPERATU
   1E)
2107 FORMAT (7F10.3)
2108 FORMAT (25H THE FOURTH ELEMENT IS   ,2A5, 22H  POSITION TEMPERATUR
   1E)
2109 FORMAT (25H THE FIFTH  ELEMENT IS   ,2A5, 22H  POSITION TEMPERATUR
   1E)
2110 FORMAT (25H THE SIXTH  ELEMENT IS   ,2A5, 22H  POSITION TEMPERATUR
   1E)
2111 FORMAT (25H THE SEVENTH ELEMENT IS  ,2A5, 22H  POSITION TEMPERATUR
   1E)
2112 FORMAT ( 32H0THE AVERAGE TEMPERATURE IN THE , 2A5,4H IS , F10.3)
2113 FORMAT (1HP,14A5/(1HP,7F10/1HP,7F10.3/1HP,7F10.3/1HP,7F10.3/1HP,7F1
   1          0.3)
2114 FORMAT (1HP, 7F10)
2115 FORMAT (1HP, 7F10.3)
2116 FORMAT ( 1H0, 19X,70H MATERIAL    RADIUS   DENSITY    THERMAL COND
   UCTIVITY  HEAT CAPACITY  /)
2117 FORMAT ( 1H0,2A5 , F10.3, F10.3, 8X,F10.3, 9X, F10.3)
2118 FORMAT (5F10.3)
2119 FORMAT(25H0 DELTA H IS REPRESENTED BY ,F10.3, 6H*EXP(-,F8.3,
   1 5H*T) +, F6.3,33H* FOR T LESS THAN OR EQUAL TO   , F8.3//
   2 28X, F10.3,1H*EXP(-,F8.3, 2H *, F8.3, 3H) +, F6.3, 2H *, F6.3,
   3 3H - , F6.3, 6H*LT - , F8.3, 1H)/67X, 18HFOR T GREATER THAN,
   4 F8.3)
2120 FORMAT(F10.3,3I10,3F10.3)
2121 FORMAT (52H0 THE WELL MIXED PORTION OF THE CORE HAS A RADIUS OF ,
   1 F10.4,13H CENTIMETERS. )
2122 FORMAT (1HP,7F10.3)
2123 FORMAT(1HP,7F10.3)
2124 FORMAT (46H0 THE WELL MIXED TEMPERATURE IN THE CORE   IS ,F10.3)
2125 FORMAT(46H0 THE DRIVING FUNCTION IS A KNOWN CORE PROFILE(
2126 FORMAT (19H0 ELEMENT,I4,27H0AS HEAT GENERATION DELHG =,F8.3,
   1          7H*EXP(-,F8.3,5H*(F8.3,2H))
2200 GO TO (2201, 2400, 2600, 2800), JLOG
2201 READ INPUT TAPE 5, 2101,(NAMFIL,J=1,2),(J=1,7),(N(I),I=1,7),
```

```
    1                                   I(I1),I=1,7),(TMRC [illegible]
    2                                   ILP(I1,I-1,7), IR[illegible]
2202 READ INPUT TAPE 5, 2102, NFREQ1, NFREQ2, N[illegible]
    1                                   NFREQ6, NFREQ7
     NPOINT = 1
     DO 2203 I = 1,7
2203 NPOINT = NPOINT + N(I)
2204 READ INPUT TAPE 5, 2107,(TEMPIM),M=1,NPOINT)
2205 READ INPUT TAPE 5, 2116, HBEG,TKON, TBREAK, SLOPE1, SLOPE2
2206 READ INPUT TAPE 5,2120,RC,JDCORE,INDEX,NELG,B2,TST,B3
2208 WRITE OUTPUT TAPE 6, 2116
2209 WRITE OUTPUT TAPE 6, 2117, (NAME(I,1), NAME(I,1), N(I), AND(I),
    1                                   THRCONI(I), CPI(I), I=1,7)
2210 WRITE OUTPUT TAPE 6,  2119, HBEG, TKON, SLOPE1, TBREAK, HBEG,
    1                                   TKON, TBREAK, SLOPE1, TBREAK, SLOPE2,
    2                                   TBREAK, TBREAK
2211 WRITE OUTPUT TAPE6,2121,RC
2212 GO TO (2,14,2213),JDCORE
2213 WRITE OUTPUT TAPE 6, 2125
2214 CONTINUE
2215 GO TO (2217,2216),INDEX
2216 WRITE OUTPUT TAPE 6,2126, NELG,B2,B3,TST
2217 CONTINUE
2399 RETURN
2400 WRITE OUTPUT TAPE 6, 2103,  NAME(I,1),  NAME(I,1)
2401 DO 2405  M= 1, J1,NFREQ1
2402 WRITE OUTPUT TAPE 6, 2104, M, TEMP(M)
2405 CONTINUE
2406 WRITE OUTPUT TAPE 6, 2105, NAME(I,2), NAME(I,2)
2407 DO 2410 M= J1,J2, NFREQ2
2408 WRITE OUTPUT TAPE 6, 2104, M, TEMP(M)
2410 CONTINUE
2411 WRITE OUTPUT TAPE 6, 2106, NAME(I,3), NAME(I,3)
2412 DO 2415 M= J2, J3, NFREQ3
2413 WRITE OUTPUT TAPE 6, 2104, I, TEMP(M)
2415 CONTINUE
```

```
2420 WRITE OUTPUT TAPE 6, 2100, [illegible]
2421 DO 2425 M=J4, J5, NFREQ4
2422 WRITE OUTPUT TAPE 6, 2100, [illegible]
2429 CONTINUE
2430 WRITE OUTPUT TAPE 6, 2100, [illegible]
2431 DO 2435 M=J4,J5, NFREQ5
2432 WRITE OUTPUT TAPE 6, 2104, M, TEMPIM)
2435 CONTINUE
2440 WRITE OUTPUT TAPE 6, 2110, NAME (1,6), NAME(2,6)
2441 DO 2445 M=J5,J6, NFREQ6
2442 WRITE OUTPUT TAPE 6, 2104, M, TEMPIM)
2445 CONTINUE
2450 WRITE OUTPUT TAPE 6, 2110,NAME (1,7), NAME(2,7)
2451 DO 2455 M=J6,J7, NFREQ7
2452 WRITE OUTPUT TAPE 6, 2104, M, TEMPIM)
2455 CONTINUE
2456 WRITE OUTPUT TAPE 6, 2104, J7, )EMPIJT)
2500 RETURN
2600 WRITE OUTPUT TAPE 6,2124,TEMPIL)
2601 DO 2602 M = 4,7
2602 SUMIM)= 0.0
2603 DO 2609 L = 2,7
2604 NELM = FJIM)
2605 NELM = FJIM +1)
2606 DO 2607 L = NELM, NELM
2607 SUMIM) = SUMIM) + TEMPIL)
2608 AVGTIM = SUMIM)/(FJIM -1) + 1.)
2609 WRITE OUTPUT TAPE 6, 2112, NAME(1,M), NAME(2,M), AVGTIM)
2610 CONTINUE
2700 RETURN
2800 WRITE OUTPUT TAPE 6, 2113,(NAME(I,J),I=1,2),J=1,7), (NI(I),I=1,7)
   1                          (RI(I),I=1,7), (THRCUN(I),I=1,7),
   2                          (CP(I),)=1,7), (RHU(I),)=1,7)
2801 WRITE OUTPUT TAPE 6, 2114, NFREQ1, NFREQ2, NFREQ3, NFREQ4, NFREQ5
   1                          NFREQ6, NFREQ7
2803 WRITE OUTPUT TAPE 6, 2115, (TEMPIM), M=1, NPOINT)
```

```
2904 WRITE OUTPUT TAPE 6, [illegible]
2905 WRITE OUTPUT TAPE 6,2[illegible]
2900 RETURN
     END
```

```
C     DYNAMIC [illegible] TRANSFER FUNCTION GENERATION FOR 7 SUBMODEL
C
20000 SUBROUTINE DERIV (X   , T, TEMP0, JDV1, JDV2, JDV3)
      COMMON IDELT, ITRUNC, X0, X1, X2, X3, X4, X0D, X1D, X2D, X3D, X4D,
     1       XI, XT, XFD
      DIMENSION IBNT112), TRUNC110, 30, 3), X0110, 30, 3),
     1          X1110, 30, 3), X2110, 30, 3), X3110, 30, 3),
     2          X4110, 30, 3), X0D110, 30, 31, X1D110, 30, 3),
     3          X2D110, 30, 31, X3D110, 30, 3), X4D110, 30, 3),
     4          XI110, 30, 3), XF110, 30, 31, XFD110, 30, 3)
      COMMON FGON., FINCR, FSONE, HO, H1, H2, H3, H4, HKO, HKL, HKZ,
     1       HK3, HKW, HLO, HL1, HL2, HLW, HMO, HM1, HMW, HOEST, HONEW,
     2       HW, I, IMAX, INCPL1, INCPL2, INCR, INCRD, J, JAMOS, JDIAG,
     3       JMAX, JOSTPT, JPUNOT, JTESTT, JTP5, JTP6, K, KMAX, NCORR,
     4       NDRV, NEG, NPRED, P1, P2, P3, P4, P5, T, TO, TERMT, TIME,
     5       TLOWER, TMDEG, TMEVO, TMPRD, TPERIN, TRESOL, TRUC, TRUCF,
     6       TRUNK, TRONUT, TRUP, TUPPER, TW, WRITME, WRTDT, XK1, XK2,
     7       XK3, XK4, XK5, XK1X
      COMMON  XANG, M, R, THRCUN, CP, RHO, PJ, AVGT, DELR, ALPHA, VOLI,
     1        VOL2, CPBAR, TCOBAR, ALPBAR, G, DELH, HBEG,
     2        NFREQ1, NFREQ2, NFREQ3, NFREQ4, NFREQ5, NFREQ6, NFREQ7,
     3        J1, J2,J3,J4,J5,J6,J7, NPUT11,TBREAK,TRON,SLOPE1,SLOPE2,RL
     4        ,JLOGRE,)ND_X,NLIG,N2,TST,B3

      DIMENSION  XAVE(2,7),N(7),R(7), THRCUN(7), CP(7), RHO(7),
     1           PJ(7), AVGT(7), DELR(7), ALPHA(7), VOL(7), VOL2(7),
     2           CPBAR(7,7), TCOBAR(7,7), ALPBAR(7,7), G(900,5),
     3           TEMP(900), TEMP1(900), SUM(7),X(900)

20100 GO TO (20200, 20500),JDV1
C
C     CALCULATE [illegible] NODES
C
20200 J1 = N(1) + 1
20202 J2 = N(2) + J1
20203 J3 = N(3) + J2
```

```
20205 J5 = NTJ1 * J4
20206 J6 = NTG1 * J5
20207 J7 = NTF1 * J6
C
C     FLOAT MODE VALUES
C
20211 FJ(1)   J1
20212 FJ(2) = J2
20213 FJ(3) = J3
20214 FJ(4)   J4
20215 FJ(5) = J5
20216 FJ(6) = J6
20217 FJ(7) = J7
C
C     CALCULATE DE[illegible] V*B[illegible]
C
20220 DELR(1)   [illegible] 3C)/(F[illegible] - 2.)
20221 DO 20220 L   2,7
20225 DELR(L)   [illegible] (L) - RIL-1)/(FJ(L) -[illegible] 1)
C
C     CALCULATE ALPHA VALUES
C
20230 DO  20235  L = 1,7
20235 ALPHA(L) =  THRCOM(L)/ICP(L)*[illegible] 1)
C
C     CALCULATION OF EQUATION C[illegible]
C
20240 CON1 = ALPHA(1)/(DELR(1)**2)
20241 CON2 = 1./ICP(1)*RHO(1)
20245 C(1,1) =(3.*ALPHA(1)/(RC*DELR(1)
20246 C(1,2) = CON2
20249 J1M1 =J1-1
20250 DO 20255  L 3, J1M1
20251 FL = L
20252 C(L,L)   CO[illegible]*FL/IFL - 1.[illegible]
```

```
20253 C(L,2)   CC I*2.
20254 C(L,3)  - CC(I*IFL - [illegible]
20255 C(L,4) - CC(2
C
C     CONSTANT FOR GENERALIZ[illegible] AT B-[illegible]
C
      B = TKO *TB(KM)
      A = HDCG*LXF(I-B) + SLOPE(I * TBREAK
C
C     CONSTANTS FOR INTERFACE EQUATIONS
C
20290 DO 20294 L = 1,6
20291 J = FJ(L)
20293 C(J,1)   IT RLONE(I*DEL(IL+1)/(D[illegible]L*DLR(IL+1) + THRCOW(L+1)
     1          *D(I(L)
20294 C(J,2) = ITI CONE(+1*D I(L)/(THRCO [illegible]L*DLR(IL+1) + THRCO[illegible]
     1          * [illegible](L)
C
C     CONSTANTS [illegible]
C
20300 DO 20320 L = 2,7
20301 A2 = ALPHA(L)/DEL[illegible]
20302 D1 = 1./DEL(IL)
20303 JNPL1 = FJ(L) 1J + 1
20304 JNM1 = FJ(L) - 1
20305  DO 20315  K  JNPL[illegible]
20306 FM  M
20307 D = 1./TRIL-1) + TFM  [illegible]
20308 C(M,1) - A2*(D1+ D)
20309 C(M,2) - A2*D1*2.
20315 C(M,3) = A2*(D1- D)
20320 CONTINUE
20324 J1P1  J1+1
20325 DO 20330 L  [illegible]
20330 C(L,4) = 0[illegible]
20331 JIM[illegible] J1 - 1
```

```
20332 J1P1   [illegible]
20333 J2M1   [illegible]
20334 J2P1   [illegible]
20335 J3M1   [illegible]
20336 J3P1   [illegible]
20337 J4M1   [illegible]
20338 J4P1   [illegible]
20339 J5M1   [illegible]
20340 J5P1   [illegible]
20341 J6M1   [illegible]
20342 J6P1   [illegible]
20343 J7M1 - [illegible]
20344 J7P1   [illegible]
20345 DO 20340 L = 1,[illegible]
20346 C(L,5) = 0.0
20347 GO TO [illegible]20500,20[illegible]
20348 L   [illegible]
20349 J1P1 = [illegible]
20350 J1M1 = [illegible] - 1
20351 D[illegible]
20352 [illegible]
C
C     DIFF[illegible]
C
20500 DO 20550 I   1,J7P1
20550 TEMP(I) = X(I)

21001 IF (T - TBREAK(  21002, 21004, 21004
21002 DELH - HDEG*EXP(-TKON*T) + SLOPE1*T
21003 GO TO 21010
21004 DELH = A - SLOPE2*(T - TBREAK)
21005 IF(DELH)21006, 21010, 21010
21006 DELH - 0.0

21010 TEMPD(I) = C(I,1)*(TEMP(3) - TEMP(2)) + C(I,2)*DELH
21011 TEMPD(2(   C(I,1)*(TEMP(3) - TEMP(2)) + C(I,2)*DELH
```

```
21012 [illegible]
21013 DE[illegible] = 0.0
21014 DO 10 I=2,[illegible]2J
21015 DELHG = J2*(XPH-B3*(T [illegible]T))
21028 TEMP(J1) = C(J1,1)*TEMP(J1-1) + C(J1,2)*(EMP(J1+1)
21029 DO 21030 L = J1,J1M1
21030 TEMP0(L) = C(L,1)*TEMP(L-1) - C(L,2)*TEMP(L) + C(L,3)*[illegible]
     1          + C(L,4)*(DELH) + C(L,5)*DELHG
21033 TEMP(J2) = C(J2,1)*(EMP(J2-1) + C(J2,2)*TEM(J2+1)
21034 DO 21035 L = J1P1,J2M1
21035 TEMP0(L) = C(L,1)*TEMP(L+1) - C(L,2)*TEMP(L) + C(L,3)*TEMP(L-1)
     1          + C(L,4)*(DELH) + C(L,5)*DELHG
21038 TEMP(J3) = C(J3,1)*EMP(J3-1) + C(J3,2)*TEMP(J3+1)
21039 DO 21040 L = J2P1,J3M1
21040 TEMP0(L) = C(L,1)*TEMP(L+1) - C(L,2)*TEMP(L) + C(L,3)*TEMP(L-1)
     1          + C(L,4)*(DELH) + C(L,5)*DELHG
21043 TEMP(J4) = C(J4,1)*EMP(J4-1) + C(J4,2)*TEMP(J4+1)
21044 DO 21045 L = J3P1,J4M1
21045 TEM0(L) = C(L,1)*TEMP(L+1) - C(L,2)*TEMP(L) + C(L,3)*TEMP(L-1)
     1          + C(L,4)*(DELH) + C(L,5)*DELHG
21048 (EMP(J5) = C(J5,1)*TEMP(J5-1) + C(J5,2)*TEMP(J5+1)
21049 DO 21050 L = J4P1,J5M1
21050 (EMP0(L) = C(L,1)*TEMP(L+1) - C(L,2)*TEMP(L) + C(L,3)*TEMP(L-1)
     1          + C(L,4)*(DELH) + C(L,5)*DELHG
21053 TEMP(J6) = C(J6,1)*(EMP(J6-1) + C(J6,2)*TEMP(J6+1)
21054 DO 21055 L = J5P1,J6P1
21055 TEMP0(L) = C(L,1)*TEMP(L+1) - C(L,2)*TEMP(L) + C(L,3)*TEMP(L-1)
     1          + C(L,4)*(DELH) + C(L,5)*DELHG
21059 DO 21060 L = J6P1,J7M1
21060 (EMP0(L) = C(L,1)*T(MP(L+1) - C(L,2)*TEMP(L) + C(L,3)*TEMP(L-1)
     1          + C(L,4)*(DELH) + C(L,5)*DELHG
21061 (EMP0)J7I    0.0

22000 JDV2    1
22010 JDV3    1
22030 RETU[illegible]
```

BIOGRAPHICAL SKETCH

Mario Ariet Antiga was born July 9, 1939, in Havana, Cuba. In June, 1956, he was graduated from Colegio de Belen, Havana, Cuba. He entered the University of Florida in September, 1956, he received the degree of Bachelor of Science in Chemical Engineering with Honors in June, 1960, and the degree of Master of Science in Engineering in December, 1962. Since that time he has been employed at the University by the Department of Chemical Engineering as a full-time engineering assistant.

He is married to the former Laudelina Rosa Suat. They have three children, Ana Maria, Maria Elena and Mario Alberto. He is a member of Sigma Tau, Tau Beta Pi, Phi Kappa Phi, and Sigma Xi.

This dissertation was prepared under the direction of the Chairman of the Candidate's Supervisory Committee, and has been approved by all members of that committee. It was submitted to the Dean of the College of Engineering and to the Graduate Council, and was approved as partial fulfillment of the requirements for the degree of Doctor of Philosophy.

April 24, 1965

Dean, College of Engineering

Dean, Graduate School

SUPERVISORY COMMITTEE:

Chairman